Biological sex differences in the gene expression and contractile function of cardiac myocytes

By Christa L. Trexler
B.S., Northern Arizona University 2010

A thesis submitted to the Faculty
of the Graduate School in partial
fulfillment of the requirements
for the degree of Doctor of Philosophy

Department of Molecular, Cellular,
and Developmental Biology
2017

This thesis entitled:

Biological sex differences in the gene expression and contractile function of cardiac myocytes

written by Christa L. Trexler

has been approved for the Department of Molecular, Cellular, and Developmental Biology

Robin Dowell, D.Sc.

Leslie Leinwand, Ph.D.

The final copy of this thesis has been examined by the signatories, and we find that both the content and the form meet acceptable presentation standards of scholarly work in the above mentioned discipline.
IACUC protocol #: 2351-16FEB2019

Trexler, Christa L. (Ph.D. Molecular, Cellular and Developmental Biology)

Biological sex differences in the gene expression and contractile function of cardiac myocytes

Thesis Directed by Leslie A. Leinwand

Abstract

Significant sexual dimorphisms have been demonstrated in the development, presentation and outcome of cardiovascular disease (CVD) in humans as well as in animal models. Biological sex is an important modifier of the development of CVD with younger women generally being protected, but this cardioprotection is lost later in life, suggesting a role for estrogen. Additionally, even though CVD is the number one killer of women in the U.S., women have traditionally been omitted from clinical trials and female animals have commonly been excluded from basic research studies. This research bias has led to the development of cardiovascular therapeutics that are not as effective in women relative to men suffering from the same disease. A more thorough understanding of sex-specific cardiovascular differences both at baseline and in disease is required to effectively treat all patients with CVD. In this thesis I characterize the baseline differences in function, gene expression and estrogen signaling that exist in the contractile cells of the heart, the cardiac myocytes. Specifically, I characterized the expression, localization and signaling characteristics of the estrogen receptor, ERα, in neonatal and adult cardiac myocytes. Because I did not observe sexual dimorphisms in the expression or localization of ERα in adult cardiac myocytes, I sought to investigate other potential mechanisms mediating the sexually dimorphic functional differences I observed in the whole heart, cardiac myocytes and myofibrils. I therefore conducted an RNA-sequencing experiment to identify cardiac myocyte gene expression differences between the sexes. In addition to demonstrating that hundreds of genes are differentially expressed between male and female myocytes, I also identified sexually dimorphic enriched pathways, such as the PKA pathway, that could be mediating the differences in contractility observed at baseline. Overall these

studies provide insight to the sex differences in cardiac function, gene expression and signaling pathways that exist during baseline conditions, which is essential for better understanding the disparity in cardiovascular disease development between the sexes.

Dedication

This thesis is dedicated to my wonderful family, whose unwavering confidence in me made this work a reality. I especially want to thank my mother for instilling me with a strong, determined work ethic and continually telling me I was capable of anything I set my mind to. To my husband, John, who deserves a medal for his constant humor and encouragement during my graduate career. And finally, to my dog Waffles for making thesis writing an adorable process.

Acknowledgements

I would first like to thank my advisor, Leslie Leinwand, for her constant support, encouragement and particularly for her patience over these six years. I also want to thank Leslie for providing an excellent one-of-a-kind laboratory environment that I am lucky to have been apart of and am unlikely to encounter in the future. The heart of the Leinwand laboratory is the group of amazingly smart, warm and hysterical people that work in the lab without whom, my graduate work would not have been possible. Specifically, Dr. Pamela Harvey and Dr. Kristen Barthel were my most valuable resources, teaching and helping me whenever I needed it, no matter what they were doing. Dr. Emily Pugach was the best role model I could have asked for in a fellow graduate student and the most supportive scientific partner I will ever have. Dr. Angela Peter is the most efficient and selfless person I have ever encountered whom I owe a great debt for the countless hours of scientific discussions, proofreading and help with cell isolations. I also have to thank Dr. Steve Langer and Dr. Massimo Buvoli for not only providing invaluable comic relief, but also for always dropping everything to help me out, no matter how small the problem, as well as for vital scientific advice. The myocyte images in this thesis were captured beautifully with the expertise of Dr. Joseph Dragavon in the BIofrontiers Advanced Light Microscopy core facility. My sequencing experiments would not have been possible without the essential help and patience of Dr. Robin Dowell and her lab, specifically Aaron Odell, soon-to-be Doctor Amber Scott and the Biofrontiers IT staff, all of whom I can never thank enough. I also thank Dr. Maureen Bjerke, Ann Robinson, Margaret Isenhart, Amy Perry, Kathy Asta and Dr. Alberto Rossi for practical support and thoughtful scientific discussions. Thank you to the American Heart Association for granting me a predoctoral fellowship (AHA14PRE20380468) and the NIH for their support through the Signaling and Cellular Regulation training grant (5-T32 GM08759). Finally, I want to thank my thesis committee members for their valuable input and advice: Drs. Robin Dowell, Zhe Chen, Timothy Mckinsey and Russell Moore.

Contents

Figures

Tables

Chapter 1 Introduction

As published in: Blenck, C. L., Harvey, P. A., Reckelhoff, J. F., & Leinwand, L. A. (2016). The Importance of Biological Sex and Estrogen in Rodent Models of Cardiovascular Health and Disease. *Circ Res, 118*(8), 1294-1312. doi:10.1161/CIRCRESAHA.116.307509

Nearly one-third of deaths in the United States are caused by cardiovascular disease (CVD) each year. In the past, CVD was thought to mainly affect men leading to the exclusion of women and female animals from clinical studies and preclinical research. In light of sexual dimorphisms in CVD, a need exists to examine baseline cardiac differences in humans and the animals used to model CVD. In humans, sex differences are apparent at every level of cardiovascular physiology from action potential duration and mitochondrial energetics to cardiac myocyte and whole heart contractile function. Biological sex is an important modifier of the development of CVD with younger women generally being protected, but this cardioprotection is lost later in life, suggesting a role for estrogen. While endogenous estrogen is most likely a mediator of the observed functional differences in both health and disease, the signaling mechanisms involved are complex and are not yet fully understood. To investigate how sex modulates CVD development, animal models are essential tools and should be useful in the development of therapeutics. This chapter will focus on describing the cardiovascular sexual dimorphisms that exist both physiologically as well as in common animal models of CVD.

Premenopausal women experience lower rates of cardiovascular disease (CVD) compared to age-matched men; a benefit thought to be mediated, at least in part, by the female sex hormone estrogen (Mosca et al., 2011; Writing Group et al., 2010). Consistent with that notion, despite a lower incidence of CVD in younger women, the rate of CVD development and mortality in women after menopause exceeds that of men (Kelsey et al., 1993; Mosca et al., 2011). These observations underscore the critical need to understand both baseline differences

in cardiovascular function and responses to pathological cardiac insults between the sexes (Huxley, 2007). Indeed, major funding agencies in the US, Canada, and Europe have emphasized the inclusion of both sexes; however, women and female animals remain vastly underrepresented in all stages of CVD research (*Gender Mainstreaming in the 6th Framework Programme – Reference Guide for Scientific Officers/Project Officers*, 2003; *Report on Governmental Health Research Policies - Promoting Gender or Sex Differences Sensitivity* 2003; Shaw et al., 2006; Yamamoto, 1985). Until only recently, consideration of both sexes was not required in clinical and preclinical studies that focus on CVD (Clayton & Collins, 2014; *Consideration of Sex as a Biological Variable in NIH-funded Research*, 2015). Characterization of baseline differences between the sexes is required to appropriately assess the utility of animal models of CVD in understanding mechanisms responsible for CVD and its treatment in women and men. In light of the need for a comprehensive understanding of sex differences in both cardiac health and pathology, I will review molecular and functional differences between healthy men and women and will relate these findings to healthy rodents used in CVD research. Although both male and female sex hormones modulate cardiac function, we focus on the genomic effects of estrogen as the major mediator of sex differences. Finally, I present molecular and functional characteristics of animal models of CVD, emphasizing sex differences in their phenotypes.

1.1 Cardiovascular biology: cardiac myocytes

The heart is an extraordinary organ that must maintain functional output at all times during a person's life, not only during rest, but also in response to a variety of physiological and pathological conditions. In order to perform this daunting task, multiple biological signals are organized to tightly coordinate and synchronize every cycle of contraction to efficiently pump blood out of the four chambers of the heart to the rest of the body. While multiple cell types within the heart such as fibroblasts, endothelial cells and smooth muscle cells contribute to

maintaining function, the cardiac myocytes contain the fundamental contractile apparatus, known as the sarcomere, which is critical for each heartbeat. Sarcomeres are highly organized structures each containing a myosin thick filament, as well as a thin filament structure composed of actin, tropomyosin, and the troponin complex. Contraction is achieved upon transient sliding interactions between the thick and thin filaments of the sarcomere, a process that is highly regulated by calcium, which upon binding to troponin C, reveals tropomyosin-covered myosin binding sites on actin allowing for actin and myosin to interact (Harvey & Leinwand, 2011). Repeated units of sarcomeres are bundled within the heart to form functional myofilaments that synchronize to propagate action potentials throughout the cells and effectively produce each contraction.

Expression and activity of sodium, calcium, and potassium channels dramatically affect the contractility of the heart through modulation of components of the action potential (Figure 1.1); the sequence and duration of ionic movement in the cardiac myocyte dictates the strength and frequency of contraction. When a sufficiently depolarizing current reaches the cardiac myocyte, sodium channels open to rapidly depolarize the cell, which promotes opening of voltage-gated L-type calcium channels (Bodi, Mikala, Koch, Akhter, & Schwartz, 2005). Increased calcium concentrations in the cardiac myocyte prolong repolarization and refractory durations and promote contraction through the interaction between calcium and troponin. The plateau phase, during which contraction takes place, is achieved through continued slow inward movement of calcium through L-type calcium channels and flow of potassium out of the cell through slow delayed rectifier channels that begin repolarizing the membrane potential (Nattel, 2008). The cardiac myocyte returns to the resting membrane potential by removal of calcium from the sarcoplasm and continued flow of potassium out of the cell through potassium channels. Importantly, this plateau and slow repolarization produces a refractory period in which the cell cannot be depolarized, thus preventing tetanus (Schmitt, Grunnet, & Olesen, 2014).

Because cardiac myocytes contain many repeated sarcomeric units as well as large numbers of mitochondria to effectively produce enough energy for repeated contractions, these cells are large in size. However, while cardiac myocytes roughly make up around 80% of total cardiac mass, they are only estimated to make up 30-50% of the total cells within the heart (Banerjee, Fuseler, Price, Borg, & Baudino, 2007). In response to increases in metabolic demand, such as exercise or high blood pressure, the heart must increase in size to maintain a functional workload. Because cardiac myocytes are largely terminally differentiated cells, (Bergmann et al., 2009; F. Li, Wang, Capasso, & Gerdes, 1996) the myocytes respond to these stressors by increasing in size, rather than dividing, in order to preserve cardiac function. The regulation of this hypertrophic response involves the coordination of many different signaling pathways and is extremely important for maintaining the heart's ability to adapt to and remodel in response to increases in metabolic demand (Bernardo, Weeks, Pretorius, & McMullen, 2010).

1.2 Sexual dimorphisms in human and rodent cardiovascular physiology at baseline.

Although baseline characteristics of cardiac function in healthy men and women differ in terms of heart rate, left ventricular ejection fraction (LVEF) and stroke volume (SV), cardiac functional advantages in healthy men compared to women have been debated in the literature for many years (Salton et al., 2002; Sandstede et al., 2000). Higher LVEF and SV in men develop after adolescence, suggesting a role for sex hormones in the regulation of cardiac function (Cain et al., 2009; Marcus et al., 1999). The mechanisms mediating these differences in the healthy heart have not been fully elucidated. The need for experimental manipulation of potential modulators requires the use of animal models to study at molecular, cellular, and systemic levels, the complicated interactions among sex, cardiac myocytes, and the cardiovascular system. As in humans, sex differences in baseline cardiovascular function are observed in many experimental rodents. In light of the dramatic effects sex has on cardiovascular function in humans, the National Institutes of Health (NIH) has called for the

inclusion of both male and female animals in preclinical CVD research (*Consideration of Sex as a Biological Variable in NIH-funded Research*, 2015).

The question of whether cardiovascular function/dysfunction in animals translates to human cardiovascular physiology has been a challenge in research for nearly a century. Basic cellular and functional differences in some experimental models are similar to those of humans, making the use of animals to model human disease possible. For example, the development of the mouse heart remarkably recapitulates that of the human heart (Krishnan et al., 2014). Notably, the role of sex hormones, particularly estrogen, in cardiovascular function is also similar in animals compared to humans (Leinwand, 2003; Luczak & Leinwand, 2009). Use of animal models has therefore allowed elucidation of specific effects of sex hormones on cardiac function that include direct and indirect modulation of contractility, ion channel expression and function, reactive oxygen species (ROS) production, and substrate utilization, among others (Murphy, 2011).

1.2.1 Cardiac contractility and ion channels.

Consistent with cardiac functional differences observed in humans, cardiac myocytes isolated from male rodents contract more strongly and rapidly than female cardiac myocytes, a difference that is reduced with age (Grandy & Howlett, 2006; Howlett, 2010; Parks & Howlett, 2013). Additionally, relaxation rates differ between the sexes. Although conflicting results have been reported, when differences are observed, it is the female cardiac myocyte that relaxes more slowly (Parks & Howlett, 2013). Sex differences in cardiac ion channel expression and function have been a focus of many studies and are implicated in the cellular basis for these differences in cardiac contractility. For example, the amplitude and frequency of calcium sparks produced by release of calcium from the SR is higher in male rat cardiac myocytes ((Farrell, Ross, & Howlett, 2010). Detailed electrophysiological measurements of action potentials in individual cardiac myocytes have revealed specific roles of many different types of ion channels

that may mediate differences in conduction and contraction in the hearts of men and women, as well as animal models of CVD. Additionally the cation currents, particularly those mediated by calcium and potassium channels, exhibit significant sexual dimorphisms. Female hearts, for example, exhibit a longer repolarization phase mediated by potassium channels than males (Figure 1.1), a characteristic that develops shortly after puberty and leaves women more prone to cardiac arrhythmias than men (Lehmann et al., 1997; Villareal, Woodruff, & Massumi, 2001). Interestingly, tissue samples from healthy hearts of female donors reveal lower levels of potassium channel gene expression than male donor hearts including the Kv1.4, Kv channel-interacting protein 2 (KChIP2), sulfonylurea receptor 2 (SUR2) and human ether-a-go-go (hERG) subunits that are responsible for cardiac myocyte repolarization;(Gaborit et al., 2010) lower levels of proteins that contribute to I_{Kr} and I_{Ks} prolongs the QT interval (X. K. Liu et al., 1998). In women, longer repolarization during normal sinus rhythm is likely attributable to a higher contribution of slow rectifying potassium channels, based on the morphology of the action potential (reviewed in (Nattel, 2008). Similar to humans, action potential duration in female rodents is longer than in males caused by a longer repolarization segment. However, mice and rats do not

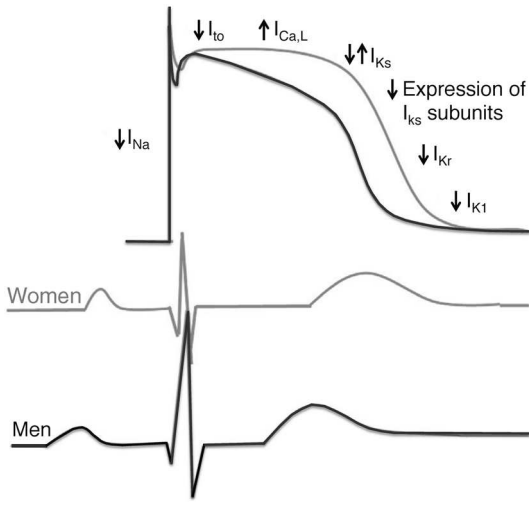

Figure 1.1 Action potential differences between sexes. Cardiac action potential waveform in men (dark gray) and women (light gray). $I_{Ca,L}$ indicates L-type slow inward calcium current; I_{kr},

rapid delayed potassium rectifier; I_{Ks}, slow delayed potassium rectifier; and I_{Na}, sodium.
Reprinted from (Zipes & Jalife) with permission of the publisher. Copyright ©2013, Elsevier.

exhibit a plateau phase and rapidly repolarize without the delayed rectifiers I_{Kr} and I_{Ks} observed in human hearts (Figure 1.2A,B) (D.M. Bers, 1991; Nerbonne, 2004).

Movement of calcium into the cell during depolarization of the cardiac myocyte activates release of calcium from the sarcoplasmic reticulum (SR) in both humans and rodents, thus producing higher intracellular calcium and initiating contraction. Although this process of electrochemical signaling through the heart is recognized as the process by which mammalian hearts contract, excitation-contraction coupling and the mechanisms that mediate it vary among species and between the sexes. Expression of several types of pumps and channels mediate movement of calcium including the sodium-calcium exchanger (NCX), SR calcium-ATPase, sarcolemmal calcium-ATPase, and a calcium uniporter expressed on the membranes of mitochondria. SR calcium-ATPase pumps are responsible for approximately 70% of calcium removal to produce relaxation in humans (D. M. Bers, 2002). By contrast, in rats and mice, more than 90% of calcium removal is mediated by the SR calcium-ATPase due to higher expression of the transporter (Hove-Madsen & Bers, 1993). Interestingly, in female rat hearts, diastolic concentrations of calcium inside the SR and the rate of reuptake after contraction is lower than in males, whereas in mice, sex differences are not observed (Parks & Howlett, 2013). Other studies in rats have revealed weaker and slower contractions in isolated female cardiac myocytes that could be explained by sex differences in calcium stored in the SR rather than differences in influx mediated by NCX or altered myofilament calcium sensitivity (Parks & Howlett, 2013). Despite evidence in rodents supporting a role for SR-mediating calcium flux as a mechanism responsible for differences in contractility, these studies have not been fully supported by human data.

Significant differences also arise between human and animal depolarizing currents mediated by calcium and sodium channels. In female dogs, for example, the density of

depolarizing calcium currents mediated by L-type calcium channels is higher than in males, consistent with a more rapid depolarizing current that causes more efficient excitation-contraction coupling in female hearts (Xiao, Zhang, Han, Wang, & Nattel, 2006).

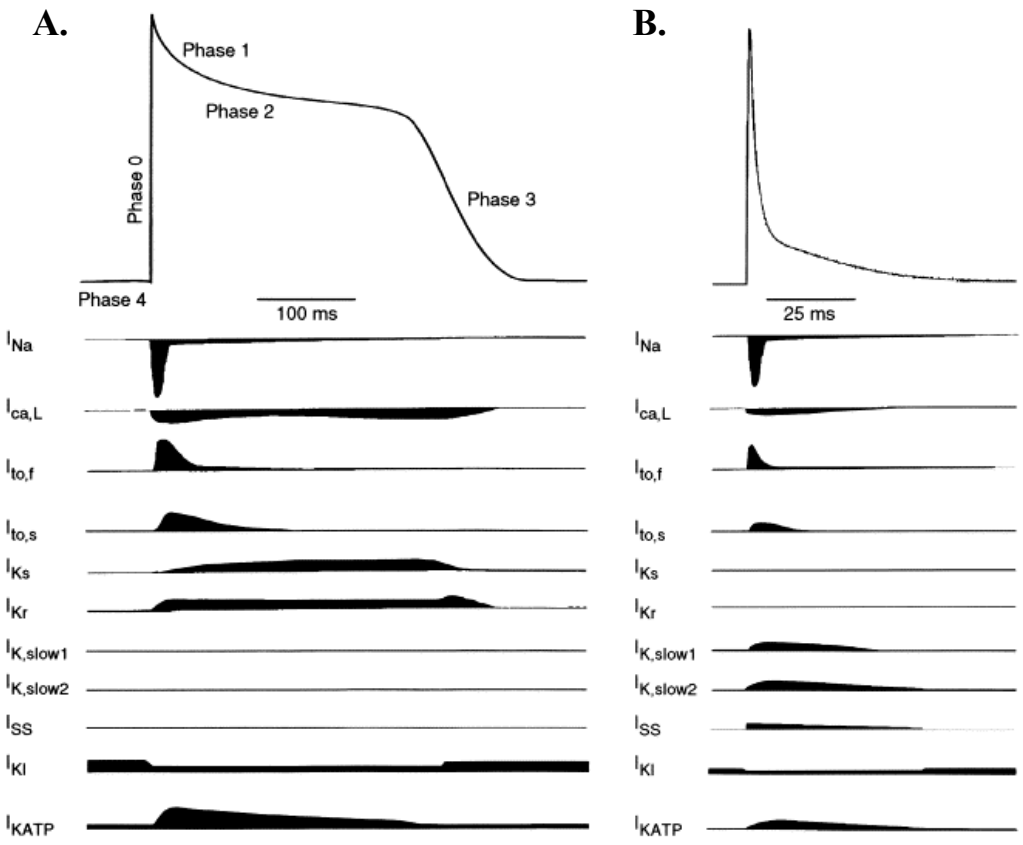

Figure 1.2: Action potential waveforms differ between human and mouse. Action potential waveform in adult human **(A)** and mouse ventricular cardiac myocytes **(B)**. Currents (I) contributing to each component of the action potential are shown below. ICaL indicates L-type slow inward calcium current; IKr, rapid delayed potassium rectifier; IKs, slow delayed potassium rectifier; INa, sodium current; Ito,f, fast transient outward potassium current; and Ito,s, slow transient outward potassium current. Reprinted from (Zipes & Jalife) with permission of the publisher. Copyright ©2003, Springer.

Indeed, estrogen-receptor deficient male mice also exhibit higher expression of L-type calcium channels (B. D. Johnson et al., 1997). Although Cav1.2, which mediates calcium entry into the cardiac myocyte and plays an important role in depolarization, is reduced by estrogen, the NCX, which is involved in repolarization is increased by estrogen; ovariectomy (OVX) reversed this expression pattern in females rats, which is significant in light of prolonged repolarization in women (Chu, Goldspink, Kowalski, Beck, & Schwertz, 2006). NCX mediates calcium influx and

maintains the action potential plateau (Eisner & Sipido, 2004). In rats, calcium concentrations in the cytosol are predominantly mediated by the sarcoplasmic reticulum rather than by NCX, as in humans (D.M. Bers, 1991). Currents mediated by L-type calcium channels are rapidly inhibited by exposure to estrogen or testosterone in rat and guinea pig cardiac myocytes (Bai, Kurokawa, Tamagawa, Nakaya, & Furukawa, 2005; Berger, Borchard, Hafner, Putz, & Weis, 1997; Nakajima et al., 1999). Opposing effects on ion currents by steroid hormones is emphasized by the decrease in potassium currents by estrogen and increase in potassium currents by testosterone could account for longer repolarization durations in the hearts of women (Bai et al., 2005; Berger et al., 1997; Nakajima et al., 1999). Despite striking differences between the action potential segment durations and heart rates, mechanisms mediating the ionic currents are conserved and sex differences observed in humans are also present in rodents. Thus, if one were interested in mechanisms mediating sex differences, rodent models are clinically relevant.

1.2.2 Molecular biology of the heart and the cardiac myocyte.

Sex differences in cardiac gene expression are present in both humans and rodents. In humans (< 40 years old) and mice (2 months old), expression of a similar number of cardiac genes is different between males and females, many of which are expressed on sex chromosomes, a mechanism requiring more study (Isensee et al., 2008; Praktiknjo et al., 2013). Cardiac genes expressed on autosomal chromosomes also differ between the sexes, and in mice, these differences appear to be independent of the estrous cycle (Isensee et al., 2008). Notably, several GeneOntology categories that are different between the sexes are similar when humans and mice are compared including genes mediating chemotaxis and inflammation. However, in humans, these categories were overrepresented in males, while in mice, these categories of enriched genes were primarily observed in the hearts of females (Isensee et al., 2008).

Sexual dimorphisms that are species-specific are also observed in expression of genes encoding contractile proteins. In the human heart, cardiac myosin expression is dominated by β-myosin heavy chain (βMyHC), with greater than 90% of total MyHC composed of βMyHC, and is higher in the atria and ventricles of healthy women compared to men (Miyata, Minobe, Bristow, & Leinwand, 2000; Reiser & Moravec, 2014). By contrast, in mice and rats, expression of αMyHC dominates the ventricles, while in the hearts of larger animal models with slower heart rates like dogs and rabbits, MyHC isoform distribution more closely resembles that of humans (D.M. Bers, 1991; Lompre et al., 1981). On average, the healthy murine heart is composed of more than 95% αMyHC (Rice et al., 2010). However, as in humans, rodent hearts exhibit sex differences in MyHC isoforms; female rat hearts, for example, express higher αMyHC and lower βMyHC compared to males (Schaible, Malhotra, Ciambrone, & Scheuer, 1984). In fact, the absence of estrogen in females reduces the levels of αMyHC,(Calovini, Haase, & Morano, 1995) again supporting a molecular advantage in premenopausal females. Conversely, removal of testosterone through gonadectomy in rats reduces expression of βMyHC (Scheuer, Malhotra, Schaible, & Capasso, 1987). αMyHC uses ATP more efficiently than βMyHC, and despite proportional differences in the isoforms between humans and rodents, increases in βMyHC are associated with reduced cardiac function in both (Scheuer et al., 1987). Expression of several other genes is higher in the hearts of female rats compared to males including skeletal actin, connexin 43, phospholamban, collagens, and transforming growth factor (TGF)-β (Gaborit et al., 2010; X. K. Liu et al., 1998; Rosenkranz-Weiss, Tomek, Mathew, & Eghbali, 1994). In fact, several of these genes have been shown to be regulated by the presence of estrogen (L. A. McKee et al., 2013; Patrizio et al., 2013). Despite dramatic differences in heart rate and ATP use, MyHC isoform ratios change in response to pathological stimuli in a manner similar to humans, therefore making smaller animals appropriate for use as CVD models.

1.2.3 Mitochondrial bioenergetics.

Alterations of cardiac bioenergetics are indicators of physiological or pathological responses to work load. Under normal conditions, the heart utilizes fatty acids as an energy substrate. However, when pathology is introduced, a switch in glucose utilization occurs, to an anaerobic process that allows ATP production even under conditions of low oxygen like ischemia (Czubryt, Espira, Lamoureux, & Abrenica, 2006). Interestingly, substrate utilization in the absence of increased workload differs between men and women. In a small study of men and women, cardiac utilization of glucose was significantly higher in males, suggesting that substrate preference may play a role in women being affected more negatively by ischemic disease like myocardial infarction (Peterson et al., 2007).

Baseline mitochondrial function in many female animal models is consistent with cardioprotection mediated by healthy cardiac metabolism. Older female rat hearts have higher oxidative phosphorylation (OXPHOS) capacity compared to age-matched males, whereas this capacity is nearly equal in younger rats of either sex (Vijay et al., 2015; Yan et al., 2004). Additionally, lower production of ROS is observed in young female rats, which is promoted by higher level of aldehyde dehydrogenase expression and activity and reduced production of ROS by α-ketoglutarate dehydrogenase, supporting observations in women, suggesting that the hearts of women suffer less oxidative damage over a lifetime (Colom, Oliver, Roca, & Garcia-Palmer, 2007; Lagranha, Deschamps, Aponte, Steenbergen, & Murphy, 2010). Young adult female Fischer 344 rat hearts also exhibit higher expression of nuclear genes with a role in β-oxidation of fatty acids compared to the hearts of young males, (Vijay et al., 2015) similar to humans where the hearts of premenopausal women favor fatty acid substrates over glucose compared to age-matched men. In fact, estrogen decreases the expression of glucose transporter type 4 via increased expression of nitric oxide synthase in both humans and rats, thereby forcing the utilization of fatty acids under normoxic conditions (Nuedling, Kahlert, Loebbert, Doevendans, et al., 1999; Peterson et al., 2007). Much remains to be learned about

how sex influences mitochondrial number and function in the heart; interactions among approximately 1,500 genes contribute to normal function (Schmidt, Pfanner, & Meisinger, 2010). At a basic level, however, rodents exhibit similar cardiac metabolic characteristics to humans.

1.3 Estrogen signaling in the cardiovascular system

1.3.1 Estrogen is implicated in mediating sexually dimorphic cardiac function.

In humans, it has long been thought that the female sex hormone estrogen and signaling through estrogen receptors (ERs) expressed in the vasculature and the heart are primarily responsible for the cardiac protection experienced by pre-menopausal women compared to age-matched men (Mendelsohn & Karas, 2005). Estradiol is synthesized through the aromatization of testosterone and interacts with two main receptors that are localized in the nucleus, cytoplasm, at the plasma membrane, and on mitochondria: ERα and ERβ. ERs are primarily localized in the nucleus where they bind to estrogen response elements (EREs) or to other transcription factors and regulate transcription of genes mediating cell growth, contractility, apoptosis, and energy substrate utilization (Gorski & Hansen, 1987; Murphy, 2011) (Figure 1.3). A third protein, G protein-coupled receptor (GPR30 or GPER), has been implicated in mediating rapid, non-genomic estrogen signaling independently of the canonical ERs (Han, Li, Yu, & White, 2013; Kang et al., 2010; Knowlton & Korzick, 2014). However, studies suggest that GPER plays a role in estrogen signaling by regulating the expression of an extranuclear ERα isoform (ERα36), not by GPER itself binding to estrogen (Kang et al., 2010). Due to multiple conflicting findings regarding GPER's ER status, I will focus on more classical estrogen signaling pathways mediated through either ERα or ERβ.

An abundance of studies in pre- and post-menopausal women including those receiving hormone replacement therapy (HRT) implicate estrogen in altering cardiovascular function. The Women's Health Initiative clinical trial suggested that HRT initiation in postmenopausal women is associated with increased CVD; the trial was halted early (at 5.2 years) due to concerns about

adverse events in the heart, pulmonary emboli, and in cancer. Additionally, results from the Heart and Estrogen/Progestin Replacement Study revealed that HRT in post-menopausal women with existing CVD did not improve, and again, a significant trend toward worse cardiac outcomes was apparent. However, most of these women had been post-menopausal for significant periods of time and with additional health conditions, complicating interpretation of the results (Hulley et al., 1998). Recently, a randomized study involving 727 women within three years of their last menses revealed that earlier hormone replacement improves some aspects of CVD risk, and participants receiving HRT did not differ in their rates of atherosclerosis progression (Harman et al., 2014). Other steroid hormones like progesterone and testosterone, that are expressed in both men and women and are also implicated in modulating cardiac function and disease phenotype, exhibit cyclic concentrations in serum, and decrease with age (Stumpf, 1990).

The attention given to HRT initiated interest in the potential therapeutic abilities of products that contain phytoestrogens, such as soy, that have the ability to initiate estrogenic signaling by binding ERα or ERβ (Bhupathy, Haines, & Leinwand, 2010). However, after several clinical trials with postmenopausal women, the cardiovascular benefits of soy supplementation remained controversial and the American Heart Association reversed its endorsement of soy products for this purpose (Bhupathy et al., 2010; Sacks et al., 2006). Additionally, phytoestrogens present in standard laboratory rodent chow, such as genistein, directly alter contractility and inhibit tyrosine kinase activation in cardiac myocytes, which should be considered when performing animal experiments (Haines, Harvey, et al., 2012a; Liew, Williams, Collins, & MacLeod, 2003; Thigpen et al., 1999).

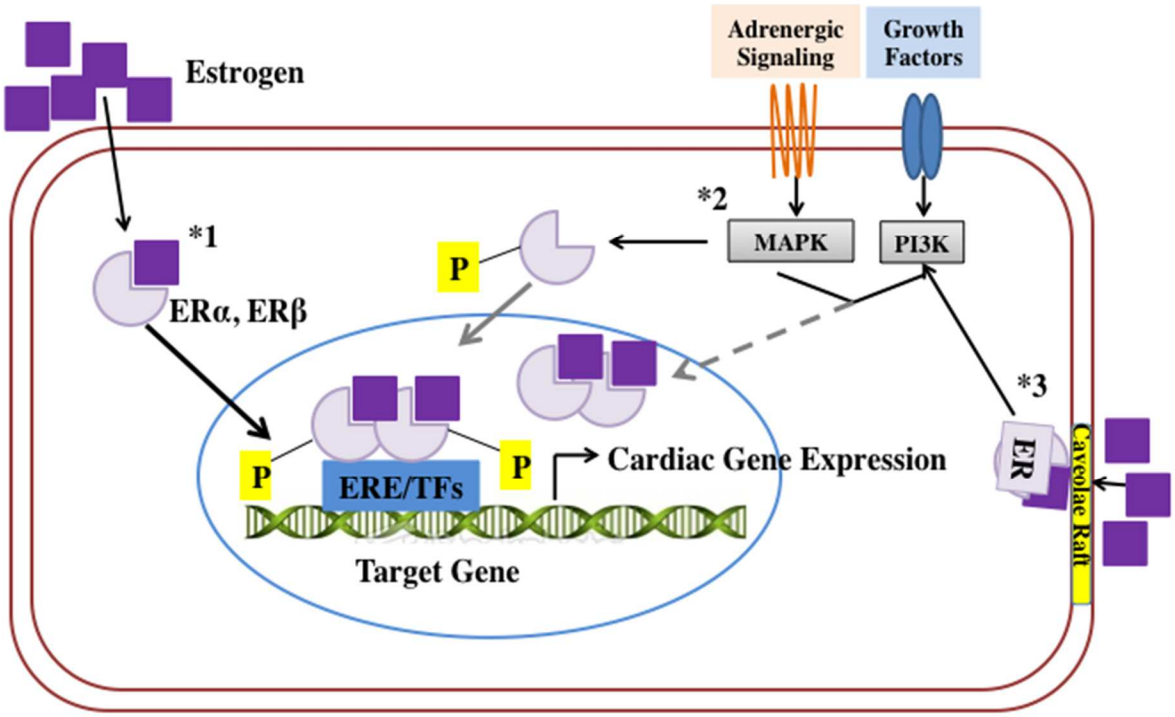

Figure 1.3: Estrogen signaling within the cardiac myocyte is involved in multiple regulatory pathways. ERα or ERβ utilize a variety of different mechanisms to elicit a biological response in cardiac myocytes, which include signaling as a transcription factor **(*1)**, in an estrogen independent fashion mediated by the activation of the MAPK and PI3K pathways by adrenergic and growth factor stimuli **(*2)** or by associating with the plasma membrane and initiating a rapid signaling response **(*3)**. ERE: Estrogen Response Element, TF: Transcription Factor, P: Phosphorylation

Clinical studies that identified sex differences in CVD where the findings are abrogated in postmenopausal women have motivated a large number of studies that manipulate levels of sex hormones, particularly estrogen, in experimental animals. Comparisons between women and female experimental animals are challenging due to significant differences in estrous cycle duration and serum estrogen levels. In mice, for example, the estrous cycle varies from 2-7 days, and decreased cycling is observed in older females (>13 months old) (Nelson, Felicio, Randall, Sims, & Finch, 1982). Female rodents do not go through a significant decline in estrogen that resembles human menopause, and there are no changes in estrogen levels between young C57Bl6 mice and older (14 month old), acyclic mice (Nelson, Felicio, Osterburg, & Finch, 1981). However, a major caveat to these studies is the notorious difficulty with which

low serum estrogen levels can be measured in rodents (McNamara et al., 2010). Removal of ovaries from mature female animals may reproduce systemic conditions in postmenopausal women. However, this strategy in mice leads to substantial weight gain beyond that which is observed in postmenopausal women. Additionally, the majority of women do not undergo menopause surgically, making ovariectomy animal models of limited use to effectively study perimenopause, which is experienced by most women and is characterized by a gradual change in ovarian hormones (Mayer, Dyer, Eastgard, Hoyer, & Banka, 2005). Therefore, these differences should be taken into consideration in studies that utilize systemic manipulations of sex hormone levels in animals to identify mechanisms of sex differences in CVD models.

1.4 Sexual dimorphisms in animal models of cardiovascular disease.

1.4.1 Hypertension.

More than 95% of hypertension cases are classified as essential hypertension without a single cause (Carretero & Oparil, 2000). Sex differences in blood pressure, like many cardiovascular features, originate during adolescence with persistently higher systolic and diastolic pressures observed in males (Boynton & Todd, 1947; Roberts & Maurer, 1977). Additionally, sex differences are also observed in pulmonary hypertension, which progressively leads to right heart failure with women being at greater risk than men (Mair, Johansen, Wright, Wallace, & MacLean, 2014). The review by Mair and colleagues (Mair et al., 2014) provides an in depth account for these differences as it is beyond the scope of this article to discuss pulmonary hypertension. The key organ for long-term control of blood pressure and body fluid volume is the kidney (Hall, Guyton, & Brands, 1995; Hall, Guyton, & Brands, 1996). According to the renal-body fluid feedback concept, chronic increases in arterial pressure occur as the result of abnormalities in the relationship between renal perfusion pressure and sodium excretion. That is, in order for long-term increases in arterial pressure to occur, a reduction in the kidneys' capacity to excrete sodium and water must be present. A common defect that has

been found in all forms of hypertension examined to date, including genetic and experimental animal models and human essential hypertension, is a rightward shift (toward increased blood pressure) in the chronic renal pressure-natriuresis relationship. The renin-angiotensin system (RAS) and other hormones including sex steroid hormones modulate baseline sexual dimorphisms in blood pressure (Jones & Hall, 2004; Weinberger, Miller, Luft, Grim, & Fineberg, 1986). In men, plasma renin activity is approximately 27% higher than in women, regardless of age, but renin activity increases in postmenopausal women, an effect that may be mediated by lower estrogen or influenced by increases in testosterone (Ushio-Fukai, Zafari, Fukui, Ishizaka, & Griendling, 1996). Additionally, dietary intake of salt can dramatically alter blood pressure, especially in African Americans. It is now recognized that blood pressure is salt-sensitive in up to 30-50% of hypertensive individuals (Weinberger et al., 1986). Interestingly, blood pressure in premenopausal women is relatively unaffected by sodium intake, but blood pressure becomes more salt-sensitive with the onset of menopause in many women (Pechere-Bertschi & Burnier, 2004). The precise mechanisms of sexual dimorphisms in hypertension have been extensively examined in several different rodent models that have revealed novel pathways for the development of hypertension (Table 1.1)

Spontaneously hypertensive rat model (SHR).

In 1963, a male rat with essential hypertension that was 25 mmHg higher than normal was identified and bred to produce a line of spontaneously hypertensive rats (Okamoto & Aoki, 1963). While this is a genetic model of hypertension, the underlying genetic variations responsible for disease development are extremely complex as quantitative trait locus mapping experiments have identified multiple genes that may be associated essential hypertension (Cowley, 2006; Hubner et al., 2005). As male and female SHR animals mature, both sexes exhibit increased systolic blood pressure; however, by 12 weeks of age this increase is significantly higher in the males compared to females, similar to humans (J. F. Reckelhoff, Zhang, H., Granger, J., 1998). This sexual dimorphism persists through adulthood; male SHR

are more hypertensive than females until after females stop estrus cycling (10 -12 months of age), when, by 16 months of age, blood pressure is higher in females than males (Chan, 2011). Male SHRs also develop signs of heart failure (HF) by 24 months, but female animals do not develop the ventricular stiffness or dilation that is observed in the males (Chan, 2011). Sexual dimorphisms are also observed at the level of the cardiac myocyte as SHR left ventricular myocyte diastolic and systolic sarcomere dynamics were reduced compared to normotensive controls; this observation was more pronounced in male SHR myocytes (Palmer, Chen, Lachapelle, Hendley, & LeWinter, 2006). The progress of disease and sexual dimorphisms are similar to those observed in men and women, making this model particularly useful (Doggrell, 1998).

Sex hormones appear to play an important role in mediating these observed sex differences. When young male and female SHRs were castrated or OVX to deplete endogenous sex hormones, castrated male SHRs exhibited reduced blood pressure similar to that of females (J. F. Reckelhoff, Zhang, H., Granger, J., 1998). In this study, OVX alone did not affect blood pressure. However, supplementing OVX females with testosterone increased blood pressure by 10 percent, suggesting that androgens may mediate the observed sex difference between SHRs, (J. F. Reckelhoff, Zhang, H., Granger, J., 1998) and that female sex hormones are not protective for hypertension in the female SHR (Brinson, Rafikova, & Sullivan, 2014; Jazbutyte et al., 2006). Interestingly, sex differences are also influenced by the RAS. When male and female SHR, both intact and gonadectomized, were treated with an angiotensin converting enzyme (ACE) inhibitor, sex differences were abrogated as reduced blood pressure was most significant in males and OVX females supplemented with testosterone after treatment (J. F. Z. Reckelhoff, H., Srivastava, K., 2000).

Table 1.1 Overview of sex differences in animal models of hypertension

Model	Age	Treatment	Reported in Males	Reported in Females	Molecules/ Pathways	References
SHR	12-20 weeks	NA	Higher systolic and mean arterial blood pressure		Testosterone; RAS signaling	(J. F. Reckelhoff, Zhang, H., Granger, J., 1998; J. F. Z. Reckelhoff, H., Srivastava, K., 2000)
SHR	9-12 weeks	NA	Isolated cardiac myocytes displayed reduced diastolic and systolic sarcomere dynamics		Not Addressed	(Palmer, Chen, Lachapelle, Hendley, & LeWinter, 2006)
SHR	3-30 months	NA	Progressed to failure by 15 months	Less hypertensive until 18 months; better mortality rates	Not Addressed	(Chan et al., 2011)
SHR	16 months	Losartan (30mg/ kg/day): 3 weeks	Displayed an enhanced depressor response after angiotensin receptor antagonism		RAS	(Yanes et al., 2006)
DSS	4-5 weeks	Low salt (0.3%) or high salt (8%) diet: 3 weeks	Higher blood pressure and increased mortality in response to high salt diet	Lower basal systolic blood pressure	Vasodilatory prostaglandins which were higher in females	(Bayorh et al., 2001)
DSS	17 weeks	Low salt (0.28%) or high salt (8%) diet: 4 weeks	Expressed higher levels of renal angiotensinogen mRNA and protein in response to high salt diet; this response was attenuated by castration		Testosterone	(Yanes et al., 2009)
DSS	14 weeks	Low salt (0.4%) or high salt (4%) diet: 2 weeks		OVX rats displayed increased blood pressure at baseline and in response to high salt diet	Estrogen potentially regulating NO	(Brinson, Rafikova, & Sullivan, 2014)
DSS	8-9 weeks	Varying salt diets: 0.15% (7days), 1% (14 days), 4% (14 days) 8% (14 days), 0.15% (14 days)	Salt dependent hypertension was greater	OVX rats developed hypertension similar to males, but their blood pressure did not normalize upon return to normal diet	Estrogen	(Laborde, Lange, & Haywood, 2000)
L-NAME treatment - rats	13-14 weeks	L-NAME (75mg/ 100mL drinking water): 5 weeks	Blood pressure in males was higher after treatment; this sex difference was abolished upon castration of males	OVX had no effect	Testosterone	(Sainz et al., 2004)
L-NAME treatment - rats	12 weeks	L-NAME (50mg/ 100mL drinking water): 4 weeks	No difference	No difference	NA	(Wu et al., 2001)
L-NAME treatment - rats	7 weeks	10 weeks L-NAME (20mg/ 100mL drinking water); withdrawal observed for 7 weeks		Developed more severe and rapid hypertension; took longer to respond to withdrawal of treatment	Not Addressed	(Y. R. Wang, Yen, Sun, & Laun, 2003)

The RAS also mediates hypertension in aged SHRs; treatment of 16 month male and female SHRs with the angiotensin receptor antagonist, losartan, decreased blood pressure in both sexes (Yanes et al., 2006). However, the decreases were greater in male SHRs, suggesting that RAS may be more important in aging male SHRs than females for maintaining blood pressure.

Dahl Salt-Sensitive (DSS) Rat Model.

Increases in dietary sodium can lead to dramatic increases in blood pressure. Men that have developed salt-sensitive hypertension are at greater risk of early death than women, even though women are more salt-sensitive than men in terms of blood pressure (Bursztyn & Ben-Dov, 2013). The DSS rat, a genetic model of hypertension induced by feeding the animals a high-sodium diet, demonstrates sex differences similar to those observed in men and women (Rapp & Dene, 1985). Prior to the addition of a high salt diet, female salt-sensitive rats have significantly lower basal systolic blood pressure compared to males (Bayorh et al., 2001). Female DSS rats have also been shown to display significantly lower systolic blood pressure than males after being fed a high salt diet for three weeks (Bayorh et al., 2001). In this same study, hypertension induced by four weeks of a high salt diet in both male and female DSS rats resulted in 50% mortality in males only (Bayorh et al., 2001; Bursztyn & Ben-Dov, 2013).

Unlike the SHR model, female sex hormones contribute to protection against hypertension, as OVX of female DSS rats increased basal blood pressure compared to intact females (Brinson et al., 2014). In addition, OVX female DSS rats fed a high salt diet developed hypertension in a manner that was not significantly different from males (Laborde, Lange, & Haywood, 2000). However, when dietary sodium was decreased to normal levels, blood pressure in the male and intact female DSS decreased, whereas in the OVX female DSS animals, it remained unchanged, suggesting that removing the female sex hormones predisposes the DSS female rats to develop hypertension, independent of sodium intake (Laborde et al., 2000). Testosterone also appears to have a role this process as castration of

male DSS rats fed a high salt diet attenuated the development of both hypertension and the increased expression of renal angiotensinogen (Yanes et al., 2009). In addition, castrated DSS male rats fed a high salt diet supplemented with testosterone had elevated blood pressure and increased renal injury (Yanes et al., 2009). Future studies are necessary to completely understand the role of male and female hormones during development of salt sensitive hypertension.

N^{ω}-nitro-L-arginine methyl ester (L-NAME) model of hypertension.

Nitric oxide (NO) exerts complex actions on the cardiovascular system through the regulation of vascular tone and renal function. In humans, inflammatory molecules cause NO synthase (NOS) II (inducible or iNOS) to produce NO, which has significant hypotensive effects. However, it is NOS III (endothelial or eNOS) that is most important in control of blood pressure. Indeed, treatment of rats with a non-selective NOS inhibitor, L-NAME, induces a NO-deficient animal model of hypertension (Glushkovskaya-Semyachkina, Anishchenko, Sindyakova, Leksina, & Berdnikova, 2006). Within five weeks of treatment, intact male rats developed a greater amount of hypertension compared to females (Sainz et al., 2004). In addition, castration of males attenuated the development of hypertension, whereas OVX of L-NAME-treated females did not affect blood pressure (Sainz et al., 2004). These results suggest that estrogen is not mediating the protective effect observed in females with L-NAME. While these results appear similar to other models of hypertension discussed earlier, there are contradictory reports regarding the sexually dimorphic response to L-NAME treatment. Other groups have observed that female animals actually develop more hypertension than males or report that there is no difference in blood pressure in response to NOS inhibition between the sexes (Y. R. Wang, Yen, Sun, & Laun, 2003; Y. Wu et al., 2001). These conflicting data could be due to the type of L-NAME treatment as each of these studies used a different dose and length of treatment to induce hypertension. Even with these discrepancies, sex differences with respect to hypertension development after L-NAME treatment are apparent in other rat models, such as

SHR animals and normotensive Sprague Dawley rats. While blood pressure in SHR males is greater than females at baseline, females exhibited a greater increase in blood pressure after L-NAME treatment, (Brinson et al., 2013) suggesting that female SHRs are more sensitive to NOS inhibition than males. However, these data are consistent with studies showing that estradiol increases NOS III and NOS I synthesis (Weiner et al., 1994).

The mechanisms responsible for hypertension are a multifactorial with a combination of genetic and environmental influences; therefore, no one animal model will completely mimic human disease development. While the SHR model is a commonly used animal model of essential hypertension, the DSS rat is a model of salt sensitive hypertension observed in humans. However, SHRs are not prone to strokes or vascular thrombosis (Pinto, Paul, & Ganten, 1998), and high salt diets cause significant renal injury and mortality within 4-6 weeks in DSS rats. Rats also do not develop signs of atherosclerosis. However, all of the discussed rodent models demonstrate increases in blood pressure in a relatively rapid and reproducible manner, providing reliable experimental systems for hypertension induced by independent mechanisms. Overall, these animal models mirror sex differences observed in humans with females developing less hypertension than males, aging confounding the hypertension in females, and estrogen signaling playing a critical role in mediating certain aspects of this protection.

1.4.2. Myocardial infarction (MI) and ischemic injury

Each year, over 600,000 Americans will experience a new MI event and nearly 40% of these cases will progress to HF (Jhund & McMurray, 2008). Sex differences with respect to MI and HF are observed, with women seemingly protected in that they develop the disease later in life compared to men (Lenzen et al., 2008; Mozaffarian et al., 2015). However, men and women often present different disease symptoms, and young women hospitalized for acute MI actually have worse outcomes than their male counterparts (Lenzen et al., 2008; Zhang et al., 2012).

Additionally, after menopause, the prognosis for women with MI is significantly worse than for age-matched men (Karlson, Herlitz, & Hartford, 1994). Cardiac remodeling in response to ischemic injury exhibits hallmarks of cardiac myocyte death, inflammatory cell infiltrations, and the development of fibrosis within the injured area in both men and women (Xie, Burchfield, & Hill, 2013). Remodeling also occurs in the surrounding healthy tissue including cardiac myocyte hypertrophy and altered ion channel expression that causes arrhythmias such that, in humans, the degree of remodeling negatively correlates with mortality (Qin et al., 1996). Additionally, trends of decreased sarcoplasmic reticulum calcium ATPase, phospholamban, and ryanodine receptors are observed, indicating reduced calcium transients and decreased contractility in human HF (Tomaselli & Marban, 1999). Similar to humans, animal models also display cardiac remodeling and sexually dimorphic characteristics with respect to ischemic injury development, severity, and response to reperfusion (Table 1.2).

Models of Myocardial injury induced by coronary artery ligation.

The complex nature of MI and HF has made developing a single animal model difficult. However, ligation of the left coronary artery in a variety of different rodent species recapitulates much of what is observed in human patients. Previous studies have utilized rodents to investigate sex differences observed both in the initial response to MI as well as the development of HF. For example, the rate of cardiac rupture and mortality within the first week after MI was greater in male mice compared to females, regardless of infarct size (Cavasin, Tao, Menon, & Yang, 2004; Cavasin et al., 2000; Q. Chen et al., 2010; Fang et al., 2007). In addition, immediately following MI, the hearts of male mice have increased neutrophil infiltration, damage to the interstitial collagen network, and matrix metalloproteinase (MMP) activity compared to their female counterparts (Cavasin et al., 2000; Fang et al., 2007). Furthermore, despite infarct size being equal at intermediate time points, during the chronic phase twelve weeks after MI, males displayed worse cardiac function, more cardiac myocyte hypertrophy, and increased ventricular dilation compared to females

Table 1.2 Sex differences in animal models of myocardial infarction

Model	Age	MI Stage/ Ischemia Protocol	Reported in Males	Reported in Females	Molecules/Pathways	References
Coronary Artery Ligation -C57BL/ 6J mice	12 weeks	Acute: 1,2,4,7 or 14 days after MI Chronic: 12 weeks after MI	Acute: Mortality was higher; Chronic: displayed worse cardiac function and more dilation		Not Addressed	(Cavasin, Tao, Menon, & Yang, 2004)
Coronary Artery Ligation-C57BL/ 6J mice	12-15 weeks	2, 3 or 60 days post MI	No difference in infarct size	Exhibited better survival and were less likely to progress to dilation	Greater induction of genes involved in angiogenesis, ECM remodeling and immune response observed in infarcted female hearts	(Q. Chen et al., 2010)
Coronary Artery Ligation -Sprague Dawley rats	12 weeks	1 & 6 weeks post MI	Greater increases in thickness of non-infarcted regions and restrictive diastolic filling patterns	No difference in infarct size	Not Addressed	(Litwin, Katz, Litwin, Morgan, & Douglas, 1999)
Coronary Artery Ligation -Sprague Dawley rats	10-12 weeks	4 weeks post MI	No difference in mortality rates	Females exhibited more pronounced LV dilation than males	Not Addressed	(Y. F. Chen et al., 2011)
I/R injury -129J & C57BL/6 mice	12-24 weeks	Ex vivo: 30 min perfusion, 20 minutes ischemia followed by 40 minutes reperfusion	Injury was greater in Iso or calcium treated hearts	No difference under basal conditions	NOS Signaling	(Cross, Murphy, & Steenbergen, 2002; Sun et al., 2006)
I/R injury -NCX Tg mice & non Tg littermates	32-36 weeks	Ex vivo: 30 min perfusion, 20 minutes ischemia followed by 40 minutes reperfusion	Post ischemic function was decreased in Tg males	No difference under basal conditions; Tg sex difference was abolished by OVX	Estrogen	(Cross, Lu, Steenbergen, Philipson, & Murphy, 1998)
I/R injury - Sprague Dawley rats	11-15 weeks	Ex vivo: 30 minutes occlusion followed by 150 reperfusion	Infarct sizes were larger; gonadectomy of both sexes produced opposite results.		Sex hormones, particularly androgens down-regulating apoptosis in response to MI	(Le et al., 2014)
I/R injury- Sprague Dawley rats	10 weeks	In vivo: 30 minutes of ischemia by clamping a coronary artery, 24 hrs reperfusion	Infarct area and percentage of apoptosis was greater		Differential regulation of apoptosis and autophagy pathways by an unknown mechanism	(C. Chen et al., 2013)
I/R injury - Sprague Dawley rats	not specified	Ex vivo: 15 minutes equilibration, 27 minutes ischemia followed by 40 minutes of reperfusion	Increased inflammatory response in response to injury	Post-ischemic cardiac function was significantly improved	Inflammatory signaling mediated by p-38 MAPK activation	(M. Wang, Baker, Tsai, Meldrum, & Meldrum, 2005)
Isolated cardiac myocytes -C57BL/ 6J mice	8-10 weeks	Cells treated with 100uM H_2O_2 for 30 minutes		Treated cells exhibited greater survival, decreased LDH release, apoptosis and necrosis	Akt and caspase signaling	(F. Wang, He, Sun, Dai, & Yang, 2010)

(Cavasin et al., 2004; Shioura, Geenen, & Goldspink, 2008). However, female mice were able to maintain contractile function over time, whereas males displayed progressive declines in contractile function associated with maladaptive cardiac remodeling (Shioura et al., 2008). The cardiac phenotypes of mice with experimentally-induced MI are consistent with humans with MI in that the hearts of women with MI exhibit lower rates of myocardial cell death and progress to HF more slowly than men (Guerra et al., 1999). Additionally, as in humans, alterations in potassium and calcium channel expression and currents that prolong the repolarization segment led to arrhythmogenicity in post-MI rats, and estrogen reduces post-MI arrhythmias associated with these ionic changes in mice (Korte et al., 2005; Qin et al., 1996).

Rats with experimental MI show variable and contrasting results compared to what has been reported in mice. In response to MI, male and female rats developed similar size infarcts and did not exhibit differences in contractile function six weeks after injury (Litwin, Katz, Litwin, Morgan, & Douglas, 1999). However, six weeks after MI, males displayed restriction of left ventricular filling, as well as greater increase in LV posterior wall thickness and myocyte diameter compared to female animals (Litwin et al., 1999). In contrast, Chen et al., demonstrated that four weeks after MI, female rats displayed more dilation than males (Y. F. Chen et al., 2011). Analysis of isolated cardiac myocytes from infarcted rat hearts also exhibited no differences in morphometrics in response to MI between sexes (Y. F. Chen et al., 2011). In a similar study that analyzed scar composition four weeks post-MI, males developed larger MI scars than females, but the overall structural composition of the scars was not different between sexes (Bogatyryov, Tomanek, & Dedkov, 2013). Aged male and female rats displayed similar patterns of overall LV remodeling, but differences were apparent in regional cardiomyocyte hypertrophy and arteriole expansion four weeks post-MI (Dedkov, Oak, Christensen, & Tomanek, 2014). Together, these studies demonstrate that sex differences do exist in rodents with experimental MI, but inconsistencies are observed between mice and rats.

The underlying causes of sex differences in MI and HF animal models have been examined at the transcriptome level. In a microarray study analyzing cardiac gene expression changes three days after MI, female mice displayed increased induction of genes involved in angiogenesis, immune response, and extracellular matrix remodeling compared to males (Q. Chen et al., 2010). In addition, female animals had a decreased amount of pathologic cardiac remodeling (Q. Chen et al., 2010). While this result may provide a general explanation for sex differences in cardiac remodeling observed after MI in men and women, the mechanism is undoubtedly multifactorial.

ER signaling appears to play a role in mediating post-MI responses. Female ERβ knockout (βERKO) mice experiencing chronic HF after MI exhibited increased mortality and altered expression of calcium handling proteins, suggesting that ERβ plays a critical role during HF (Pelzer et al., 2005). Additionally, estrogen treatment of OVX ERα knockout (αERKO) mice resulted in smaller infarcts (Babiker et al., 2007). This was not observed in wild-type controls, and the opposite was observed in βERKO animals, further implicating that ERβ is important for mediating estrogen's effects in the heart post-MI (Babiker et al., 2007). These results are complicated by the observation that estrogen treatment increased post-MI mortality in wild-type controls and αERKO animals, suggesting that estrogen signaling is not universally protective (Babiker et al., 2007). Other models, however, provide evidence of the cardioprotective effects of estrogen. For example, estrogen treatment of OVX rats 24 hours after MI resulted in increased expression of connexin 43, which allowed for critical cell-gap junctions to be maintained and reduced fatal ventricular arrhythmias (C. C. Chen, Lin, & Lee, 2010). OVX alone in wild type mice worsened LV function and dilation, suggesting a protective role for estrogen (Cavasin, Sankey, Yu, Menon, & Yang, 2003). In contrast, testosterone worsened cardiac function in both intact and OVX wild type females, and castration of wild type males decreased the amount of cardiac ruptures and improved cardiac function (Cavasin et al., 2003).

Histone deacetylases (HDACs) are key modulators of MI by regulating the activity of cardiac transcription factors, such as myocyte enhancer factor 2 (MEF2) (van Rooij et al., 2010). While HDACs have become therapeutic targets for cardiac hypertrophy, they appear to have sex specific effects, which should be considered. Female, but not male, HDAC 5 or 9 KO mice were protected against pathological cardiac remodeling after MI in an ERα dependent manner (van Rooij et al., 2010). Thus, active class II HDACs repress ERα expression and appear to promote pathological cardiac remodeling specifically in females. Increased ERα expression due to HDAC inhibition could protect females by regulating expression of genes such as vascular endothelial growth factor (VEGF), thus promoting angiogenesis (van Rooij et al., 2010). These data provide a novel explanation for how cardiac ERα expression is regulated post-MI, and give insight into the potential protective effects of HDAC inhibitors in humans, particularly women.

Ischemia/reperfusion (I/R) studies.

Animal models utilizing I/R provide valuable mechanistic information in terms of surgical reconstitution of blood flow to damaged cardiac tissue after MI in humans (Kalogeris, Baines, Krenz, & Korthuis, 2012). Under basal conditions, there was no difference in susceptibility to I/R injury or infarct size between male and female mice (Cross, Lu, Steenbergen, Philipson, & Murphy, 1998; Cross, Murphy, & Steenbergen, 2002; Sun et al., 2006). Despite this lack of difference at baseline, over-expression of NCX increased I/R injury in male but not female mice, suggesting that females are less prone to injury when calcium homeostasis is perturbed (Cross et al., 2002). Exposure to isoproterenol (Iso) or calcium pre-treatment supports this conclusion; I/R injury is increased to a greater extent in male mice compared to females (Cross et al., 2002). The hearts of male mice treated with Iso prior to I/R accumulate more intracellular sodium than do female hearts (Imahashi, London, Steenbergen, & Murphy, 2004). In contrast, several other studies report that under basal conditions female hearts displayed preserved contractile function, smaller infarct size, and fewer apoptotic cells compared to males after I/R (Brown et al., 2005; C. Chen et al., 2013; M. S. Johnson, Moore, & Brown, 2006; Le et al., 2014; M. Wang,

Baker, Tsai, Meldrum, & Meldrum, 2005). These differences are also apparent at the cellular level as intracellular sodium tended to be higher in isolated cardiac myocytes from male mice, and female cardiac myocytes survived at a higher rate than males when exposed to an oxidative stressor (Sugishita, Su, Li, Philipson, & Barry, 2001; F. Wang, He, Sun, Dai, & Yang, 2010). The variation in results of I/R injury between sexes could be due to differences in I/R experimental protocol as many of these studies used different lengths of time to induce an ischemic event.

Examination of the mechanisms mediating sexual dimorphisms in response to I/R also support a role for calcium homeostasis and involves differences in NO signaling, specifically S-nitrosylation between sexes (Murphy & Steenbergen, 2007). NO production was higher in the hearts of female mice at baseline, and female cardioprotection in I/R injury models after Iso exposure was lost upon treatment with the L-NAME (Cross et al., 2002). Furthermore, female hearts lacking NOS I or NOS III exhibited increased contractility and were also not protected from I/R injury (Sun et al., 2006). NO may be mediating this effect by altering intracellular sodium levels as L-NAME treatment of hypercontractile hearts blocked differences in intracellular sodium levels, which were higher in males (Imahashi et al., 2004). Non-specific NOS inhibition also increased calcium in female hypercontractile hearts to levels similar to males, a process that is regulated by the S-nitrosylation state of the L-type calcium channel (Sun et al., 2006). Thus, sex differences in I/R injury animal models may be attributable to increased intracellular calcium in male hearts.

Survival and apoptotic signaling pathways also play important roles in mediating sex differences during ischemic events. For example, cardiac myocytes isolated from female mice displayed higher levels of phosphorylated Akt both before and after oxidative stress (F. Wang et al., 2010). Caspase 3 activity was also lower in female rat cardiac myocytes treated with an oxidative stressor compared to males, possibly contributing to the greater survival observed in the female cells (F. Wang et al., 2010). Apoptotic signaling differences are also observed in the

whole heart. After I/R injury, levels of the anti-apoptotic protein, Bcl-2, were significantly lower, while levels of the pro-apoptotic protein, Bax, were unchanged in males, but not females (C. Chen et al., 2013). Furthermore, phospho-p38 levels that promote apoptosis were significantly increased in males after I/R whereas in the hearts of females, increased autophagy was observed (C. Chen et al., 2013).

In I/R injury studies, sex hormones promote opposing effects in terms of infarct size. OVX of female rats led to larger infarct sizes, but estrogen supplementation attenuated this response (Le et al., 2014). Testosterone, however, aggravated the response to I/R by down-regulating the anti-apoptotic protein Bcl-xL leading to the enhanced cardiac injury observed in males (Le et al., 2014). βERKO mice (but not αERKO mice) displayed less functional recovery if exposed briefly to Iso before I/R injury making them similar to what was observed in wild type males, suggesting that cardioprotection in females is mediated by ERβ signaling (Gabel et al., 2005). Furthermore, hearts of βERKO mice had altered expression of multiple metabolic genes compared to wild-type and αERKO females, which could explain functional differences in response to I/R injury (Gabel et al., 2005). The protective effects of estrogen are also observed in a cellular model of ischemia as estrogen treatment led to decreases in intracellular calcium and sodium during metabolic inhibition in male cardiac myocytes, abolishing observed sex differences (Sugishita et al., 2001).

The complexity of MI or I/R injury in mouse models discussed here parallels that of humans by producing more severe phenotypes in male mice, but this is less apparent in rats. Additionally, female mouse hearts display less cell death after injury and are less likely to progress to HF, which is in agreement with human studies (C. Chen et al., 2013; Guerra et al., 1999). The role of estrogen in mediating the observed protection in females continues to be unclear since estrogen supplementation has conflicting effects on MI outcome, which is also representative of reports in humans (Babiker et al., 2007; Hulley et al., 1998).

1.4.3 Cardiac Hypertrophy.

Pathological stimuli, such as hypertension, aortic stenosis, or cardiac injury, results in cardiac hypertrophy that may initially compensate for disrupted function; however, prolonged exposure to these pathological stressors leads to decreased cardiac function, increased fibrosis and an increased risk of HF (Rohini, Agrawal, Koyani, & Singh, 2010). The phenotypic appearance and development of cardiac hypertrophy are distinct between males and females (Table 1.3) and are modulated by hormones as well as rodent diets that contain high levels of phytoestrogenic compounds (Konhilas et al., 2004; Stauffer, Konhilas, Luczak, & Leinwand, 2006).

Pathological hypertrophy induced by pressure overload.

In humans with aortic valve stenosis or hypertension, left ventricular hypertrophy develops to maintain functional cardiac output and up to 50% of those patients will progress to HF (Himmelmann, 1999). Pressure overload is commonly studied in animal models by banding either the ascending or transverse aorta and is particularly useful since development of cardiac hypertrophy is gradual and progresses to HF (deAlmeida, van Oort, & Wehrens, 2010; Patten & Hall-Porter, 2009). As with other CVD animal models, sexual dimorphisms are apparent in pressure overload studies with males consistently developing more severe disease symptoms in a variety of experimental settings, consistent with studies in men and women (Figure 1.4) (Douglas et al., 1998; Fliegner et al., 2010; Kararigas, Fliegner, et al., 2014; Previlon, Pezet, Vinet, Mercadier, & Rouet-Benzineb, 2014; Skavdahl et al., 2005; Weinberg et al., 1999). In studies of both mice and rats, male hearts developed eccentric cardiac hypertrophy, while female hearts exhibited concentric hypertrophy, as observed in men and women with aortic stenosis (Carroll et al., 1992; Fliegner et al., 2010).

The hearts of males exposed to pathological stimuli were more likely to exhibit decreased contractility and increased fibrosis compared to their female counterparts (Douglas et

al., 1998; Fliegner et al., 2010; Karanigas, Fliegner, et al., 2014; Previlon et al., 2014; Skavdahl et al., 2005; Weinberg et al., 1999).

Table 1.3 Sexual dimorphisms in animal models of pathological hypertrophy

Model	Age	Hypertrophic Stimulus	Reported in Males	Reported in Females	Molecules/Pathways	References
Pressure overload -Wistar rats	3-4 weeks	Aortic banding: 6 & 20 weeks	By 20 weeks progressed to heart failure	Hypertrophic response is similar after 6 weeks	Not addressed	(Douglas et al., 1998)
Pressure overload -Wistar rats	Not specified	Aortic banding: 6 weeks	Exhibited increased expression of fetal genes	Extent of hypertrophy was similar between sexes	Not addressed	(Weinberg et al., 1999)
Pressure overload - C57BL/6J WT & ERβ KO mice	8 weeks	Aortic banding: 9 weeks	WT males developed more hypertrophy, fibrosis and heart failure; this difference was abolished upon ERβ KO		Estrogen signaling through ERβ regulating apoptosis and fibrosis	(Fliegner et al., 2010; Karanigas et al., 2014)
Pressure overload -B6D2/ F1 mice	5 weeks	Aortic banding: 4 weeks	Exhibited more fibrosis	Extent of hypertrophy was similar between sexes	CaMKII activation regulating MEF2 transcription	(Previlon, Pezet, Vinet, Mercadier, & Rouet-Benzineb, 2014)
Volume overload -Sprague Dawley rats	8 weeks	AV fistula: 8 weeks	Increased mortality and development of heart failure		Not addressed	(Gardner, Brower, & Janicki, 2002)
Volume overload -Sprague Dawley rats	6 weeks	AV shunt: 4 or 16 weeks	By 16 weeks, exhibited decreased cardiac function which progressed to heart failure	Maintained cardiac function by 16 weeks	Estrogen up regulating phospho-Bcl2 to attenuate apoptosis & β-adrenergic signaling in female hearts	(Dent, Tappia, & Dhalla, 2010a, 2010b, 2011)
Chemical - C57BL/6J mice	4 months	Isoproterenol treatment: 7 days		Developed less hypertrophy	Estrogen broadly regulating the activation of kinase signaling	(Haines, Harvey, & Leinwand, 2012)
Chemical - Sprague Dawley rats	Weight matched (270-290g)	Acute Isoproterenol treatment (1uM) of isolated myocytes	In response to Iso, cells displayed greater cell shortening, calcium current density and cAMP production.		β-adrenergic signaling differences between sexes	(Vizgirda, Wahler, Sondgeroth, Ziolo, & Schwertz, 2002)
Genetic HCM - mice	4 & 10 months	R403Q mutation in alpha MYHC	By 10 months, developed cardiac dilation and dysfunction,	Developed hypertrophy by 4 weeks, maintained function by 10 weeks	Not addressed	(Olsson, Palmer, Leinwand, & Moore, 2001)
Genetic HCM - mice	12 weeks	Truncated cTnT or missense R92Q mutation in cTnT	In both mouse models, treatment with Iso or PE resulted in sudden cardiac death in all males	At baseline, R92Q hearts were larger, exhibited decreased hypertrophic gene expression and fibrosis.	Not addressed	(Maass, Ikeda, Oberdorf-Maass, Maier, & Leinwand, 2004)
Genetic HCM - mice	13 weeks	Knock-in model with a heterozygous point mutation in MYBPC3	Isolated cardiac myocytes and myofilaments displayed reduced maximal force generating capacity		Not addressed	(Najafi et al., 2015)

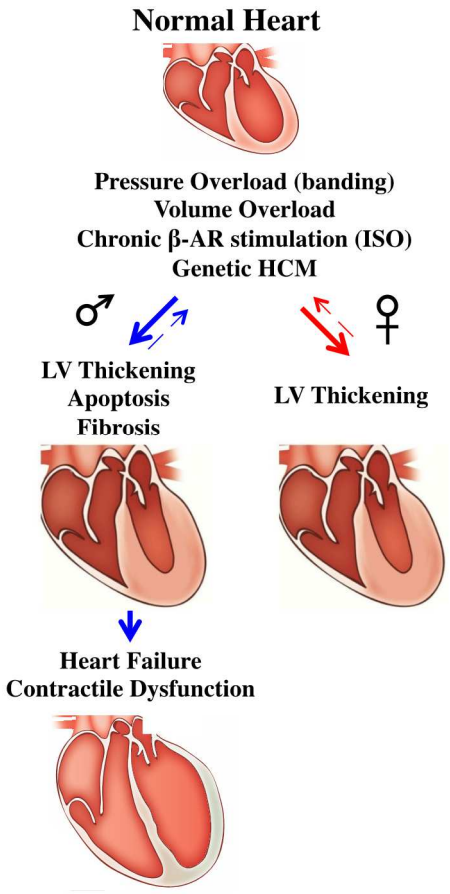

Figure 1.4 Male and female rodent hearts adapt differently to pathological stimuli. Although left ventricles of both sexes increase in size to response to increases in metabolic demand, male hearts are more likely to develop fibrosis, apoptosis, and progress to heart failure. HCM indicates hypertrophic cardiomyopathy; LV, left ventricle; and ISO, isoproterenol. Reprinted with permission, Heart image copyright ©2016 Abcam.

While female hearts hypertrophied after aortic constriction, sometimes even to a similar degree as the males, cardiac function was preserved over time, and cardiac expression of fetal genes, such as atrial naturietic peptide, β-MyHC, and MMP, was lower compared to males (Douglas et al., 1998; Weinberg et al., 1999). In addition, the proteomic response of the heart to pressure overload was very different between the sexes, with increased expression of cytoskeletal proteins in females whereas mitochondrial proteins were more prominently regulated in males,

suggesting that male and female animals utilize different mechanisms to respond to the same pathological stimulus (Kararigas, Fliegner, et al., 2014).

Consistent with clinical studies that demonstrate postmenopausal loss of cardioprotection in women, estradiol supplementation of OVX rats ameliorated cardiac dysfunction as well as hypertrophic development induced by transaortic constriction, suggesting that estrogen provides a cardioprotective role in female animals (Patten et al., 2008). Furthermore, in female mice lacking either ERα or ERβ, the hearts of βERKO mice displayed a more pronounced response to aortic banding, whereas αERKO mice were indistinguishable from wild type mice, suggesting that signaling through ERβ may be mediating the protection observed in normal females (Babiker et al., 2006; Skavdahl et al., 2005). Female βERKO mice also exhibited increased fibrosis relative to wild-type controls in response to pressure overload, and ERβ appears to mediate this effect by regulating the expression of repressors of the MAPK-ERK1/2 pathway (Fliegner et al., 2010; Queiros et al., 2013). The cardiac proteomic response to pressure overload was also dramatically different between βERKO and wild-type animals of both sexes, suggesting that ERβ also plays a role in the male heart (Kararigas, Fliegner, et al., 2014). However, ERβ gene expression was not detectable in adult cardiac myocytes from male mice or rats of either sex, suggesting this ERβ signaling is mediated in cardiac fibroblasts, endothelial, or vascular cells (O'Meara et al., 2015; Pugach, Blenck, Dragavon, Langer, & Leinwand, 2016).

Evidence exists for other signaling pathways involved in mediating sex differences observed in response to pressure overload. The calcium-calmodulin-dependent kinase-MEF2 (CaMKII-MEF2) pathway may be important as CaMK-phosphatase compartmentalization differed between sexes after pressure overload, leading to differences in MEF2 activation, which can promote cardiac hypertrophy (Previlon et al., 2014). In addition, cardiac expression of a dominant-negative form of p38α MAPK resulted in severe hypertrophy and mortality in female, but not male mice after pressure overload (J. Liu et al., 2006). However, OVX abolished the

increased hypertrophic responses observed in transgenic females (J. Liu et al., 2006). Additionally, male rats exhibited increases in NOS1 expression, a factor that has consistently been up-regulated in HF, after aortic banding much earlier than females; once again demonstrating the importance of NO in mediating cardiac sexual dimorphisms (Loyer et al., 2007). Complex signaling mechanisms mediate sexual dimorphisms associated with pressure overload hypertrophy, and further studies are required to elucidate interactions among those implicated.

Pathological hypertrophy induced by volume overload.

Anatomical defects that cause conditions such as mitral or aortic valve regurgitation result in increased ventricular blood volume and cause the thickness of ventricular walls to increase to maintain cardiac function (Lorell & Carabello, 2000). Similar to pressure overload, the consequences of volume overload were less severe in females; males exhibited decreased contractile function, increased mortality rates, and were more likely to progress to HF (Dent, Tappia, & Dhalla, 2010b; Gardner, Brower, & Janicki, 2002). Males also displayed higher levels of plasma catecholamines, and increased cardiac expression of angiotensin II (Ang II) type 1 receptor as well as pro-apoptotic proteins such as BAX, caspase 3 and 9 (Dent, Tappia, & Dhalla, 2010a; Dent et al., 2010b). This sex-specific alteration in apoptotic signaling in animals agrees with increased fibrotic gene expression observed in cardiac biopsies from men, but not women experiencing LV hypertrophy due to aortic stenosis (Petrov et al., 2010).

As in pressure overload, estrogen protects from development of pathological hypertrophy induced by volume overload. OVX of female rats resulted in more pronounced hypertrophy that progressed to ventricular dilation (Gardner et al., 2002). Interestingly, supplementation of OVX rats with 17β-estradiol did not fully attenuate the development of hypertrophy, suggesting that other ovarian hormones may be mediating protection (Dent et al., 2010b). However, this contradicts studies that demonstrated rescue of cardiac function with estrogen administration in similar volume overload models (Dent et al., 2010a; Dent, Tappia, &

Dhalla, 2011). Additionally, estrogen regulates apoptosis during this hypertrophic response as OVX rats exhibited increased cardiac pro-apoptotic signaling similar to levels observed in males, but this response was abrogated with estrogen supplementation (Dent et al., 2010a). Estrogen also regulates fibrosis in a sexually dimorphic manner in that collagen gene expression increased upon estrogen treatment in male, but decreased in female adult rat cardiac fibroblasts, which is consistent with sex differences observed clinically (Petrov et al., 2010).

Estrogen may also be regulating other signaling pathways in response to volume overload. Male but not female rats displayed decreased cardiac expression of β-adrenergic receptors (β-ARs) and adenylyl cyclase in response to arteriovenous shunt (Dent et al., 2011). However, OVX females also exhibited decreases in β-AR and adenylyl cyclase expression in response to volume overload, and estrogen supplementation brought these values back to levels observed in intact females, suggesting that estrogen may maintain cardiac function in response to volume overload stress by up regulating the β-AR signaling pathway (Dent et al., 2011).

Chemical induction of cardiac hypertrophy.

Chemical agonism of cardiac pathways, such as the β-adrenergic and Ang II pathways, also promotes pathological cardiac hypertrophy. After one week of Isoproterenol (Iso) treatment, male mice developed greater cardiac hypertrophy than females and also displayed altered contractile function (Haines, Harvey, & Leinwand, 2012). Sex differences are also apparent at the cellular level as Iso treatment increased SR calcium levels in male but not female cardiac myocytes (J. Chen et al., 2003). Additionally, Iso treatment elicited a greater increase in cAMP production, cell shortening, and intracellular calcium transients in male cardiac myocytes (Curl, Wendt, & Kotsanas, 2000; Vizgirda, Wahler, Sondgeroth, Ziolo, & Schwertz, 2002). However, at higher Iso concentrations, male but not female cardiac myocytes exhibited signs of calcium overload (Curl et al., 2000). Ang II promoted a different sex-specific response; cardiac myocytes

isolated from aged female mice overexpressing Ang II were more prone to contractile dysfunction than their male counterparts (Mellor et al., 2014). However, these female cells also exhibited stable SR calcium stores, whereas the male cells displayed increased spontaneous contractility, once again suggesting female myocytes are protected from calcium overload by unknown mechanisms (Mellor et al., 2014).

Acute estrogen treatment of isolated male cardiac myocytes also treated with Iso inhibited cAMP production and increased peak calcium (H. Y. Li, Bian, Kwan, & Wong, 2000). Similarly, myocytes isolated from the hearts of OVX rats treated with Iso exhibited increased calcium transients, force of contraction, and PKA activity compared to sham controls, but estrogen supplementation restored these parameters to sham levels (Kam, Kravtsov, Liu, & Wong, 2005). Myocytes from OVX rats displayed altered expression of β-ARs compared to sham controls, which could explain functional differences in response to Iso (Q. Wu et al., 2008). Estrogen appears to protect from Ang II-induced hypertrophy as OVX mice supplemented with estrogen during Ang II treatment developed less hypertrophy and fibrosis than the vehicle treated animals (Pedram et al., 2008). This response appears to be mediated by ERβ signaling because OVX βERKO animals supplemented with estrogen were no longer protected from developing hypertrophy or fibrosis, as was observed in αERKO or wild type OVX animals (Pedram et al., 2008).

Genetic hypertrophic cardiomyopathy animal models.

Hypertrophic cardiomyopathy (HCM) is a well-characterized autosomal dominant genetic disease, which affects about 1 in 500 individuals. Disease-causing mutations have been found in at least 11 different genes that are important for maintaining contractile function, such as components of the sarcomere and calcium handling genes. A variety of different mouse models have been created that harbor disease-causing mutations reported in humans (A. Maass & Leinwand, 2000). One of the most commonly used mouse models has a missense mutation (R403Q) in α-myosin heavy chain (α-MyHC,) which when present in the β-MyHC human gene

produces a severe form of HCM (Olsson, Palmer, Leinwand, & Moore, 2001). These mice develop HCM similar to human patients in a manner that is modulated by sex over time (Olsson et al., 2001). While males and females both developed cardiac hypertrophy to a similar extent at four months of age, only the males displayed LV dilation and systolic dysfunction at ten months (Olsson et al., 2001). In young HCM mice, the R403Q α-MyHC mutation enhanced LV myofilament performance, but myofilament function was not different between sexes (Palmer et al., 2008). However, in a more recent study analyzing older mice with established HCM, 10-month-old female HCM mice had larger hearts, and their trabeculae were more sensitive to calcium than their male counterparts (L. A. McKee et al., 2013). This difference in calcium sensitivity could be due to higher expression of sarco/endoplastic reticulum calcium transport ATPase (SERCA2A) in female HCM hearts, or the reduced phosphorylation of cardiac troponin T observed in the male HCM hearts (L. A. McKee et al., 2013). Furthermore, the signaling pathways activated in this HCM model appear to be different between sexes as HCM males also expressing a constitutively activated glycogen synthase kinase 3β exhibited contractile dysfunction, decreased SERCA2A expression, and premature death, but this was not observed in their female counterparts (Luckey et al., 2007). Interestingly, removal of phytoestrogens from rodent chow abrogated the severe dilated cardiomyopathy observed in HCM males (Stauffer et al., 2006). However, female HCM mice did not progress to HF on either phytoestrogen-free or soy-based diets (Stauffer et al., 2006). The predominant phytoestrogen in soy, genistein, activates apoptotic pathways in the male HCM heart contributing to the development of cardiac dysfunction (Haines, Harvey, et al., 2012a). Additionally, estrogen treatment was not protective in either male or female HCM animals and actually increased mortality in phytoestrogen-fed male HCM animals (Haines, Harvey, et al., 2012a).

Mice harboring a truncated cardiac troponin T (cTnT) protein displayed smaller ventricles and contractile dysfunction, but not fibrosis, whereas transgenic mice with a missense mutation (R92Q) in the cTnT gene exhibited severe fibrosis and induction of hypertrophic markers (A. H.

Maass, Ikeda, Oberdorf-Maass, Maier, & Leinwand, 2004). In addition, while no significant differences at baseline were observed in the truncated cTnT animals from either sex, the male R92Q animals displayed smaller heart weights, increased expression of hypertrophic markers, as well as increased fibrosis compared to their female counterparts (A. H. Maass et al., 2004). Both of these cTnT models displayed sex differences with respect to exposure to adrenergic stimuli. Treatment with either Iso or phenylephrine (PE) resulted in sudden cardiac death of all male, but not female HCM animals (A. H. Maass et al., 2004). Unlike the R403Q α-MHC model, estrogen appears to be cardioprotective in the R92Q cTnT female animals. OVX further decreased contractile function as well as myocardial energy metabolism, but estrogen supplementation restored these parameters and reduced cardiac oxidative stress (Y. Chen et al., 2015). In another model of HCM, in which mice carry a point mutation in myosin-binding protein C, isolated cardiomyocytes and myofilaments from male animals exhibited reduced maximal force generating capacity compared to females (Najafi et al., 2015).

While the mechanisms for the observed sex differences in genetic HCM models are not well understood, they should be taken into account when choosing a genetic model of the disease. Directly extrapolating results from genetic HCM animal studies to humans should also be done carefully due to the phenotypic diversity of HCM patients, which is not as apparent in the animal models (Arad, Seidman, & Seidman, 2002). Whether this limitation of HCM animal models is due to unknown modifiers of the human disease or a result of the difference in MyHC isoform predominance between mice and humans, caution should used when relating results to the human population. Additionally, it is not quite clear how the observed sex differences in animal HCM models relate to humans since understanding the effect of sex on the development and mortality associated with HCM is complicated by women being diagnosed later in life due to multiple environmental factors, such as clinical screening biases (Kubo et al., 2010).

1.5 Summary & Questions addressed in this study

Over the past 20 years, awareness of heart disease in women has dramatically increased, but gaps remain in knowledge among women about their cardiovascular risk. Increasing our knowledge of sex differences in basic cardiac physiology is critical for effectively treating patients of both sexes suffering with CVD. Human and animal studies have demonstrated that cardiovascular sexual dimorphisms exist in normal and diseased states from the level of cardiac myocyte to the whole heart. Despite several differences in cardiac physiology compared to humans, small rodent models have been extremely useful for better understanding the mechanisms responsible for mediating these observed sex differences. At baseline, differences in excitation-contraction coupling and mitochondrial function are apparent between the sexes, providing evidence that mechanisms involved in maintaining cardiac function are in place prior to the onset of any disease. Estrogen is believed to mediate this protection both prior to and after disease onset, but the exact mechanism is still not well understood and appears to be context dependent since estrogen supplementation can also be detrimental in some cases. As observed in humans, female animals are generally protected from developing multiple CVDs in genetic, surgical, and chemically-induced models. In many disease states, such as cardiac hypertrophy or hypertension, this protection in females or increased risk in males is lost upon the depletion of endogenous sex hormones. To appropriately investigate the mechanisms underlying CVD development, biological sex is an important experimental variable that needs to be addressed both in basic and clinical research studies. Although this introduction cited many different studies that focused on cardiac sex differences, most studies have not taken sex into account. More research needs to include animals of both sexes; not only to better understand the responsible signaling mechanisms, but to also ensure that therapeutics will work effectively in both men and women. With the new guidelines recently released by the National Institutes of Health that require biological sex to be included as a potential experimental variable in vertebrate animal and human studies, more

insight into mechanistic studies of the sexual dimorphisms observed in the cardiovascular system may be gained.

In this thesis I will present data that characterizes the baseline sexual dimorphisms that exist from the level of the whole heart function, down to the cardiac myocyte transcriptome. I will also discuss data that investigates the role of ER signaling in both neonatal and adult cardiac myocytes. In Chapter 2, due to a successful collaboration with Dr. Emily Pugach, I present experiments in which we analyzed the expression, localization and signaling characteristics of the estrogen receptor, ERα, in cardiac myocytes (Pugach et al., 2016). In the ER experiments in Chapter 2, I also investigated if sexual dimorphisms exist in the cardiac myocyte expression pattern or localization of ERα, but did not observe any differences between the sexes. This led me to investigate other potential mechanisms mediating the functional differences I observed in the whole heart, myofibrils and cardiac myocytes that I discuss in Chapter 3. I therefore characterized cardiac myocyte gene expression differences between the sexes and identified sexually dimorphic enriched pathways, such as the PKA pathway, that could be mediating the differences in contractility observed at baseline. Overall these studies provide insight to the sex differences in cardiac function, gene expression and signaling pathways that exist during baseline conditions, which is essential for better understanding the disparity in cardiovascular disease development between the sexes.

Chapter 2 Estrogen receptor profiling and activity in cardiac myocytes

As published in: Pugach, E.K.*, Blenck, C.L.*, Dragavon, J.M., Langer, S.J., Leinwand, L.A., Estrogen receptor profiling and activity in cardiac myocytes, Molecular and Cellular Endocrinology (2016), doi: 10.1016/j.mce.2016.05.004. (* These authors contributed equally). The work in this chapter was performed in collaboration with Dr. Emily Pugach. All figures are given the appropriate attribution when necessary.

Abstract

Estrogen signaling appears critical in the heart. However a mechanistic understanding of the role of estrogen in the cardiac myocyte is lacking. Moreover, there are multiple cell types in the heart and multiple estrogen receptor (ER) isoforms. Therefore, we studied expression, localization, transcriptional and signaling activity of ERs in isolated cardiac myocytes. We found only *ERα* RNA (but no *ERβ* RNA) in cardiac myocytes using two independent methods. The vast majority of full-length *ERα* protein (ERα66) localizes to cardiac myocyte nuclei where it is competent to activate transcription. Alternate isoforms of *ERα* encoded by the same genomic locus (ERα46 and ERα36) have differential transcriptional activity in cardiac myocytes but also primarily localize to nuclei. In contrast to other reports, no *ERα* isoform is competent to activate MAPK or PI3K signaling in cardiac myocytes. Together these data support a role for *ERα* at the level of transcription in cardiac myocytes.

2.1 Introduction

Sex hormone status correlates strongly with cardiovascular health in men and women (P. A. McKee, Castelli, McNamara, & Kannel, 1971; Mozaffarian et al., 2015). This observation, in conjunction with numerous experimental animal models, suggests sex hormones (like estrogen (E2)), and their receptors may be important regulators of cardiac health and disease (Pare et al., 2002; Skavdahl et al., 2005). Decades of research have demonstrated the importance and

complexity of estrogen's actions through its two receptors; particularly in breast cancer cells. It has been demonstrated that both estrogen receptors, ERα and ERβ, can signal in a variety of ways. The classical, genomic mechanism of estrogen signaling involves ligand-dependent DNA or transcription factor binding and subsequent regulation of transcription (Yamamoto, 1985). Palindromic hormone response elements in DNA called estrogen response elements (EREs, AGGTCAnnnTGACCT) provide an optimal recognition sequence for liganded ER dimer and heterodimer binding (Berg, 1989), although transcription regulation can also occur through interaction of ER's with other transcription factors or ER recognition of variants of the consensus ERE sequence (Batistuzzo de Medeiros, Krey, Hihi, & Wahli, 1997; Galien & Garcia, 1997).

Nongenomic mechanisms of estrogenic action have been more recently described (reviewed in (Farach-Carson & Davis, 2003)). These estrogen-initiated signaling events occur on the order of seconds to minutes and are considered much too rapid to be attributable to traditional genomic signaling mechanisms. Thus, E2-ER action can occur through at least two distinct mechanisms. Whether both mechanisms of estrogen signal transduction occur in cardiac myocytes remains understudied.

While reports using overexpression of *ERs* or *ER* knockout mice (KO) suggest these receptors have important and distinct cardiac roles, these studies are confounded by the systemic effects of global ER deletion, as ERαKO mice have increased levels of circulating estrogen, are obese, and have metabolic syndrome and ERβKO mice exhibit hypoxia and high blood pressure (Babiker et al., 2006; Bryzgalova et al., 2006; Kararigas, Nguyen, & Jarry, 2014; Morani et al., 2006; Pedram, Razandi, O'Mahony, Lubahn, & Levin, 2010; Rissman, Wersinger, Taylor, & Lubahn, 1997) (Figure 2.1). These studies highlight the need for additional studies to better understand ER-E2 signaling within specific cell types in the heart. Because experiments described here demonstrate that *ERβ* mRNA is undetectable in cardiac myocytes (see Figure 2.3), we focused on understanding the signaling mechanisms of *ERα* in cardiac myocytes.

Similar to other nuclear hormone receptor genes, the human *ERα* locus is complex and

undergoes alternative splicing and promoter usage with the isoform encoding a 66 kDa protein (ERα66) considered full length (Flouriot, Griffin, Kenealy, Sonntag-Buck, & Gannon, 1998; Kastner et al., 1990). Several *ERα* isoforms have been reported (Figure 2.2).

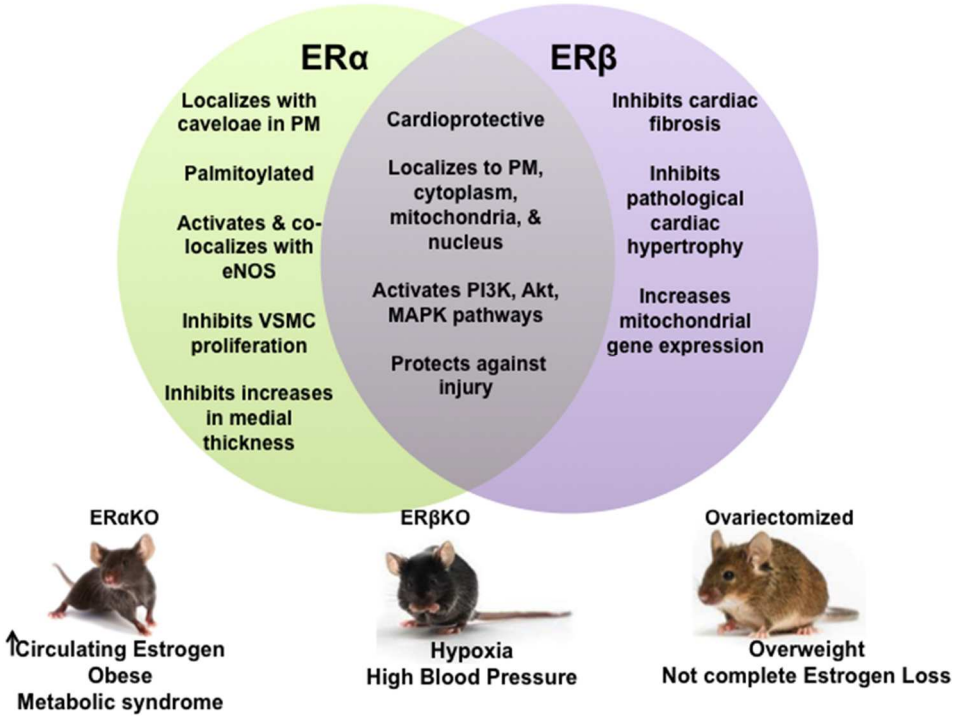

Figure 2.1: Overview of the cardiac functions attributed to ERα and ERβ. Both estrogen receptors have been described to have multiple overlapping and distinct functions within the cardiovascular system. However, many of the experiments describing the roles utilized ERα or ERβ knockout (KO) or ovariectomized animal models, which have systemic phenotypes that could influence cardiac function. PM: Plasma Membrane, eNOS: endothelial Nitric Oxide Synthase

A 46 kDa N-terminal truncation of full length *ERα* was first identified in human MCF7 breast cancer cells (Flouriot et al., 2000). *ERα46* is transcribed from an alternative promoter and lacks the AF-1 transactivation domain of full length *ERα66* but is otherwise identical. *ERα46* expression has been observed in endothelial cells, ovary, lung and kidney (Flouriot et al., 2000; L. Li, Haynes, & Bender, 2003). Interestingly, a 46 kDa band was also identified in the membrane fraction of adult cardiac myocyte lysates using an ERα antibody (Ropero et al., 2006), suggesting a potential role for this ERα variant in cardiac myocytes.

Microscopic and biochemical analyses have localized the *ERα46* splice variant to

the plasma membrane and cytosol of cell types in which it has been identified (L. Li et al., 2003; Ropero et al., 2006) although it is also competent to activate transcription (Figtree, McDonald, Watkins, & Channon, 2003).

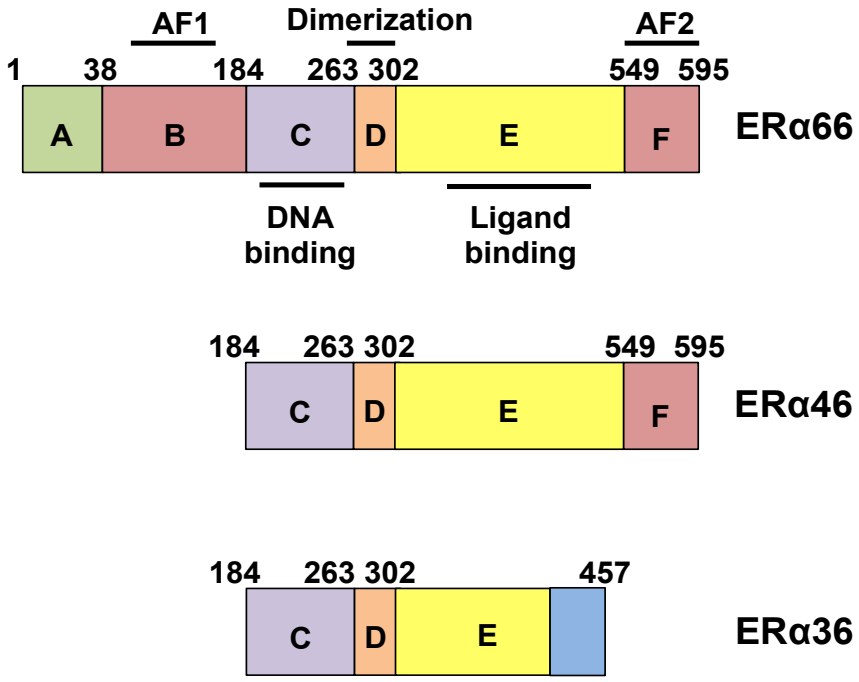

Figure 2.2: Gene structure and isoform variants of ERα. Full length ERα is a 66 kDa protein that includes 2 transactivation domains, AF1 **(A/B)** and AF2 **(F)**, **(C)**, a DNA binding/dimerization domain **(D)** and a ligand binding domain **(E)**. ERα46 and ERα36 are N-terminal truncations that lack the AF-1 domain. ERα36 includes a unique shorter C-terminus. Figure adapted from Dr. Emily Pugach

A single report suggests colocalization of cardiac myocyte membrane ERα46 with α-actinin at T-tubular membranes using immunofluorescence of rat cardiac myocytes (Ropero et al., 2006). Similarly, immunofluorescence was used to localize ERα to myocyte sarcolemma and intercalated discs in human cardiac myocytes (Mahmoodzadeh et al., 2006). Although these data are suggestive of a role for ERα46 in regulating myocyte contraction dynamics or structure, these findings remain to be recapitulated using an antibody-independent assay. Consistent with its localization at the membrane or in the cytosol, ERα46 has been reported to induce rapid, non-genomic signaling in human breast cancer cells and endothelial cells (L. Li et al., 2003;

Marquez & Pietras, 2001). Whether ERα46 plays a similar role in cardiac myocytes remains to be determined. Given the troublesome nature of steroid hormone receptor antibodies (Pugach et al., 2016; Schonbrunn, 2014), antibody-independent localization for ERα isoforms could better support their specific cellular roles.

A more recently identified human *ERα* variant, *ERα36,* is also truncated at the N-terminus and therefore lacks the A/B AF-1 domain. Additionally, *ERα36* lacks the C-terminal activation domain of full length ERα66 and ERα46 and instead contains a unique C-terminal sequence encoded further downstream (Z. Wang et al., 2005). *ERα36* is transcribed from a promoter located in the first intron of *ERα* and its expression has been observed in multiple cell and tissue types including several breast cancer cell lines and a number of different mouse tissues (Irsik, Carmines, & Lane, 2013; Z. Wang et al., 2005; Zheng et al., 2010)**.** When overexpressed in HEK293 (Human Embryonic Kidney) cells or MCF7 breast cancer cells *ERα36* has been shown to regulate rapid signaling pathways such as the pERK/MAPK pathway (Kang et al., 2010)**.** The demonstrated ability of cardiac myocytes to also respond rapidly to estrogen treatment through activation of analogous pERK/MAPK signaling (Nuedling, Kahlert, Loebbert, Meyer, et al., 1999) and the importance of the pERK/MAPK pathway in regulating cardiac myocyte biology (Bueno et al., 2000; Ueyama et al., 2000) call for a more thorough investigation of the ability of specific *ERα* isoforms to regulate these pathways in cardiac myocytes.

As described above, ERα isoforms can function both as nuclear transcription factors and cytoplasmic signaling activators when bound by E2. Further, ERs have been shown to differentially localize depending on cell type or stimulus (Nuedling, Kahlert, Loebbert, Doevendans, et al., 1999; Ropero et al., 2006). Both ERα and ERβ mRNA and protein have been reported in total heart lysates, but there are many cell types in hearts (Lizotte, Grandy, Tremblay, Allen, & Fiset, 2009; Mahmoodzadeh et al., 2006). Overall ER abundance in cardiac myocytes remains controversial due to the use of antibodies of questionable specificity (Schonbrunn, 2014). Live-cell and/or antibody-independent imaging of ER localization in cardiac

myocytes have not yet been reported. This type of analysis may provide clues to ER function in the heart. Considering the ubiquity of hormone replacement therapy, these data also provide important guidance for studies focusing on both cardiac and non-cardiac disease prevention and intervention. Therefore, we examined ER expression along with nuclear, cytoplasmic, and membrane distribution of three ERα isoforms and the contribution of estrogen signaling from each subcellular compartment in rodent cardiac myocytes. These studies help reveal the cellular location from which important downstream signaling events originate in cardiac myocytes and may inform more targeted cardiac myocyte-relevant ER therapeutics.

2.2 Materials and Methods

Animals

All animal protocols were approved by the Institutional Animal Care and Use Committee at the University of Colorado at Boulder. Mice and rats were fed *ad libitum* standard rodent chow and housed in a facility with a 12 hour light, 12 hour dark cycle. Wild-type C57Bl/6J mice (Jackson Laboratories) were used for left ventricular gene expression studies. For sample collection, mice were sedated using 1–4% inhaled isoflurane and sacrificed by cervical dislocation. Hearts were excised and perfused in ice cold PBS. Left ventricles (LVs) were then isolated and flash frozen in liquid nitrogen.

Cardiac myocyte isolation

Neonatal rat ventricular myocytes (neonatal-RVMs) were isolated from 1 day old Spague-Dawley pups (Charles River Laboratories) as previously described (A. H. Maass & Buvoli, 2007). Briefly, hearts were harvested, atria removed, and ventricles digested with trypsin. Fibroblasts were removed by preplating the trypsin-digested cell preparations. Adult rat ventricular myocytes (adult-RVMs) were isolated from Sprague-Dawley rats (Charles River Laboratories) as previously described (Haines, Harvey, et al., 2012b). Briefly, hearts were

harvested then digested with collagenase (Worthington Biochemical) using a Langendorff perfusion apparatus. Following dissection of the left ventricle, myocytes were enriched using mesh filtration and successive centrifugation in increasing amounts of calcium solution. Neonatal-RVMs were cultured as described (A. H. Maass & Buvoli, 2007) except for experiments in which phenol red was omitted from the culture medium. For these experiments, cells were maintained in MEM 1X 51200-038 (ThermoFisher) with 2 mM L-glutamine (Gibco 25030-081).

Gene expression

Total RNA was purified using TRI Reagent (Ambion) according to the manufacturer's protocol. cDNA was synthesized using SuperScript III reverse transcriptase (Invitrogen) and random hexamer primers. Gene expression was determined by qRT-PCR using SYBR Green dye (Invitrogen) and gene specific primer sets (Appendix I). Data were collected and analyzed using a Bio-Rad CFX-96 Real-Time PCR system.

ERα *overexpression studies*

For studies of *ERα* localization, the human *ERα66*, *ERα46,* or *ERα36* cDNA open reading frame was cloned into pEGFP-N1 (Addgene) using *EcoRI* and *BamHI* restriction sites to terminally tag each isoform with EGFP. For each construct, a flexible linker (CCACCGGTCGCCACCATG) was placed between the *ERα* sequence and the EGFP sequence. The EGFP tag was placed on the carboxy-terminus as previous studies suggest that accessibility of the N-terminus is critical for palmitoylation-regulated targeting of ERα to the cell membrane (L. Li et al., 2003).

Subcellular fractionation and western blotting

Cells were fractionated according to the manufacturer's protocol (Cell fractionation kit, NEB 9038). Following fractionation, lysates were sonicated in a water bath, boiled, and centrifuged. Fractions were then analyzed by western blot as follows. 15 µL of lysate was loaded onto a 10% SDS-PAGE gel. Fractionation was confirmed using the following antibodies:

Histone 3 (Cell Signaling 4499s): Nuclear fraction, Caveolin-3 (Santa Cruz 5310): Membrane fraction, and Gapdh (Cell Signaling 2118): Cytoplasmic fraction. EGFP-tagged ERα was then detected using anti-GFP (Santa Cruz 8334). GFP quantification in each fraction was performed using ImageJ.

Adenoviral constructs

Adenovirus production was performed using the AdEasy-1 kit (Qbiogene) with modifications (Resnicow, Deacon, Warrick, Spudich, & Leinwand, 2010). Briefly, after subcloning each GFP-tagged isoform from pEGFP-N1 into pShuttle-CMV, the shuttle vector was linearized with *PmeI* and homologously recombined with pAdEasy in bacteria. Successfully recombined plasmids were linearized with *PacI* and transfected into HEK293 cells stably expressing the E1 protein to complement pAdEasy for replication competence. Virus was amplified by serial passage on HEK293 cells (ATCC), then virus was isolated from the lysates by sequential step and equilibrium density CsCl gradients. Purified virus was stored at -20°C in 100 mM Tris pH 7.5, 250 mM NaCl, 1 mM $MgCl_2$, 1 mg/ml BSA, 50% glycerol. Infectivity of each viral preparation was determined by plaque titering on HEK293 cells. Multiplicity of infection (MOI) for each virus was chosen such that final protein expression was comparable between *ERα* isoforms and >90% of cells were EGFP-positive for *ERα*-containing adenoviruses. MOIs used for Adeno-*EGFP*-only, Adeno-*ERα36*, Adeno-*ERα46*, and Adeno-*ERα66* were 2, 0.5, 6, and 0.3 respectively for neonatal-RVMs and 70, 15, 60, and 33 for ARVMs.

Microscopy

Cells were plated on 1% gelatin (neonatal-RVMs) or 10 μg/mL laminin in PBS (adult-RVMs) coated glass coverslips. Twenty-four hours post-infection, cells were treated with vehicle (0.1% ethanol) or 100 pM 17β-estradiol for 5 minutes. For the antagonist experiment in Figure 2.6, cells were treated with vehicle or 100nM Fulvestrant (ICI 182,780 – Sigma) one hour prior to the addition of 17β-estradiol. Cells were then fixed in 2.5% paraformaldehyde for 5 minutes and stained with F59 (anti-myosin) and nuclei were visualized with DAPI. All samples were

imaged on a Nikon TiE inverted microscope. Fixed neonatal-RVMs in Figure 2.5 were imaged using a Nikon Plan Apo 100x 1.45NA oil objective and illuminated with a Sola Light Engine with the appropriate filter cubes for DAPI, GFP, and TRITC. Widefield fluorescent images of neonatal-RVMs used for Figure 2.6 were acquired with a Nikon Plan Apo 20x 0.75 NA air objective and an Andor Ixon 897 EMCCD with the EM gain set to 300 and a bin factor of 1. The exposure times were unique for each channel as to utilize the dynamic range of the camera, and were applied consistently for all the acquired images. A 5x5 matrix of images using 5% overlap was acquired for analysis with the Nikon Perfect Focus System engaged. Confocal fluorescent images of the Adult-VRMs in Figure 2.8 and Figure 2.9 were acquired using a Nikon A1R laser scanning confocal on an inverted Ti-E microscope. A Nikon Plan Apo 100x 1.45 NA oil objective was used to capture each z-stack, ensuring that each stack encapsulated the entirety of the mycoyte. The step size was set to 300nm. The XY resolution was set to 120nm pixels (Nyquist sampling rate), and the pinhole was set to 1.2 Airy units. From the laser combiner, 405nm, 488nm, and 561nm lasers were used to sequentially excite the corresponding fluorophores of DAPI, GFP, and TRITC. An Andor Ixon3 DU897 was used to acquire all of the fluorescent images. All of the widefield neonatal-RVM images quantified in Figure 2.6 were analyzed using Fiji version 2.0.0-rc-43/1.50g. Briefly, TRITC channel was used to determine the perimeter of each myocyte, with each cell identified by a unique region of interest number. Then, individual threshold values were applied to the DAPI and GFP channels in order to remove the background signal before each was converted to a binary image. The ROIs determined by TRITC were then applied to the binary DAPI and GFP channels. The total area of each ROI and the percent areas covered by the DAPI and GFP channels were then determined. The data was then segmented to determine the number of infected cells as well as the number of cytosolic infections. Once the appropriate thresholding conditions were determined, these values were applied to all of the acquired data sets using a custom Fiji macro.

Reporter assays (ERE-luciferase)

Neonatal-RVMs plated in 6-well dishes (400,000 cells/well) were serum starved for 24 hours and infected with *ERα-EGFP* adenoviruses or control *EGFP*-only adenovirus along with *ERE-luciferase* and control *β-galactosidase* encoding adenovirus. *ERE-luciferase* adenovirus encodes 3 tandem ERE sites (from the *Gallus gallus Vitellogenin* sequence) upstream of the *E1A* TATA box. *β-galactosidase* adenovirus encodes the *E.coli β-lactamase* gene behind the *CMV* promoter. 4 hours after infection, cells were treated with either vehicle (0.1% ethanol) or 100 pM 17β-estradiol (Sigma). 12 hours after hormone treatment (16 hours post infection), cells were lysed in 200 µL of Reporter Lysis Buffer (Promega E3971). Luciferase activity was quantified using 50 µL LARI substrate (Promega E1500) and 10 µL of cell lysate. Luciferase activity was normalized to β-galactosidase activity using β-Galactosidase Enzyme Assay System (Promega E2000).

Signaling activation

24-hour serum-starved neonatal-RVMs were isolated and infected with *ERα-EGFP* adenoviruses or control, GFP-only adenovirus. 36-40 hours post-infection, *ERα-EGFP* expression was confirmed using live-cell fluorescence microscopy. Cells were treated with either vehicle (0.1% ethanol), EGF (recombinant rat EGF, ScienCell #145-04, 0.01 µg/mL), or 100 pM 17β-estradiol for 5 minutes, washed in PBS, and lysed in RIPA buffer (50 mM Tris pH 8.0, 150 mM NaCl, 1% NP40, 0.5% Na-deoxycholate, 0.1% SDS, complete protease inhibitor cocktail (Roche) and the following phosphatase inhibitors: 1 mM PMSF, 2mM NaF, 2 mM NaPPi, 1 mM Beta-Glycerophosphate, 1 mM Na-molybdate dihydrate, and 1 mM Na-Orthovanadate). Lysates were sonicated in a water bath and precleared by centrifugation. Lysate protein concentration was determined by Bicinchoninic Acid (BCA) assay (Pierce 23225) for protein quantification. 10 µg of protein were then resolved on a 4-12% Bis-Tris SDS-PAGE gel (Life Technologies) and probed with antibodies for pAkt (Cell Signaling 9275s, 1:1000 dilution), Akt (Cell Signaling 9272, 1:2000 dilution), ppERK (Cell Signaling 9101s, 1:1000

dilution), ERK (Cell Signaling 9102s, 1:2000 dilution), and Tubulin (Sigma t7816). Quantification was performed using ImageJ.

ERα immunoblot

Total cell lysates were generated using RIPA buffer as described above. ERα antibody was purchased from Santa Cruz Biotechnology (sc-542).

Data and statistical analysis

Data are presented as mean ± SEM. Differences between groups were evaluated for statistical significance using Student's two-tailed t test (two groups) or one-way ANOVA (more than two groups) followed by Tukey's post-hoc test for pairwise comparisons. For comparisons between multiple treatments and groups, two-way ANOVA was performed followed by Tukey's post-hoc test. *P* values less than 0.05 were considered significant unless otherwise noted. Nuclear size outliers in the image analysis datasets shown Figure 2.6 were identified using the ROUT method (Motulsky & Brown, 2006) with a Q value of 1 and were excluded from the final analysis.

2.3 Results

2.3.1 ER expression in cardiac myocytes

ER mRNA expression was quantified in isolated rat cardiac myocytes as well as mouse left ventricular myocardium (LV) (Figure 2.3). We measured and compared expression of *ERα* and *ERβ* mRNA in the LV of 3 month- and 6 month-old adult mice of both sexes. (Figure 2.3A,B). *ERα* expression was readily detectable while *ERβ,* had average Threshold Cycle (C_T) values >38 for all mouse LV samples analyzed. Both *ER*s were abundantly expressed in positive control mouse ovary (Figure 2.3A,B). *ERα* expression did not differ between male and female mouse LV's nor between ages, in agreement with human studies (Mahmoodzadeh et al., 2006).

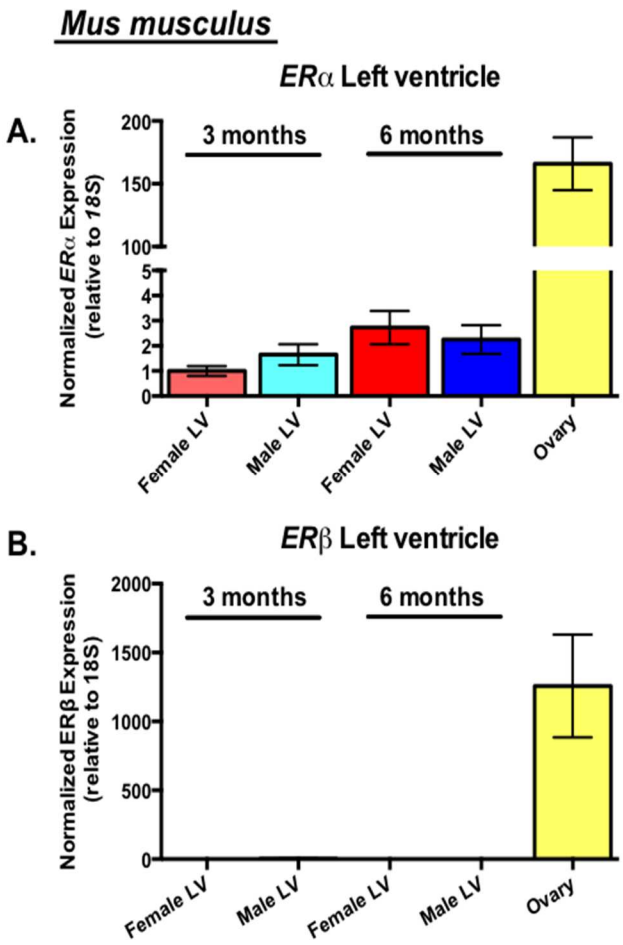

Figure 2.3: *Estrogen Receptor-α* is the predominant estrogen receptor transcript expressed in cardiac myocytes. (A) *ERα* and **(B**) *ERβ* gene expression by qRT-PCR in 3 and 6 month-old mouse left ventricular (LV) homogenates and ovary (positive control). N=3-5 animals/group (excluding ovary: N=2 animals). Figure was produced by Dr. Emily Pugach.

Similarly, only *ERα* mRNA was detectable in both neonatal rat ventricular myocytes (neonatal-RVMs) and female and male adult rat ventricular myocytes (adult-RVMs) (Figure 2.4). Expression of *ERα* was approximately 3-fold higher in adult-RVMs compared to neonatal-RVMs (Figure 2.4). *ERβ* was undetectable in neonatal-RVMs and adult-RVMs from either sex (data not shown). Additionally, RNA-sequencing (RNA-Seq) experiments demonstrated that *ERα* was expressed in both male and female adult-RVMs, but *ERβ* expression was not detectable (data not shown, Trexler *et al.*, in preparation, see Chapter 3).

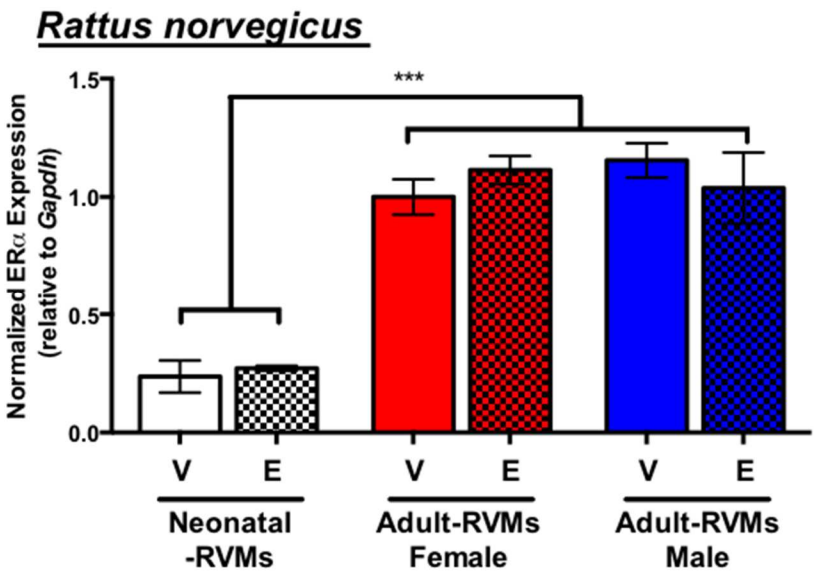

Figure 2.4: *Estrogen Receptor-α* transcript expression increases with age similarly in male and female rat ventricular myocytes and its expression is not modified by estrogen treatment. *ERα* expression by qRT-PCR in mixed male and female neonatal rat ventricular myocytes (RVMs) and isolated male and female adult-RVMs following 24 hours vehicle (V) or 100 pM 17β-estradiol treatment (E). ****P* < 0.001 vs. groups specified. N=3-4 animals/group excluding neonatal-RVMs: N=3 independent cell preparations from 70-100 pups each.

To determine whether *ERα* expression was altered by estrogen treatment, we isolated neonatal-RVMs and adult-RVMs from male and female animals and treated each with either vehicle or a physiological dose (100 pM) of 17β-estradiol (estrogen) (Figure 2.4). In agreement with *ERα* mRNA levels in male and female mouse myocardium, we found that *ERα* mRNA levels in isolated rat cardiac myocytes were similar between males and females. Further, in both neonatal-RVMs and male and female adult-RVMs *ERα* mRNA levels were not changed following 24 hours of estrogen treatment.

2.3.2 ERα localization in cardiac myocytes

We next asked whether the subcellular localization of ERα could inform its mechanism of action in cardiac myocytes. Since ERα variants have been implicated in non-genomic signaling (Kang et al., 2010; Ohshiro, Schwartz, Levine, & Kumar, 2012; Z. Wang et al., 2006), we also asked whether alternate ERα isoforms displayed differential localization and/or signaling

competencies compared to full length ERα, as has been observed in other cell types (Kang et al., 2010; Kim, Toomre, & Bender, 2011; Ohshiro et al., 2012; Ropero et al., 2006; Z. Wang et al., 2005).

Multiple antibodies for ERα demonstrated poor specificity in our hands, therefore GFP-tagged ERα isoforms were studied (see Methods). Adenoviruses were made using the fluorophore-tagged *ERα* constructs to allow for increased efficiency and uniformity of expression in neonatal-RVMs as well as expression in adult-RVMs which cannot be transfected. Appropriately sized ERα-EGFP proteins were easily detectable in neonatal-RVMs at no obvious cost to cell health or viability (data not shown).

Localization of each ERα isoform was assessed following 5 minutes of 100 pM estrogen treatment or vehicle using both high resolution fluorescence microscopy (Figure 2.5) and subcellular fractionation followed by immunoblot analysis (Figure 2.7). Following adenoviral-mediated ERα-EGFP overexpression, neonatal-RVMs were estrogen treated and immunostained with an anti-myosin antibody (F59) and stained with DAPI to label DNA and imaged using confocal microscopy. As shown in Figure 2.5, all three EGFP-tagged ERα variants displayed primarily nuclear localization, independent of estrogen treatment. We did not observe any EGFP-tagged ERα36, ERα46 or ERα66 co-localizing with myosin or another striated structure, in contrast to previous reports with antibody localization (Mahmoodzadeh et al., 2006; Ropero et al., 2006). Similar patterns of ERα localization were also observed using N-terminal EGFP tags and a comparably smaller, Myc tag (data not shown). ERα localization was not affected by pre-treatment with an ER antagonist (ICI 182,780) nor the presence of phenol red in media (Figure 2.6).

To confirm our microscopic finding of nuclear localization of all three ERα variants, we performed subcellular fractionation of neonatal-RVMs. Neonatal-RVMs were infected with adenoviruses encoding EGFP-tagged ERα variants. Cells were then briefly treated with estrogen (or vehicle) and partitioned into cytoplasmic, nuclear/cytoskeletal, and

membrane/organelle fractions. Lysates from each fraction were run on an SDS-PAGE gel and probed for ERα-EGFP abundance using a GFP antibody. Quantification of these experiments is shown in Figure 2.7A. To confirm efficiency of fractionation, fractions were also

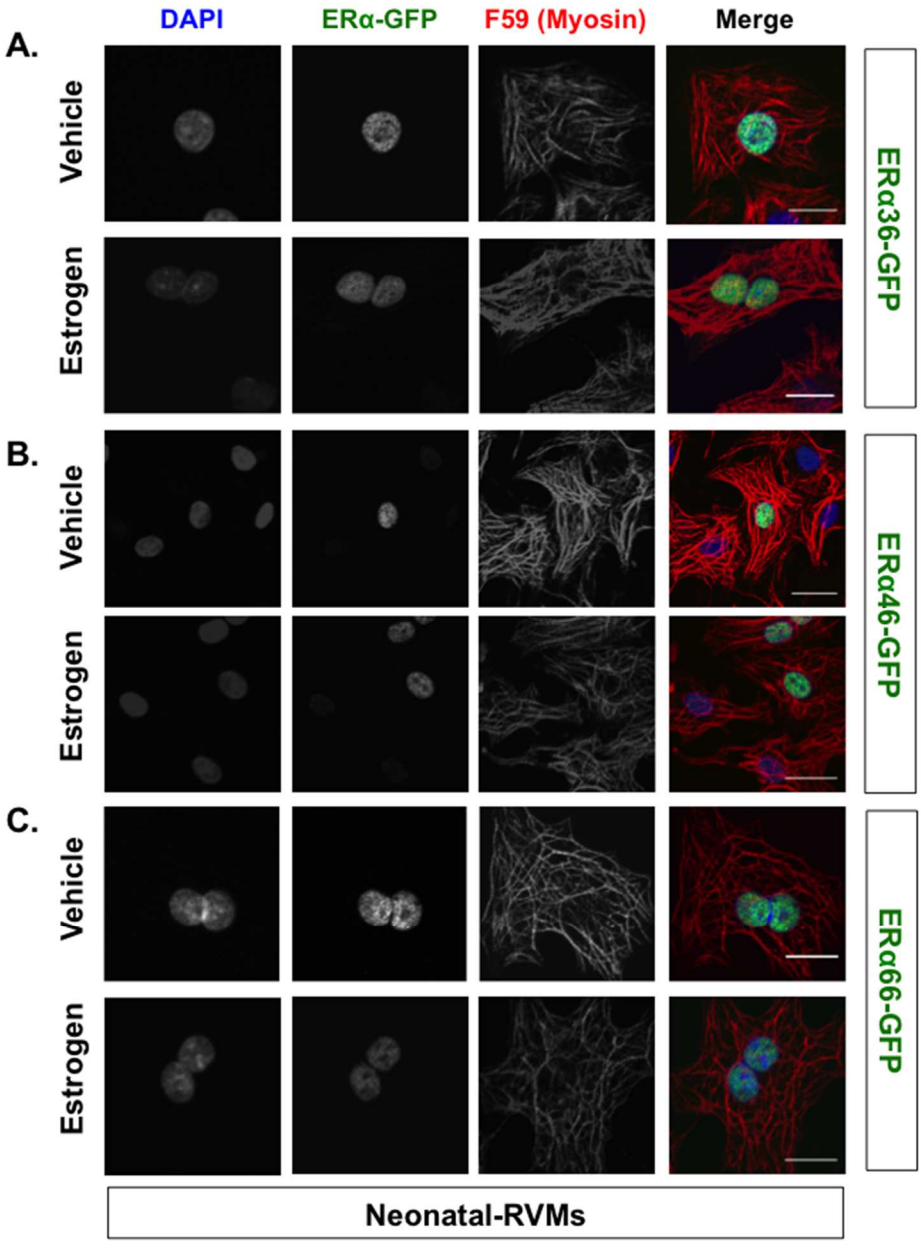

Figure 2.5: Three different isoforms of Estrogen Receptor-α predominantly localize to neonatal ventricular myocyte nuclei: fluorescence microscopy. (A-C) Fluorescence based subcellular localization of each EGFP-tagged ERα variant relative to DNA (DAPI) or myosin (F59) following treatment with either vehicle or 100 pM 17β-estradiol using confocal microscopy. Scale bar: 50μM. This figure was produced by Dr. Emily Pugach.

probed for markers of each fraction (Figure 2.7B). This biochemical analysis revealed similar subcellular localization patterns for all three ERα isoforms. In all cases and in agreement with our fluorescence microscopy studies, regardless of estrogen status, each ERα isoform localized primarily to cardiac myocyte nuclei. The nuclear subcellular localization of each ERα variant was also confirmed in both male and female adult-RVMs using fluorescence microscopy (Figure 2.8 & Figure 2.9).

2.3.3 ERα isoform transcription activity in cardiac myocytes

Each ERα isoform was then interrogated for its ability to regulate transcription of a synthetic estrogen responsive (*ERE*) reporter construct. Neonatal-RVMs were infected with adenovirus encoding each of the three *ERα* isoforms and concurrently infected with adenovirus encoding a synthetic *ERE-luciferase* reporter as well as with adenovirus encoding *β-galactosidase* under the control of a constitutive promoter for normalization purposes. Cells were then treated with either vehicle or 100 pM estrogen for 12 hours after which luciferase activity was quantified. As shown in Figure 2.10A, luciferase induction varied among *ERα* isoforms with *ERα66-EGFP* mediating the greatest induction. As expected, based on its truncated N-terminal transactivation domain, *ERα46-EGFP* showed lower activation of *ERE-luciferase* similar to what has been observed in other cell types (Figtree et al., 2003). *ERα36-EGFP* was incapable of inducing *ERE-luciferase* in response to E2 treatment, a finding that is consistent with its lack of both N- and C-terminal transactivation domains and with what has been observed in other cell types (Z. Wang et al., 2006). Moreover, luciferase activity resulting from ERα36-EGFP was not statistically different from uninfected or GFP control-infected cells.

Importantly, *ERE-luciferase* was not inducible by estrogen treatment in the absence of *ERα* overexpression; consistent with the very low basal expression of endogenous *ERα* in

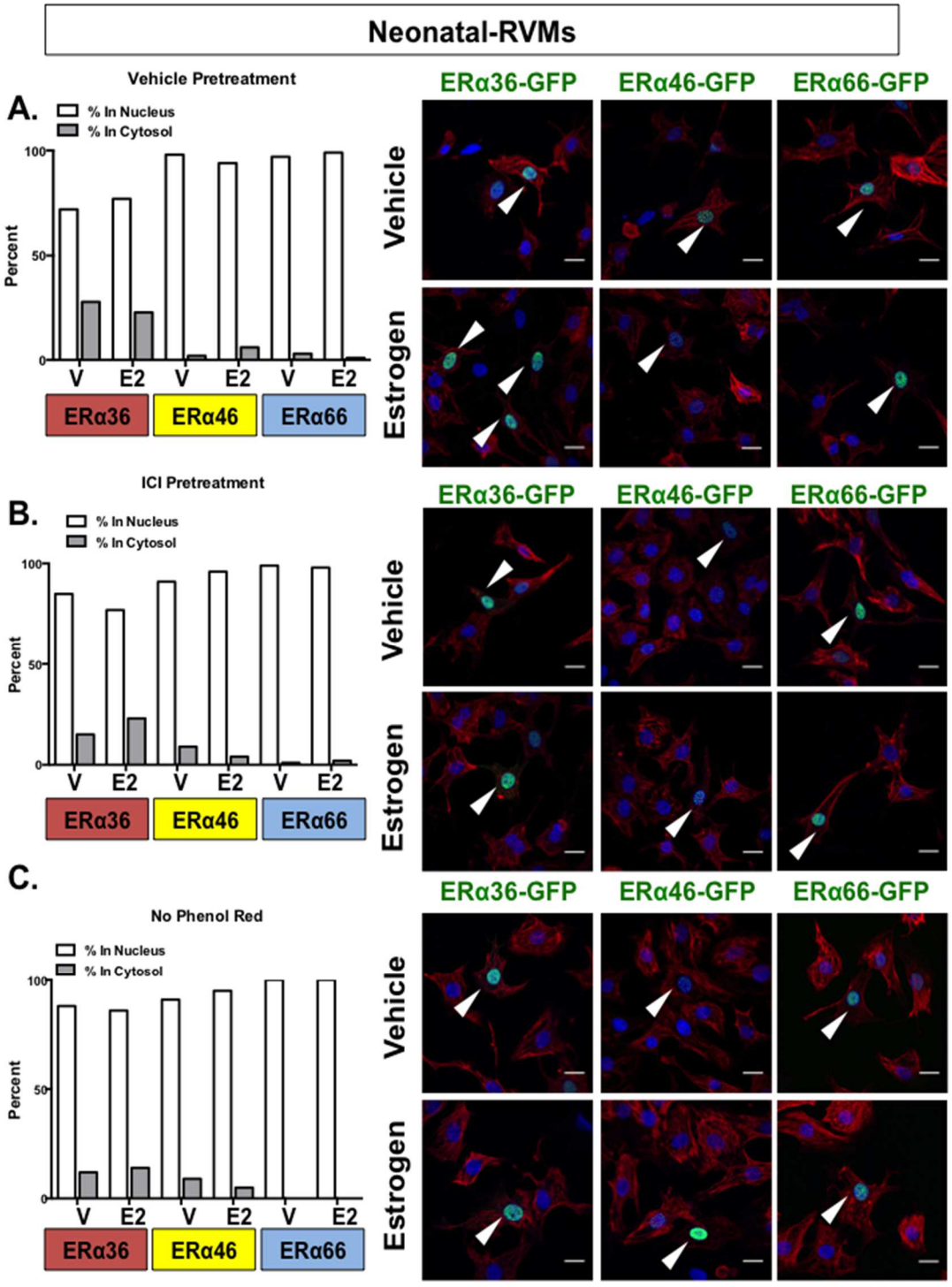

Figure 2.6: ERα-EGFP localization is not affected by pre-treatment with an ER antagonist (ICI 182,780) nor the presence of phenol red in media. Representative images and percent ERα-EGFP in neonatal-RVM nuclei and cytoplasm following 1 hour vehicle pretreatment **(A)** or 100 nM ICI 182,780 pretreatment **(B)** followed by 5 minutes vehicle or 100 pM 17β-estradiol (E2) treatment. **(C)** Percent ERα-EGFP in neonatal-RVM nuclei and cytoplasm following 5 minutes vehicle or 100 pM 17β-estradiol (E2) treatment in phenol red-free media. At least 29

cells were analyzed per condition from a cell preparation of 50 pooled neonatal rat hearts. Scale bar: 15 μM.

neonatal-RVMs (Figure 2.4). However overexpression of full length *ERα* in the absence of estrogen treatment was sufficient to activate the reporter. Together these results indicate that, in neonatal-RVMs, ERα-EGFP is capable of both estrogen-independent and estrogen-dependent activity.

2.3.4 Rapid signaling activity of ERα in neonatal-RVMs

Since estrogen has been shown to rapidly activate both the MAPK and PI3K signaling pathways in cardiac myocytes and other cell types (Nuedling, Kahlert, Loebbert, Meyer, et al., 1999; Simoncini et al., 2000), we next asked whether any ERα-EGFP variant was capable of rapid activation of either of these pathways in isolated cardiac myocytes. To this end, neonatal-RVMs were infected with corresponding adenoviruses and treated briefly (5 minutes) with 100 pM estrogen or vehicle. Following treatment, cell lysates were harvested and probed for relevant signaling activation using phosphorylation-specific antibodies (Figure 2.10B).

Neither Akt activation, nor ERK1/2 MAPK activation (Thr202/Tyr204 ERK1, Thr185 and Tyr187 of Erk2) was observed following overexpression of any *ERα* variant, independent of estrogen status, except following treatment with a known agonist, EGF (Pierce et al., 2001) (Figure 2.10B). Thus, although neonatal-RVMs are capable of rapid activation of PI3K and MAPK signaling, neither treatment with E2 nor overexpression of ERα alone or in combination with E2 treatment was sufficient to activate these pathways in neonatal-RVMs.

2.4 Discussion

2.4.1 ER expression in cardiac myocytes

To our knowledge, this is the first report of ER expression data in pure populations of isolated neonatal and adult cardiac myocytes using qRT-PCR. Several other groups have reported ER expression and localization patterns using ER antibodies; but ER antibody

specificity remains controversial (Lizotte et al., 2009; Ropero et al., 2006). Our data also suggest an absence of *ERβ* in both neonatal and adult cardiac myocytes despite reported protein expression in myocytes and ventricular lysates using antibody-based assays (Grohe, Kahlert, Lobbert, & Vetter, 1998; Lizotte et al., 2009; Nuedling, Kahlert, Loebbert, Doevendans, et al., 1999).

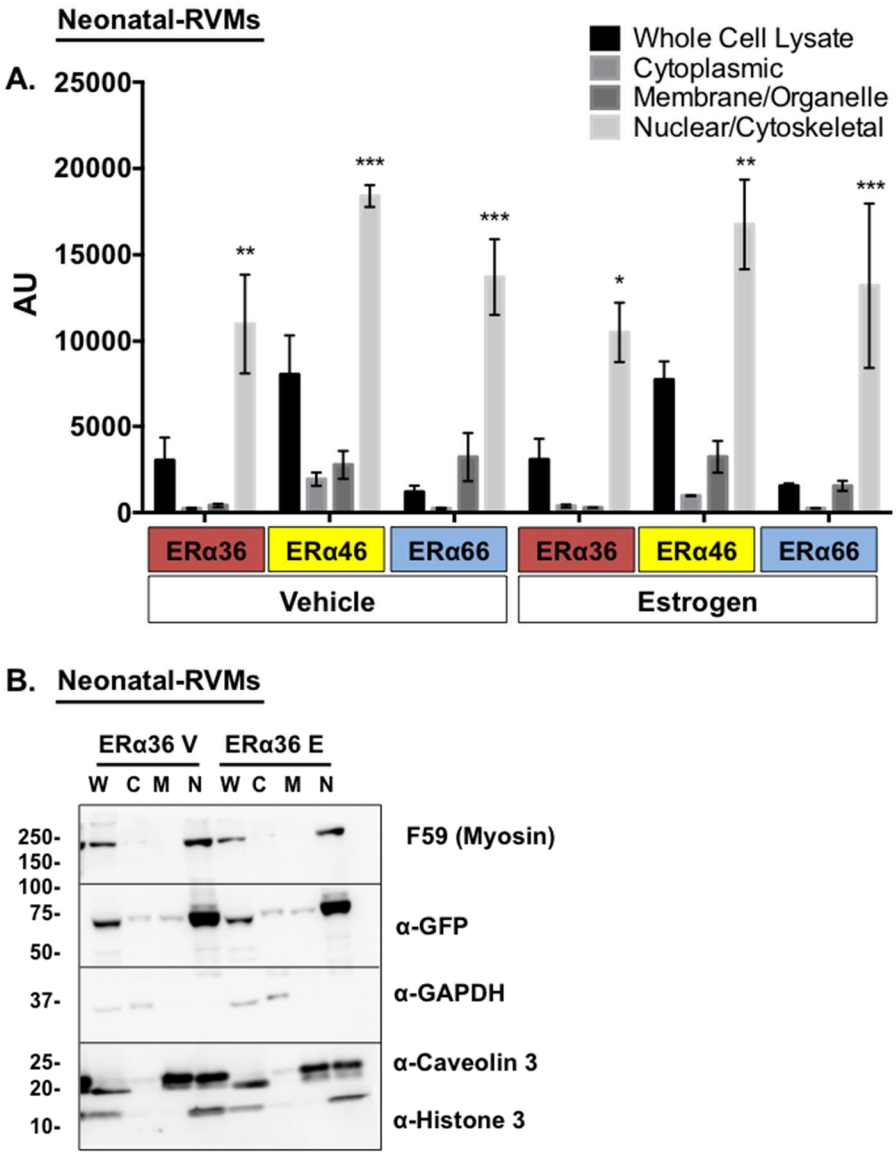

Figure 2.7: Three different isoforms of ERα predominantly localize to neonatal ventricular myocyte nuclei by subcellular biochemical fractionation. (A) Quantification of each EGFP-tagged ERα variant by subcellular fractionation followed by immunoblot for GFP. **(B)** Representative immunoblot of neonatal-RVMs following infection with ERα36-GFP. Following overexpression by adenoviral infection and treatment with either vehicle or 100pM 17β-estradiol,

ERα-EGFP localization was quantified in fractionated cell lysates. Subcellular fraction identity was verified by the presence of either GAPDH (cytosol), Caveolin-3 (membrane), or Histone-3 (nucleus). F59 antibody was used to determine sarcomeric protein localization relative to other fractions. *$P < 0.05$, **$P < 0.01$, ***$P < 0.001$ vs. all other ERα isoform- and treatment-matched fractions. 17β-estradiol treatment: 100pM, 1 hour. N=3 experiments. W: Whole cell lysate, C: Cytosolic lysate, M: Membrane/organelle lysate, N: Nuclear/cytoskeletal lysate, V: Vehicle, E: 17β-estradiol, AU: Arbitrary Units. This Figure was produced by Dr. Emily Pugach.

Further, published RNA-Seq data of mouse LV, isolated cardiac myocytes, and our own unpublished data support our findings that *ERα* is the only detectable cardiac myocyte ER transcript (Matkovich, Edwards, Grossenheider, de Guzman Strong, & Dorn, 2014; O'Meara et al., 2015).

Several models of *ERβ*-deficient mice support a role for *ERβ* in the heart and vasculature although our data suggest this role is likely in non-myocyte cells in the heart (Babiker et al., 2006; Pedram et al., 2010). Indeed, many studies support the importance of *ERβ* in non-cardiac myocyte cell and tissue types including cardiac fibroblasts, lung septa, and platelets (Jayachandran et al., 2010; Morani et al., 2006; Pedram et al., 2010). These cell and tissue types can directly and indirectly influence cardiac myocyte function and viability so cardiac phenotypes in mice with systemic loss of *ERβ* may actually be secondary phenotypes (Babiker et al., 2006; Babiker et al., 2007; Pelzer et al., 2005; Skavdahl et al., 2005). Even though cardiac myocyte expression of *ERβ* was not detected in this study, this receptor may still have an important cardiac role. Because cardiac myocytes account for approximately 75% of the myocardial volume, other non-myocyte cells, such as fibroblasts or endothelial cells may express *ERβ*, but this expression would be diluted out in the whole left ventricle (Jugdutt, 2003). Additionally, in the current study, all analysis was performed with tissue or cells from the left ventricle only. *ERβ* expression could potentially be enriched in the atria, which would explain why it was undetectable in our experiments. This is supported by differential gene expression analysis of right and left mouse atria in which *ERβ* was detectable (Kahr et al., 2011).

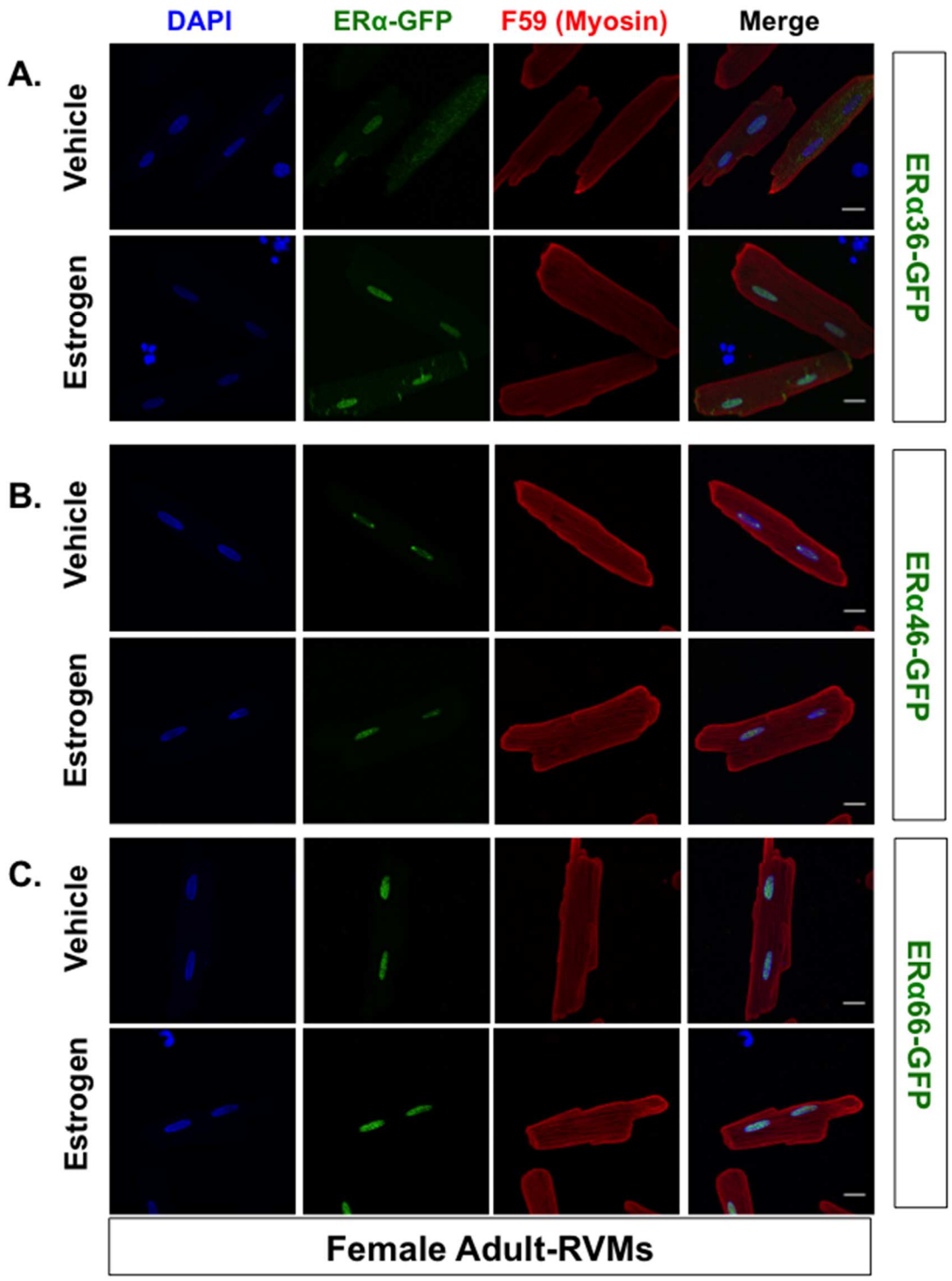

Figure 2.8: Three different isoforms of Estrogen-Receptor-α predominantly localize to nuclei of female adult ventricular myocyte by fluorescence microscopy. Fluorescence-based subcellular localization of each GFP-tagged ERα variant relative to DNA (DAPI) or myosin (F59) following treatment with either vehicle or 100 pM 17β-estradiol using confocal microscopy. **(A)** ERα36-GFP, **(B)** ERα46-GFP, **(C)** ERα66-GFP. Scale bar: 15 μM.

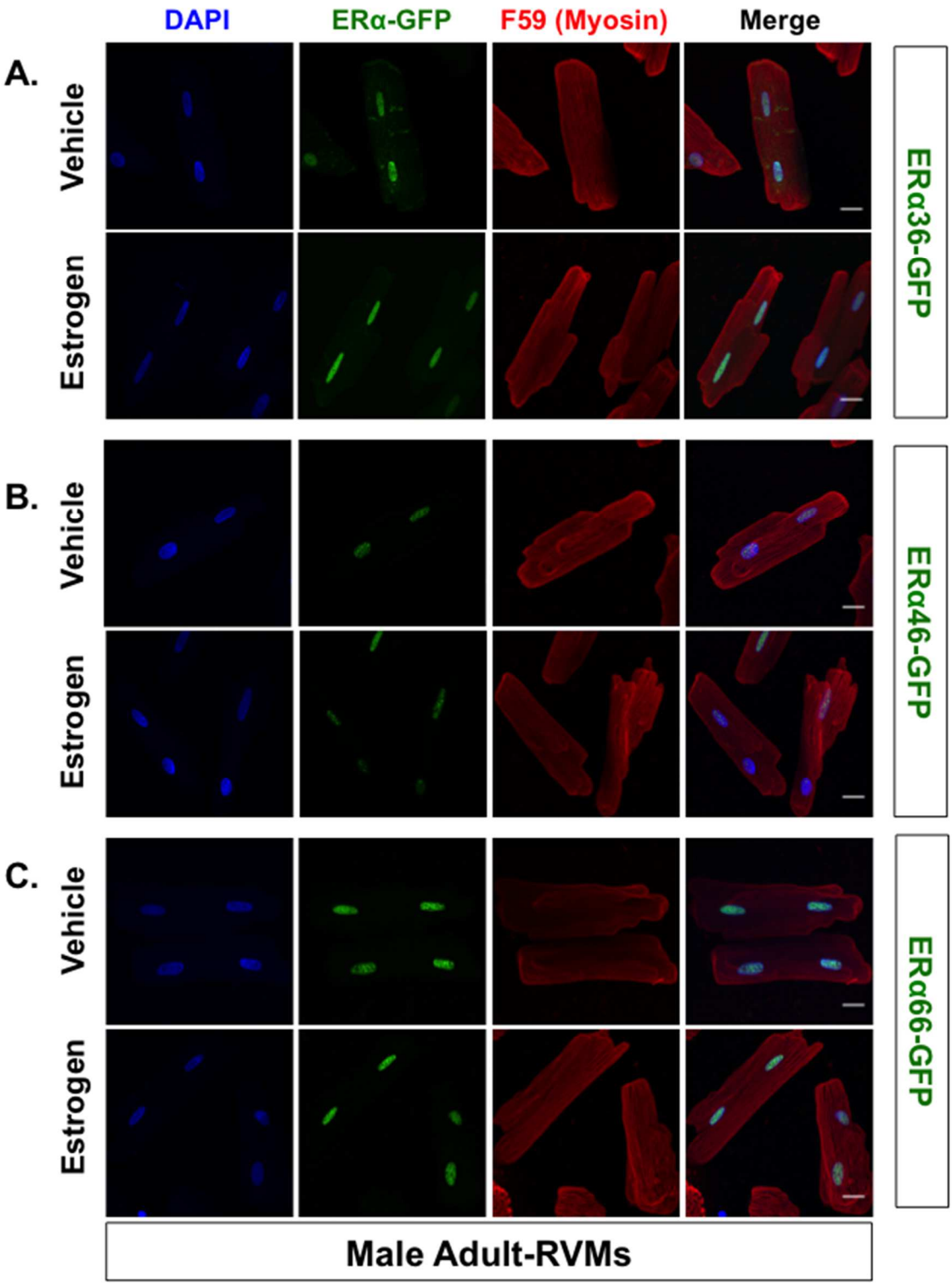

Figure 2.9: Three different isoforms of Estrogen-Receptor-α predominantly localize to male adult ventricular myocyte nuclei by fluorescence microscopy. Fluorescence based subcellular localization of each GFP-tagged ERα variant relative to DNA (DAPI) or myosin (F59) following treatment with either vehicle or 100 pM 17β-estradiol using confocal microscopy. **(A)** ERα36-GFP, **(B)** ERα46-GFP, **(C)** ERα66-GFP. Scale bar: 15 μM

2.4.2 Full-length and alternate ER isoform localization and signaling in cardiac myocytes

Estrogen and ERα signaling have been shown to act in many subcellular compartments and to be very powerful in a number of cell types; most prominently in breast cancer cells (Kang et al., 2010; Kim et al., 2011; Ohshiro et al., 2012; Z. Wang et al., 2006). Further, there have been reports of sarcomeric, nuclear, and cytoplasmic immunolocalization of ERα in cardiac myocytes (Mahmoodzadeh et al., 2006; Ropero et al., 2006). Localization of full-length and alternatively spliced isoforms of *ERα* were carefully assessed in this study. Predominantly nuclear localization was observed for all three EGFP-tagged *ERα* variants (Figure 2.5 - Figure 2.9). Although it is conceivable that the EGFP tag could interfere with ERα trafficking, several pieces of evidence support a lack of effect of EGFP on ER localization. First, broad distribution of EGFP alone was observed suggesting EGFP is capable of targeting to all of the subcellular compartments that were assessed (Pugach et al., 2016). Second, full length *ERα* localization was similar regardless of EGFP tag orientation (amino- or carboxy-terminus; data not shown). Finally, when a comparably smaller Myc tag was substituted for the N-terminal EGFP tag, nuclear localization was also observed (Pugach et al., 2016). Previous reports using GFP-tagged ERα isoforms have demonstrated comparable GFP-ERα localization (Htun, Holth, Walker, Davie, & Hager, 1999; Stenoien et al., 2000).

Interestingly, sarcomeric proteins co-fractionated with nuclear proteins during the subcellular extraction process (Figure 2.7B). Co-fractionation of sarcomeric and nuclear extracts does not allow biochemical resolution of ERα. This is important since sarcomeric localization of ERα has been reported in adult cardiac myocytes using immunofluorescence (Ropero et al., 2006). However, high magnification, high resolution fluorescence microscopy of the EGFP-tagged receptors in cardiac myocytes confirms its primarily nuclear localization pattern (Figure 2.5 - Figure 2.9).

It is possible that the dose of estrogen used (100 pM) may be insufficient to elicit a localization or rapid signaling effect in our assays. However, this dose was chosen based on

reported serum concentrations of estrogen in rodents (Dubal et al., 1998; Haines, Harvey, et al., 2012b; H. Wang et al., 2013) and the reported binding affinity of ERα for estrogen (Escande et al., 2006; Kuiper et al., 1997). Further, this concentration of estrogen was demonstrated to induce strong effects in cells endogenously expressing ERα (H. J. Li et al., 2011).

Others have reported a range of subcellular localizations for *ERα* and its splice variants. Primarily nuclear localization with significant membrane and cytosolic localization of both ERα66 and ERα46 was observed in COS7 fibroblast-like cells and EA.926 immortalized endothelial cells following overexpression of GFP-tagged constructs (Figtree et al., 2003). Another group reported enrichment of ERα46 in the cytosol and plasma membrane relative to the nucleus in EA.926 cells (L. Li et al., 2003). Our results in cardiac myocytes are inconsistent with these findings as the majority of ERα46 and ERα66 was localized in the nucleus. While it might seem unexpected to observe nuclear ER localization in the absence of ligand, previous studies of both GFP-tagged ER constructs and other nuclear hormone receptors have demonstrated similar localization patterns (Htun et al., 1999; Maruvada, Baumann, Hager, & Yen, 2003). Additionally, ligand-independent activation of mammalian ER has been previously documented *in vitro* and *in vivo* (Weigel & Zhang, 1998).

The most recently discovered *ERα* variant, *ERα36,* appears to be transcriptionally incompetent at a canonical ERE site in cardiac myocytes (Figure 2.10A). While we do not show that each of these isoforms transcriptionally activate different targets, we do demonstrate that each of the isoforms have different transcriptional activities as demonstrated by our ERE-luciferase assay. This is an established method as many other reports have utilized this ERE-luciferase system as a surrogate for measuring transcription of ER targets (Figtree et al., 2003) (Fujimoto, Jinno, & Kitamura, 2004).

None of the three isoforms was capable of inducing PI3K or MAPK signaling (Figure 2.10B). This does not rule out another mechanism of *ERα36* action in neonatal-RVMs or adult cardiac myocytes or a human-specific cardiac myocyte function for this variant. Importantly,

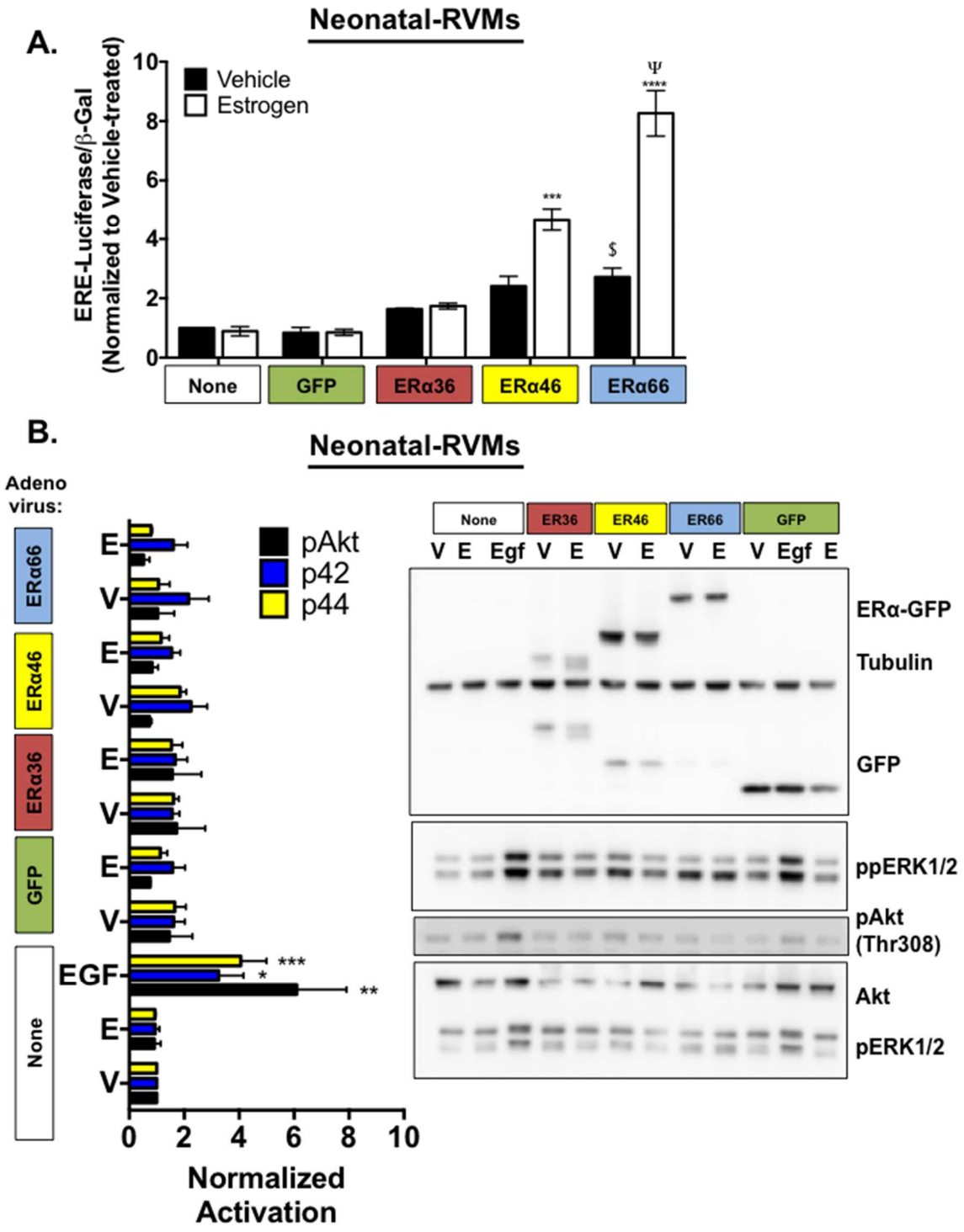

Figure 2.10: Cardiac myocyte ERα predominantly regulates cardiac myocytes through control of transcription, not activation of cytoplasmic signaling. (A) Induction of synthetic ERE-luciferase reporter by EGFP alone, or EGFP-tagged ERα variants with and without 12 hours 100 pM 17β-estradiol treatment. *** $P < 0.001$ vs. matched V, Ψ $P < 0.001$ vs. ERα46-EGFP, $ $P < 0.05$ vs. uninfected vehicle. N=3 experiments. **(B)** MAPK (phospho-p44/phospho-

p42 ERK) and PI3K/Akt (phospho-Akt) activation in neonatal-RVMs by GFP alone or EGFP-tagged ERα variants with and without 5 minutes 100 pM 17β-estradiol treatment. EGF: 0.01 μg/mL 5 minutes (positive control). α-tubulin: loading control, **P* < 0.05, ***P* < 0.01, ****P* < 0.001 vs. vehicle treated. V: Vehicle, E: 17β-estradiol N=3 experiments. This figure was produced by Dr. Emily Pugach

ERα36 transcript expression has been identified solely in human tissues (Z. Wang et al., 2005; Zheng et al., 2010). A corresponding mouse or rat transcript has yet to be identified. Rodent models were utilized due to relative availabilities of cells and molecular and physiological similarities between human and rodent. Further studies investigating human isoforms in human cardiac myocytes are needed but beyond the scope of this report.

The nuclear localization pattern of ERα36 (Figure 2.5 - Figure 2.9) is consistent with its retention of the DNA binding domain and nuclear localization sequence while its inability to activate transcription (Figure 2.10A) agrees with its lack of N- and C-terminal transactivation domains. Nevertheless, our findings using an EGFP-tagged *ERα36* construct do not recapitulate membrane and cytoplasmic localization patterns seen in other cell types using immunofluorescence or subcellular fractionation in conjunction with isoform-targeted ERα antibodies (Lee et al., 2008; Z. Wang et al., 2006). Interestingly we observed increased variability of ERα36-GFP localization in adult-RVMs (Figure 2.8 & Figure 2.9). In some instances, EGFP-ERα36 puncta were observed throughout the cytoplasm or at the distal ends of adult-RVMs (Figure 2.8 & Figure 2.9). The EGFP-ERα36 distal end localization was in a pattern reminiscent of gap junction protein distribution at intercalated discs (Severs, Bruce, Dupont, & Rothery, 2008). Although this was only observed in Adult-RVMs from two animals of each sex it may warrant further investigation.

There is ample precedence for the importance of nongenomic ERα signaling in the heart. Recent generation of a transgenic mouse in which membrane-associated ERα signaling is disrupted revealed the importance of membrane-localized ERα in protecting the heart from vascular injury (Bernelot Moens et al., 2012; Lu et al., 2004). Endothelial cells isolated from transgenic mice that are unable to initiate membrane ERα signaling were deficient in their ability

to activate E2-dependent phosphorylation of Akt and ERK, suggesting the importance of these two pathways in mediating the effect of E2-ERα rapid-signaling-induced cardioprotection. Data presented here point to the importance of non-myocyte cardiac cell types in facilitating this effect.

The inability of each ERα variant to regulate rapid E2 signaling effects does agree with the lack of extra-nuclear ERα in cardiac myocytes that we observed compared to what has been previously reported for other cell types. Together, these results support a primarily nuclear function for ERα in cardiac myocytes. The relevant gene targets for ERα46 and ERα66 in cardiac myocytes warrant further investigation and may reveal novel cardiac myocyte-specific targets for estrogen-liganded ERα.

Although EGFP-tagged *ERα46* and *36* isoforms could be robustly expressed in neonatal-RVMs and adult-RVMs, their relevance to adult cardiac myocyte biology remains in question. Although *ERα46* mRNA has been detected in murine tissues (Flouriot et al., 2000), an orthologous *ERα36* isoform remains to be identified in rodent cells. Neonatal-RVMs were chosen for most cardiac myocyte studies due to the extremely low endogenous levels of *ERα* compared to adult-RVMs where expression of *ERα* is much higher (Figure 2.4). In this way, we were able to study each ER isoform individually in the absence of reported inhibitory effects of one *ERα* isoform on another (Figtree et al., 2003; Zou, Ding, Coleman, & Wang, 2009). However, ERα46 and ERα36 protein expression have been observed by others using western blot of lysates from adult cardiac myocytes or total ventricular extracts (Irsik et al., 2013; Ropero et al., 2006). In our hands, the antibodies used in these studies were not specific so it is unclear how much of each isoform exists in adult cardiac myocytes. From the studies reported here, which follow fluorescently tagged ERα, full-length ERα is the functionally relevant isoform for cardiac myocytes and its principal mechanism of signaling is through transcriptional activation.

Chapter 3 The Transcriptome and Functional Profile of Cardiac Myocytes is influenced by Biological Sex

Currently in preparation: Christa L. Trexler B.S., Aaron T. Odell B.S., Mark Y. Jeong, M.D., Robin D. Dowell D.Sc., Leslie A. Leinwand, Ph.D.

Abstract

Background: Even though cardiovascular disease (CVD) is the number one killer of women in the U.S., women have traditionally been omitted from clinical trials and female animals have either not been included in preclinical research studies or the two sexes have been combined. In studies where both sexes have been studied, significant sexual dimorphisms have been demonstrated in the development, presentation and outcome of CVD in humans as well as in animal models. However, there is little understanding of the mechanisms underlying sexually dimorphic cardiac disease. A more thorough understanding of sex-specific cardiovascular differences both at baseline and in disease is required to effectively treat all patients with CVD.

Methods & Results: We analyzed contractility in the whole heart, adult rat ventricular myocytes (ARVMs) and myofibrils from both sexes and observed functional sex differences at each level. Hearts and ARVMs from female rats displayed greater fractional shortening than males, and female ARVMs and myofibrils took longer to relax. To define factors underlying these functional differences, we performed an RNA-sequencing experiment ARVMs from male and female rats and identified ~600 genes whose expression was sexually dimorphic. Further analysis revealed sex-specific enriched signaling pathways and regulators, such as Protein Kinase A (PKA), Wnt/Ca^{2+} and inducible nitric oxide synthase being activated in the female dataset, whereas integrin, Rac, and insulin receptor pathways were enriched in male cells. At the protein level, female ARVMs exhibited higher PKA kinase activity, consistent with the RNA-seq data. Additionally, activating the PKA pathway by treating male and female ARVMs with a cAMP mimic diminished the contractile sexual dimorphisms previously observed.

Conclusions: These data support the notion that sex-specific gene expression differences at baseline influence cardiac function, particularly through the PKA pathway, and could be potentially responsible for differences in CVD presentation and outcomes.

3.1 Introduction

3.1.1 Sex differences in baseline cardiac function & disease

Cardiovascular disease (CVD) is the leading cause of death of American men and women (Mozaffarian et al., 2015). Even though CVD causes one in three women's deaths each year, women have traditionally been excluded from clinical trials and female animals have also been utilized less in basic research studies (Miller & Best, 2011; Mozaffarian et al., 2015). Until recently, consideration of both sexes was not required in clinical and preclinical studies focusing on CVD (Clayton & Collins, 2014; *Consideration of Sex as a Biological Variable in NIH-funded Research*, 2015). This research bias has led to the development of CVD therapeutics that are either ineffective or have detrimental side effects in women (Regitz-Zagrosek, 2006). Sex-specific differences in baseline cardiac function are observed in healthy adults, with women typically displaying higher heart rate, due to the smaller size of women's hearts (Prabhavathi, Selvi, Poornima, & Sarvanan, 2014). In terms of left ventricular ejection fraction (LVEF) and stroke volume (SV), cardiac functional advantages between healthy men and women have been debated in the literature (Salton et al., 2002; Sandstede et al., 2000). Higher LVEF and SV in men develop after adolescence, suggesting a role for sex hormones in the regulation of cardiac function (Cain et al., 2009; Marcus et al., 1999). Studies have also reported that women display better diastolic function compared to men, and women have preserved systolic function compared to men over the course of aging (Prabhavathi et al., 2014). Similar to humans, baseline differences in cardiac function have been reported in mice and rat studies, with females generally having better function compared to their male counterparts (A. K. Chung et al., 2006; Haines, Harvey, & Leinwand, 2012; Litwin et al., 1999). While studies focused on sex

differences in cardiac myocyte function have reported variable findings, likely due to different experimental conditions, most studies observed that sex differences are also apparent at the level of the cardiac myocyte with isolated male rodent cardiac myocytes contracting more strongly and rapidly than female cells, but this difference diminishes with age (Grandy & Howlett, 2006; Howlett, 2010; Parks & Howlett, 2013). Additionally, some reports have observed that relaxation rates also differ between the sexes with female cardiac myocytes relaxing more slowly than male cells (Parks & Howlett, 2013). Healthy cardiac contraction is maintained by strictly regulating calcium handling within cardiac myocytes, which also appears to be regulated in a sexually dimorphic manner. For example calcium sparks produced by the release of calcium from the sarcoplasmic reticulum are greater in amplitude and frequency in male rat cardiac myocytes compared to females (Farrell et al., 2010). Similarly, peak calcium transient amplitudes are generally smaller in female rat cardiac myocytes (Parks & Howlett, 2013). However, the physiological mechanisms responsible for these functional differences at the level of the whole heart as well as the cardiac myocytes are not well understood.

Additionally, sex differences are apparent in the development, presentation and outcome of a variety of CVDs in humans as well as in animal models (Mahmoodzadeh, Fliegner, & Dworatzek, 2012). Sex differences in blood pressure, like many cardiovascular features, originate during adolescence, with persistently higher systolic and diastolic pressures observed in men (Boynton & Todd, 1947; Roberts & Maurer, 1977). Women have increased incidences of pulmonary hypertension, which can progressively develop into right heart failure (Mair et al., 2014). With respect to myocardial infarction (MI) and heart failure, with women seemingly are protected in that they develop the disease later in life compared to men (Lenzen et al., 2008; Mozaffarian et al., 2015). However, after menopause, the prognosis for women with MI is significantly worse than for age-matched men (Karlson et al., 1994). Furthermore, women are more likely to develop heart failure with preserved ejection fraction (HFpEF), but this clinical disparity is not understood and treatment options for HFpEF are lacking (den Ruijter et al.,

2015; Komajda & Lam, 2014). Similar sexually dimorphic responses to cardiac disease conditions are also observed in a variety of animal models, making them excellent model systems to investigate responsible molecular mechanisms. For example, female animals are less likely to progress to heart failure in response to a variety of different pathological stressors and male hypertensive rats typically develop greater increases in blood pressure (Reviewed in (Blenck, Harvey, Reckelhoff, & Leinwand, 2016). Several mechanisms, particularly estrogen signaling, have been extensively studied and suggested to be responsible for the cardioprotection observed in women (Knowlton & Lee, 2012). However, the contradictory results from many of these studies reveals that this issue is still not completely understood and highlights that pathways other than estrogen signaling are undoubtedly playing a role. To effectively understand these sex specific disease dimorphisms, a better understanding of the mechanisms underlying these differences, particularly during baseline conditions, is needed.

3.1.2 The complexity of cardiac estrogen signaling

Menopause results from a 10-fold decline in circulating estradiol, the most biologically active estrogen, which has prompted many researchers to focus on the potential protective effects of estrogen on CVD (Y. Liu et al., 2001). For example, estrogen maintains vascular tone and cardiomyocyte survival, effects that are generally mediated by binding to either of the two distinct nuclear hormone receptors, estrogen receptor-alpha or -beta (ERα or ERβ) (Murphy, 2011). Once bound to estrogen, ERs alter transcription of target genes involved in a wide variety of processes such as growth and differentiation (Bjornstrom & Sjoberg, 2005). Estrogen has also been shown to mediate non-genomic effects by binding to ERs associated with the plasma membrane and activating kinase signaling cascades such as phosphoinositide 3-kinase (PI3K) (Murphy, 2011). Hormone replacement therapy (HRT) was used to potentially maintain the cardioprotection experienced by younger women. While early studies appeared promising, more detailed examination of the study design revealed that administering HRT to

postmenopausal women does not uniformly improve cardiac function, likely due to the timing of replacement or type of HRT administered (X. P. Yang & Reckelhoff, 2011). While much research has focused on the role of estrogen in cardiovascular function, conflicting results suggest that the role of estrogen is complex and incompletely understood at the cellular and molecular levels (Mahmoodzadeh et al., 2012). Also, there are undoubtedly factors other than estrogen signaling that may be important in mediating the observed sex-specific functional differences, but these have not be explored in depth.

3.1.3 Baseline sexual dimorphisms in cardiac gene expression

Left ventricular gene expression is sexually dimorphic in both humans and rodents. In reports analyzing human and mouse left ventricles, cardiac genes were differentially expressed between males and females, many of which are expressed on sex chromosomes (Fermin et al., 2008; Isensee et al., 2008). Autosomal cardiac genes also differ between the sexes, and in mice, these differences are not affected by the estrous cycle, suggesting that these differences are not due to differences circulating estrogen levels (Isensee et al., 2008). Upon further investigation, GeneOntology categories such chemotaxis and inflammation were enriched in the female hearts, however, in humans, these categories were overrepresented in males (Isensee et al., 2008). While these sexual dimorphisms are intriguing and inevitably contribute to the differences in baseline function and disease response, these studies analyzed whole ventricles, which are a complex mixture of cardiovascular cells such as fibroblasts, myocytes, smooth muscle and endothelial cells (Figure 3.1). Additionally, these previous studies utilized microarrays to detect sexual dimorphisms in cardiac gene expression whereas using next generation sequencing methods would provide a more unbiased and in-depth approach. To address how biological sex impacts the genetic profile of the contractile cells of the heart, we conducted an RNA-sequencing experiment to analyze baseline gene expression differences between male and female rat cardiac myocytes. This study defines the basic gene expression

profiles in cardiac myocytes from each of the sexes and describes the functional consequences of sex-specific gene expression. We believe these findings could be useful in the development of cardiovascular therapeutics for both men and women.

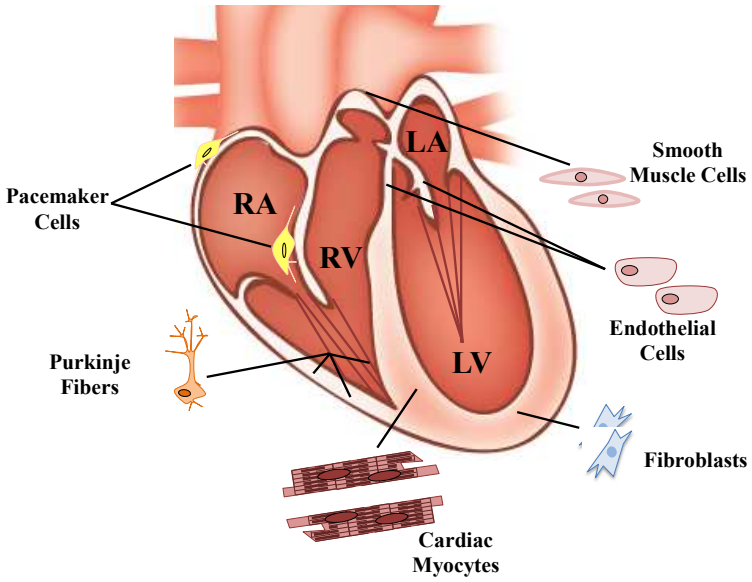

Figure 3.1: The heart is made up of multiple cell types to maintain function. The four-chambered heart contains more than just cardiac myocytes to function appropriately. Fibroblasts, purkinje fibers as well as endothelial, epithelial and pacemaker cells all provide vital functions such as maintaining the vasculature and conducting electrical impulses. Adapted from (Xin, Olson, & Bassel-Duby, 2013). RA/LA: right and left atrium, RV/LV: right and left ventricle.

3.2 Materials and Methods

Animals

All animal protocols were approved by the Institutional Animal Care and Use Committee at the University of Colorado at Boulder. Rats were fed *ad libitum* standard rodent chow and housed in a facility with a 12 hour light, 12 hour dark cycle. Male and Female (250-300g) Sprague-Dawley, CD, rats were purchased from Charles River Laboratory and allowed to acclimate to the facility prior to the described experiments.

Echocardiography

One week prior to cardiac myocyte isolation, all rats were subjected to transthoracic echocardiography. Non-invasive echocardiographic images and measurements were made

using the Philips Sonos 5500 system. Rats were placed on a heating pad and maintained on 2% isoflurane via spontaneous inhalation. The fur was first removed from the ribcage using a depilatory cream, and an image-potentiating gel was then applied for image acquisition. M-(motion) mode images were captured for each animal at the level of the papillary muscles (A2 view). LV dimensions and function was calculated from the M-mode images, where wall thickness of the anterior and posterior walls and the chamber diameter were measured using the ASE leading edge convention. Heart rate measurements were not different between groups with an average of 373.0 ± 13.6 beats per minute (bpm) for males and 347.2 ± 5.6 bpm for the females (Table 3.1).

Table 3.1: Echocardiography data of male (blue) and female (pink) hearts.

Animal ID	LVAW;d (cm) avg	LVID;d (cm) avg	LVPW;d (cm) avg	LVAW;s (cm) avg	LVID;s (cm) avg	LVPW;s (cm) avg
CB1	0.118	0.801	0.114	0.229	0.479	0.195
CB2	0.114	0.831	0.136	0.263	0.470	0.242
CB3	0.140	0.864	0.131	0.263	0.547	0.220
CB4	0.123	0.805	0.136	0.216	0.491	0.246
CB5	0.127	0.733	0.127	0.246	0.377	0.254
CB6	0.136	0.826	0.140	0.280	0.474	0.204
CB7	0.127	0.784	0.127	0.220	0.466	0.242
CB8	0.140	0.695	0.144	0.301	0.305	0.275
CB9	0.140	0.670	0.153	0.242	0.309	0.326
CB10	0.144	0.652	0.153	0.288	0.301	0.258
CB11	0.114	0.767	0.118	0.263	0.398	0.233

Animal ID	LV Vol;d (ul)	LV Vol;s (ul)	%EF	%FS	LV Mass corrected (mg)	Heart Rate (bpm)
CB1	345.6	106.8	69.1	40.2	496.6	383
CB2	374.7	102.4	72.7	43.4	579.3	419
CB3	409.3	145.4	64.5	36.8	689.9	340
CB4	349.8	113.5	67.5	39.0	573.8	360
CB5	283.3	60.8	78.5	48.6	478.2	400
CB6	370.4	104.6	71.8	42.6	652.0	336
CB7	329.1	100.3	69.5	40.5	535.8	356
CB8	251.1	36.4	85.5	56.1	508.0	364
CB9	231.1	37.7	83.7	53.8	498.5	340
CB10	217.8	35.2	83.8	53.9	487.6	333
CB11	313.7	69.2	77.9	48.1	460.6	343

Adult rat ventricular myocyte isolation and culture

Cardiac myocytes were isolated from the left ventricle of adult rats using a Langendorff apparatus with modification of previously published protocols (Haines, Harvey, et al., 2012a). Briefly, rats were injected with 250U heparin (Sagent, Schaumberg, IL), then after ten minutes, animals were injected intraperitoneally with 35mg/kg of sodium pentobarbital solution (Vortech, Dearborn, MI). Once the animal was completely anesthetized, the heart was quickly excised, rinsed in cold saline solution and cannulated onto the perfusion apparatus by the aorta. The heart was then perfused first with an isotonic buffer heated to 37°C and then digested with a collagenase Type II (Worthington, Lakewood, NJ) solution. For myocytes being used for contractility experiments, blebbistatin (30mmol/liter) was added to the collagenase solution. After isolation, myocytes were enriched using mesh filtration (250 um) and successive centrifugation at 100 x g for 5 minutes in buffered calcium solution, Media 199 (Invitrogen, Carlsbad, CA) and Springhorn media (0.2% BSA, 1.6 mmol/liter L-carnitine, 4.4 mmol/liter creatine monohydrate, 5 mmol/liter L-taurine, 4 _mol/liter L-glutamine, 5 _mol/liter sodium pyruvate, 10 mmol/liter 2,3-butanedione monoxime, 174 nmol/liter insulin). Cells were plated on 60-mm plates coated with 10ug/ml laminin (Invitrogen, Carlsbad, CA) in Springhorn media and allowed to settle. After 45 minutes, the media was removed and the cells were flash frozen in liquid nitrogen for downstream analysis.

Cardiac myocyte contractility assay and analysis

ARVMs were isolated as described above, plated on laminin-coated coverslips and allowed to settle for two hours in culture prior to the beginning of each contractility experiment. The coverslips were then transferred to the microscope (Nikon Diaphot) and superfused in Tyrode's solution [137mmol/liter NaCl, 2.7mmol/liter KCl, 1 mmol/liter $MgCl_2$, 1.8mmol/liter $CaCl_2$, 0.2mmol/liter Na_2HPO_4, 12mmol/liter $NaHCO_3$ & 5.5mmol/liter D-Glucose, pH 7.4]. Myocytes were electrically paced via field stimulation at room temperature by using the IonOptix MyoPacer with a stimulus duration of 4ms, voltage of 1.2x stimulation threshold and frequency

of 1Hz. Transients from at most five randomly selected myocytes per coverslip were recorded for at least 30 seconds per cell. Cell length measurements and shortening dynamics were determined by edge detection IonWizard software (IonOptix, Westwood, MA) in which at least ten transients per cell were averaged and analyzed. To analyze differences in contractile function in response to alterations in the PKA pathway, ARVMs from both sexes were plated on laminin coated coverslips and then treated with bucladesine (Cayman Chemical, Ann Arbor, MI) or DMSO two hours after isolation for 30 minutes. Contractility experiments were then performed as described above with the Tyrode's solution supplemented with either bucladesine or DMSO for the respective treatments.

Left ventricular myofibrillar isolation and analysis

In collaboration with Dr. Mark Jeong, we used previously published techniques to measure the force and kinetics of isolated myofibrils activated and relaxed by fast solution switching (Colomo, Nencini, Piroddi, Poggesi, & Tesi, 1998; Demos-Davies et al., 2014; Tesi, Colomo, Nencini, Piroddi, & Poggesi, 2000). Briefly, a small section of left ventricular tissue is skinned using Triton X-100 and homogenized to obtain a myofibril slurry. A small bundle of myofibrils were mounted between two microtools. One tool was connected to a motor that could produce rapid length changes (Mad City Labs). The second tool was a calibrated cantilevered force probe (4-8 μm/μN; frequency response 2-5 KHz). Myofibrils were set 5-10% above slack myofibril length. Average sarcomere length and myofibril diameter were measured using ImageJ (NIH). Mounted myofibrils were activated and relaxed by rapidly translating the interface between two flowing streams of solutions of different pCa (Tesi, Colomo, Nencini, Piroddi, & Poggesi, 1999; Tesi et al., 2000). Data was collected and analyzed using a customized LabView software. Measured mechanical and kinetic parameters were defined as follows: rate constant of early slow force decline (Linear k_{REL}) - the slope of the linear regression normalized to the amplitude of relaxation transient and the linear relaxation duration.

RNA extraction, Library Preparation and Sequencing

Total RNA was isolated using the miRNeasy mini kit (Qiagen, Valencia, CA) according to the manufacturers protocol with the on-column DNase digestion. RNA concentration was determined using the Qubit RNA BR Assay (Invitrogen, Carlsbad, CA) and RNA integrity was analyzed with the Agilent Bioanalyzer (Agilent, Santa Clara, CA) with all of the RNA samples used for sequencing having a RNA integrity number (RIN) of at least 9. Ribo-zero gold depleted paired-end sequencing libraries were then constructed from 650ng total RNA using the TruSeq Stranded Total RNA Sample Kit (Illumina, San Diego, CA) according to the manufacturers protocol. All libraries were sequenced using Illumina's HiSEQ2500 with 2x125bp v4 chemistry.

RNA-sequencing mapping, differential gene expression analysis & pathway analysis

All paired-end reads were demultiplexed with the Casava pipeline (v1.8.2) and adapter trimmed with Trimmomatic (v0.32). RNA-sequencing reads were aligned to the rat rn6 genome using Tophat (v2.0.12). Both the rn6 fasta reference file as well as the gene annotation (gtf) file was downloaded from the UCSC genome brower database (http://genome.ucsc.edu). To be able to distinguish between multiple isoforms, the UCSC rn6 gtf file was converted with UCSC genome browser's genePredToGtf Utility and then used for all mapping and differential expression analysis. Aligned reads that mapped to genes were counted with HTseq count (v0.6.1) and differentially expressed genes were identified using DESeq (v1.10.1). Genes identified to be statistically differentially expressed between sexes by at least 1.5 fold with a padj value of <0.01 by DESeq were then analyzed using Qiagen's Ingenuity Pathway Analysis (IPA) software (Content version: 24718999) to identify enriched networks. All genes with a padj ≤ 0.01 by DESeq are listed in Appendix II. We noticed inconsistencies with the gene annotation of *Hsp90aa1* between NCBI, Ensemble and UCSC, so this gene was excluded from our DESeq and IPA analysis. To investigate for enrichment of estrogen response elements (EREs) within the genes that were differentially expressed between the sexes, I analyzed my gtf file for the presence of EREs within 10kb of the start site of each gene using the PWMScan genome-wide

position weight matrix (PWM) scanner (http://ccg.vital-it.ch/pwmtools/pwmscan.php) as well as python script kindly given to me by Dr. Mary Allen. To scan genes within my gtf for ERE sites I utilized the Jasper 2014 core vertebrate motif library with the ESR1 MA0112.2 motif.

Quantitative PCR

cDNA was synthesized using SuperScript III reverse transcriptase (Invitrogen, Carlsbad, CA) and random hexamer primers. Gene expression was determined by qRT-PCR using SYBR Green dye (Invitrogen, Carlsbad, CA) and gene specific primer sets. All genes were normalized to 18S expression. All primer sequences used are listed in Appendix I. Data were collected and analyzed using a Bio-Rad CFX-96 Real-Time PCR system.

Protein Kinase A Activity Assay

Sexual dimorphisms in Protein Kinase A activity in ARVMs was determined using the Protein Kinase A activity kit (Abcam, Cambridge, United Kingdom). ARVMs from both sexes were isolated as described above and after 45 minutes of culture the cells were washed with phenol-red free media (ThermoFisher, Rochester, NY) and flash frozen. ARVMs were collected in lysis buffer [20 mM MOPS, 50 mM β-glycerolphosphate, 50 mM sodium fluoride, 1mM sodium vanadate, 5 mM EGTA, 2 mM EDTA, 1% NP40, 1 mM dithiothreitol (DTT), 1mM benzamidine, 1 mM phenylmethane- sulphonylfluoride (PMSF) and 10 µg/mL leupeptin and aprotinin] and this crude enzyme lysate was used for the remainder of the assay according the manufacture's protocol. Protein concentrations were determined by performing a BCA assay (Thermo Fisher Scientific, Waltham, MA).

Phospho-Kinase Antibody Array

ARVMs were isolated, plated and cultured for 45 minutes as previously described. The Proteome Profiler Human Phospho-Kinase array kit (R&D Systems, Minneapolis, MN) was used to detect the phosphorylation status of 45 proteins simultaneously in the ARVM lysates according to the manufacturer's protocol. ARVM lysates from two animals of each sex were

pooled per array and the arrays were incubated with equivalent amounts of protein (600µg), as deemed by BCA assay assay (Thermo Fisher Scientific, Waltham, MA).

Western Blot

ARVM protein lysates were prepared by collecting the cells in 50 mM Tris pH 8.0, 150 mM NaCl, 1% NP40, 0.5% Na-deoxycholate, 0.1% SDS, complete protease inhibitor cocktail (Roche, Basel, Switzerland) and the following phosphatase inhibitors: 1 mM PMSF, 2 mM NaF, 2 mM NaPPi, 1 mM beta-glycerophosphate, 1 mM Na-molybdate dihydrate, and 1 mM Na-orthovanadate. Protein concentrations were determined by performing a BCA assay (Thermo Fisher Scientific, Waltham, MA) and then 25µg was resolved on a NuPAGE 4-12% Bis-Tris gel (Invitrogen, Carlsbad, CA) and probed with the following antibodies: GAPDH (Cell Signaling Technologies, Danvers, MA, 2118S) and p-Troponin I (Cell Signaling Technologies, Danvers, MA, 4004S). All blots were imaged using the ImageQuant LAS 4000 (GE Healthcare Bio-Sciences, Pittsburg, PA) system and analyzed with the ImageQuant software.

Statistical analysis

Statistical analysis of differentially expressed genes were performed with DESeq (v1.10.1) with Benjamini-Hochberg adjusted p-value (padj) <0.01 deemed statistically significant. Differences between two groups were evaluated for statistical significance using Student's two-tailed t test using GraphPad PRISM 6 software with data presented as mean ± SEM. P <0.05 was considered significant. Significance was determined by using a two-way ANOVA for experiments that involved two or more independent variables, which was followed by a Tukey's multiple comparisons *post hoc* test to examine interactions between specific groups. Hypergeometric probability analysis for the ERE enrichment experiment (Figure 3.8) was performed with the calculator provide by geneprof.org (https://www.geneprof.org/GeneProf/tools/hypergeometric.jsp)

3.3 Results

3.3.1 Sex differences are apparent in baseline cardiac function from the level of the whole heart to cardiac myofibrils.

At the level of the whole heart, *in vivo* echocardiography demonstrated that cardiac function was enhanced in the female animals as displayed in Figure 3.2A with fractional shortening being higher in the female hearts compared to their male counterparts. The internal dimensions of the left ventricle were larger in male hearts both during diastole and systole, but the overall left ventricular mass was not different between sexes (Figure 3.2A). Similar functional differences between the sexes were also observed in isolated ARVMs with female cells displaying greater percent shortening than the male myocytes (Figure 3.2B). Interestingly, female ARVMs also took more time than male cells to reach peak contraction as well as return to baseline. This sex-specific difference during the relaxation phase was also observed at the level of the myofibril. Female myofibrils exhibited slower relaxation duration and kinetics of slow phase duration (Figure 3.2C).

3.3.2 Cardiac myocyte gene expression is sexually dimorphic

We next asked what molecular mechanisms could be responsible for the functional differences we observed in the cardiac myocytes by performing an RNA-sequencing experiment with ARVMs from both sexes. All paired-end sequencing reads were mapped to the rat rn6 genome using the Tophat pipeline leading to around 100 million reads mapping per sample with an overall mapping rate of at least 80% (Table 3.2). Differential expression analysis carried out using DESeq identified ~600 genes that are differentially expressed between male and female cardiac myocytes at baseline by at least 1.5 fold (Figure 3.3). These differences in gene expression appear to be sex-specific and not merely differences among biological replicates since there are almost no statistical differences in gene expression when the samples were analyzed with DESeq randomly (Figure 3.4).

Table 3.2 Tophat mapping statistics of male (blue) and female (pink) samples.

Sample	# reads mapped	Overall mapping rate
CB1	138611090	81.60%
CB2	144741248	82.30%
CB3	133684910	82.40%
CB4	158742168	80.60%
CB5	169837416	80.50%
CB6	168417496	80.90%
CB7	158436486	81.40%
CB8	166296856	82.10%
CB9	189128974	82.90%
CB10	150660844	81.80%
CB11	149957806	82.40%

Furthermore, the two genes with the largest difference in expression between sexes were *Ddx3* and *Eif2s3y*, are located on the Y chromosome (Figure 3.3)**.** Additionally, there were ~300 genes that were statistically differentially expressed by at least 1.5 fold in one sex compared to the other (Figure 3.3B). To validate our results, we performed qPCR on a subset of mRNAs that were differentially expressed between the sexes and observed the same expression profile as was indicated by the RNA-sequencing results (Figure 3.5). For example, genes such as the transferrin receptor (*Tfrc)* and cytochrome C oxidase (*Cox6c*) were more highly expressed in the male cardiac myocytes by both qPCR and RNA-sequencing methods (Figure 3.5A). Similarly, expression of the uncoupling protein 2 (*Ucp2*) and P450 oxidoreductase (*Por*) genes were higher in the female myocytes in both the RNA-sequencing and qPCR datasets (Figure 3.5B).

3.3.3 Enriched pathways and regulators are distinct between the sexes

We next wanted to investigate the functional relevance of the sex-specific gene expression differences observed in cardiac myocytes by performing pathway analysis on genes that were up-regulated in either sex. Ingenuity pathway analysis (IPA), which integrates data across previously published studies, was used to identify different pathways, functions and

upstream regulators enriched in genes that were at least 1.5 fold higher in expression between male or female cardiac myocytes. We observed that canonical pathways predicted to be activated by IPA were distinct between sexes (Figure 3.6A). For example, signaling pathways such as Protein Kinase A (PKA), Wnt/Ca^{2+} and inducible nitric oxide synthase (iNOS) were activated in the female dataset, whereas integrin, Rac, and insulin receptor pathways were enriched in genes up-regulated in male cardiac myocytes. Furthermore, genes that were more highly expressed in female cardiac myocytes are involved processes such as gene expression, lipid and energy metabolism, and small molecular biochemistry (Figure 3.6B). However, the male enriched genes are more likely to function in regulating cell growth and movement, the cell cycle and cellular death processes. To understand more about the effectors responsible for the observed gene expression and pathway differences observed between male and female cardiac myocytes, we took advantage of the upstream regulator tools provided by IPA. We discovered that the types of upstream regulators enriched when analyzing genes abundant in either the male or the female cardiac myocytes were largely distinct, similar to what we observed with the activated pathways and cellular functions (Figure 3.6C). While there are some upstream regulators common in both the male and female datasets, the majority was specific to one sex. In total, appears that the sexually dimorphic gene expression differences in cardiac myocytes are focused in a pathway specific manner, which could have functional contractile consequences.

To further investigate the sex differences in activated signaling pathways in cardiac myocytes, I performed a phospho-kinase array with ARVM lysates. This method allows for the activation state of 45 signaling molecules to be analyzed simultaneously. Similar to the RNA-sequencing results, the differences in activated signaling molecules were not dramatic between the sexes (Figure 3.7). While only a few of the sex differences observed were statistically significant, the molecules that were differentially activated between sexes are consistent with the pathway analysis of our RNA-sequencing data.

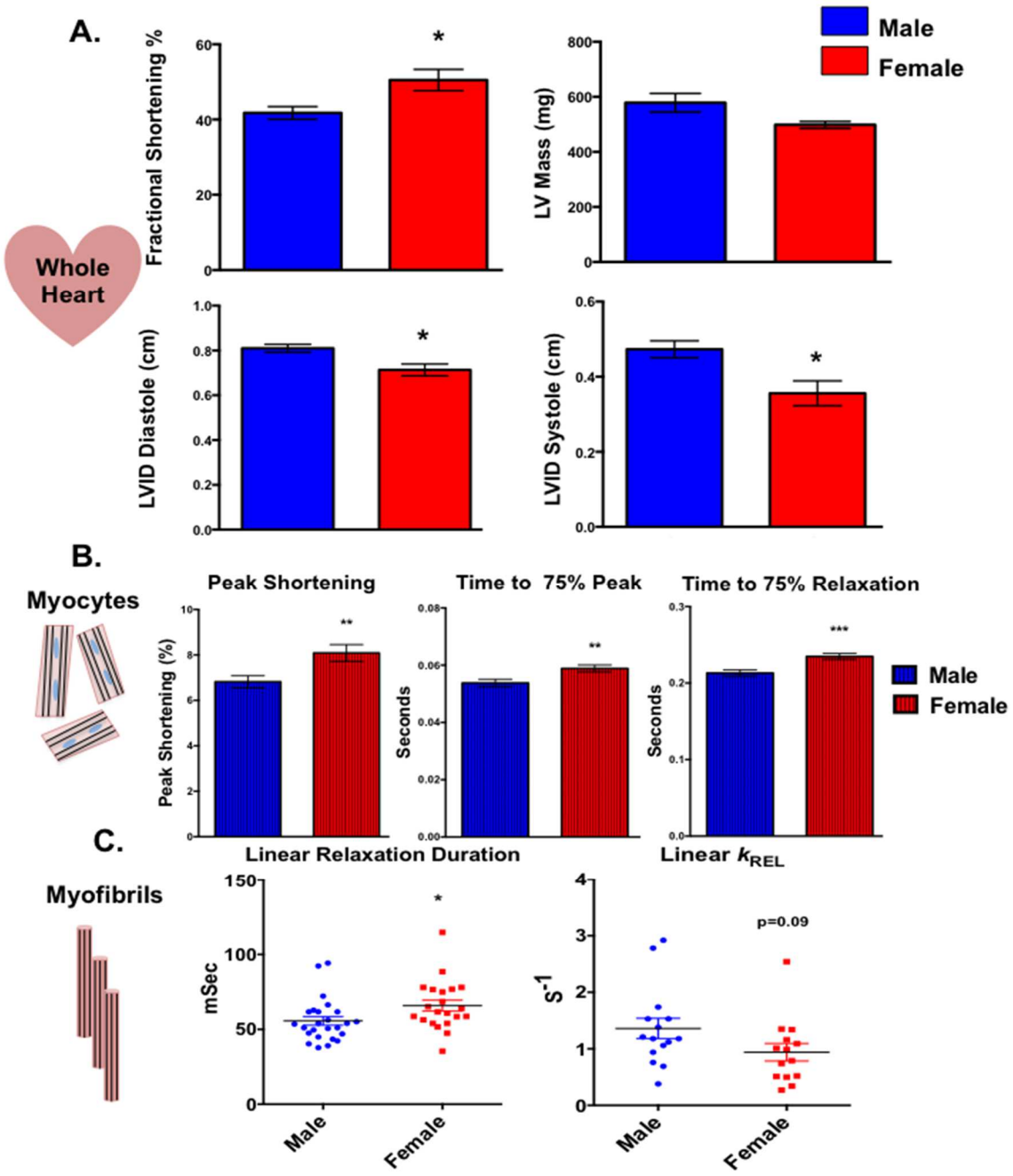

Figure 3.2: Cardiac function is sexually dimorphic from the level of the whole heart down to the myofibril. (A) *In vivo* whole heart function as measured by echocardiography in male and female rats. *p<0.05 relative to male, N=5 female and 6 males. **(B)** Contractile function of electrically paced ventricular myocytes from rats of both sex. **p<0.01, ***p<0.001 relative to male, N=97 female cells and 110 male cells pooled from 6 animals of each sex. **(C)** Kinetic properties of left ventricular myofibrils isolated from male and female rats. Linear relaxation duration: *p<0.05 relative to female, N=21 female and 25 male myofibrils from 3 separate animals. Linear KREL: N= 15 female and 14 myofibrils from 3 separate animals. All data

reported as mean ± SEM.

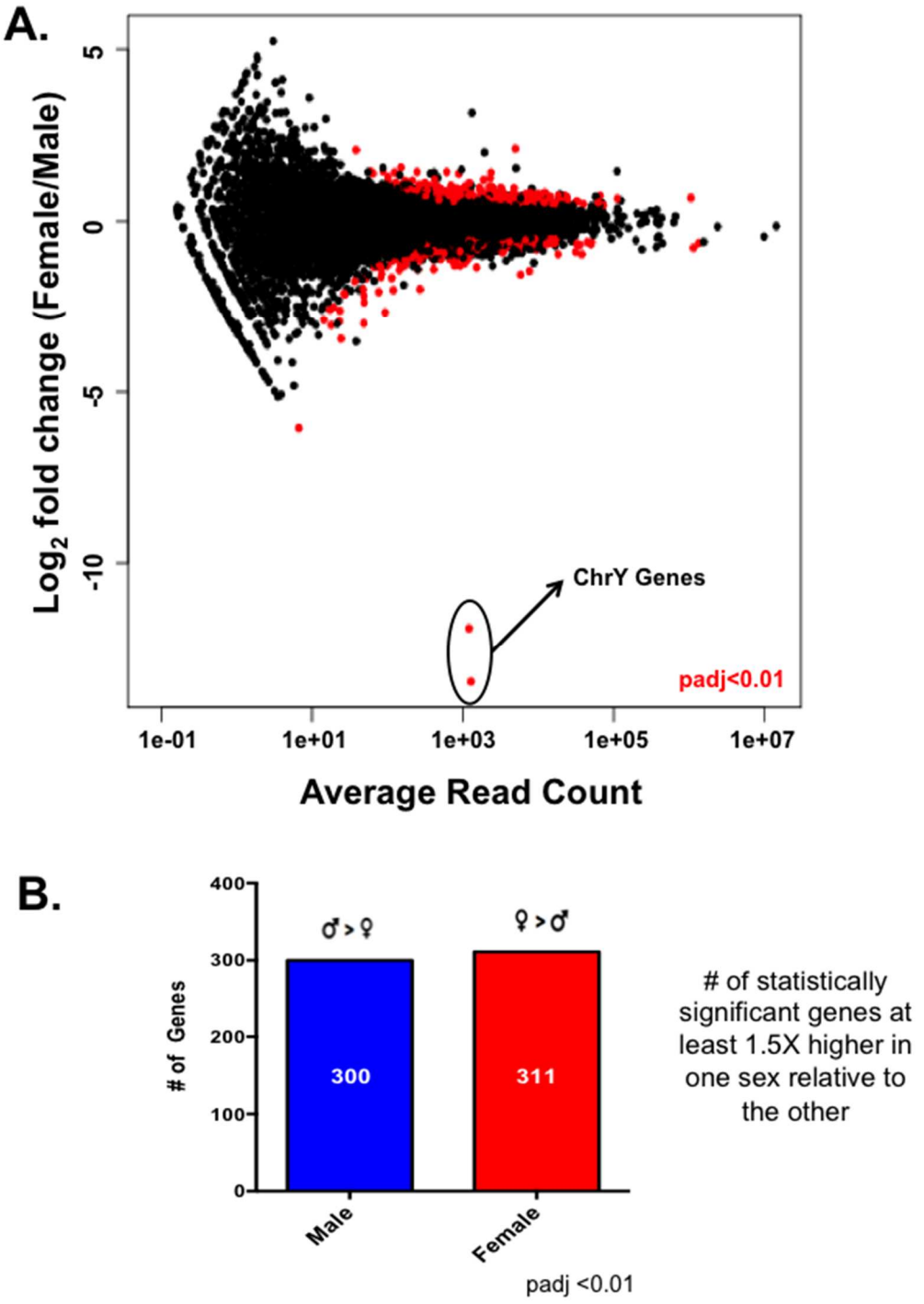

Figure 3.3: Male and female cardiac myocytes exhibit different transcriptome profiles. (A) Differential gene expression analysis between male and female cardiac myocytes as measured with DESeq. Statistically significant differentially expressed genes between the sexes are indicated by the red circles; padj <0.01 female relative to male, N=5 female and 6 male isolated cardiac myocyte preparations. **(B)** The number statistically significant (padj<0.01) genes at least 1.5X higher in one sex relative to the other as measured by DESeq; this list of genes was used for downstream analysis with IPA.

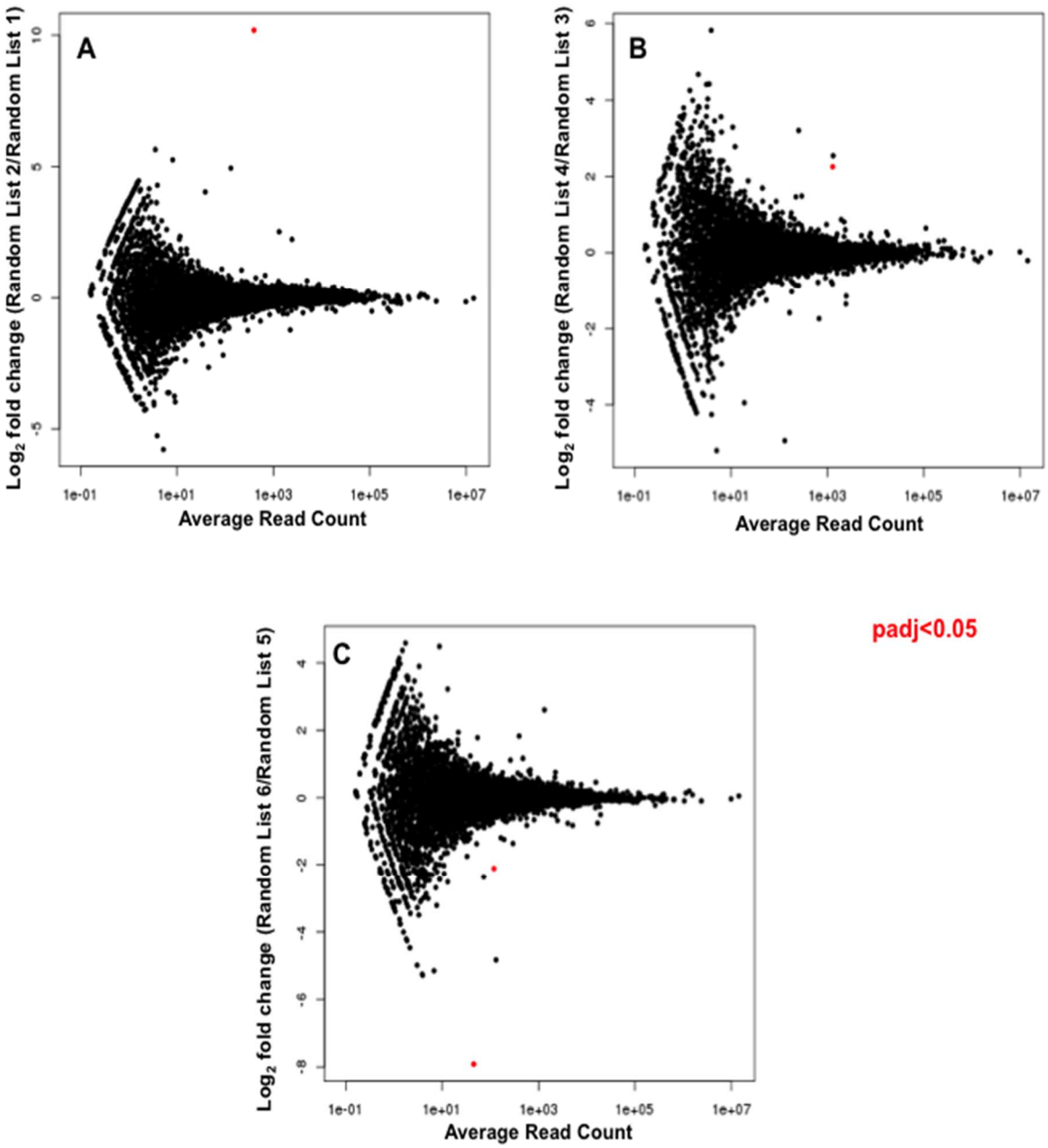

Figure 3.4: Differential gene expression is not observed when samples are randomly analyzed. Differential gene expression analysis using DESeq was performed with the cardiac myocyte samples randomly assigned to two groups, not based on sex. This random analysis was performed three separate times **(A, B, C).** Statistically significant differentially expressed genes between the sexes are indicated by the red circles; padj <0.05.

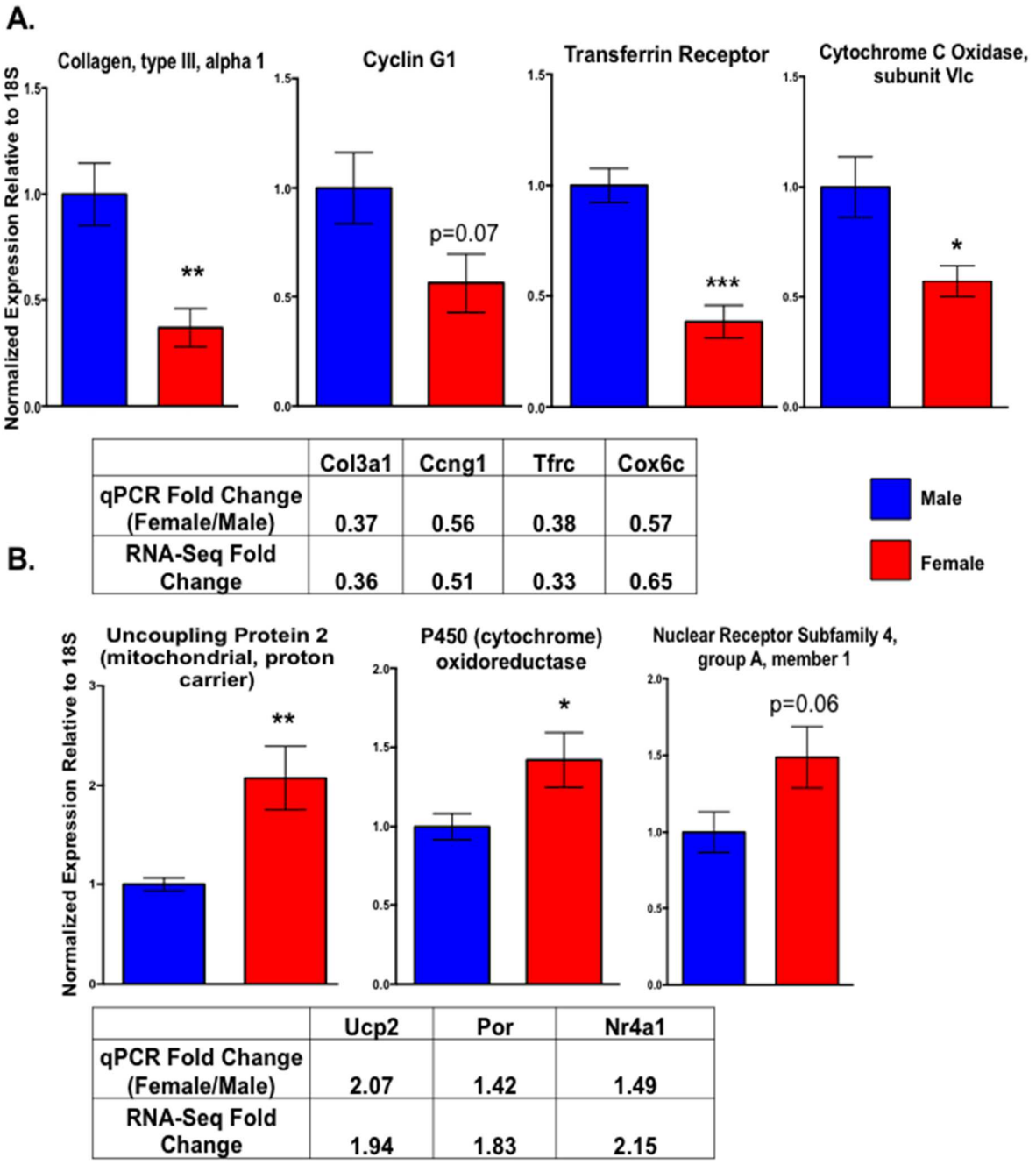

	Col3a1	Ccng1	Tfrc	Cox6c
qPCR Fold Change (Female/Male)	0.37	0.56	0.38	0.57
RNA-Seq Fold Change	0.36	0.51	0.33	0.65

	Ucp2	Por	Nr4a1
qPCR Fold Change (Female/Male)	2.07	1.42	1.49
RNA-Seq Fold Change	1.94	1.83	2.15

Figure 3.5: Validation of differentially expressed genes with qPCR also demonstrates that cardiac myocyte gene expression is sexually dimorphic. Expression of *Col3a1, Ccng1, Tfrc, Cox6c* **(A),** *Ucp2, Por, and Nr4a1* **(B)** as measured by qPCR in male and female cardiac myocytes. The mean fold changes (female relative to male) for each gene as found by qPCR and the RNA-sequencing experiment are indicated in the supplied tables. All genes were normalized to levels of 18S; *p<0.05, **p<0.01, ***p<0.001 female relative to male; N=5 female and 6 male isolated cardiac myocyte preparations. All data reported as mean ± SEM.

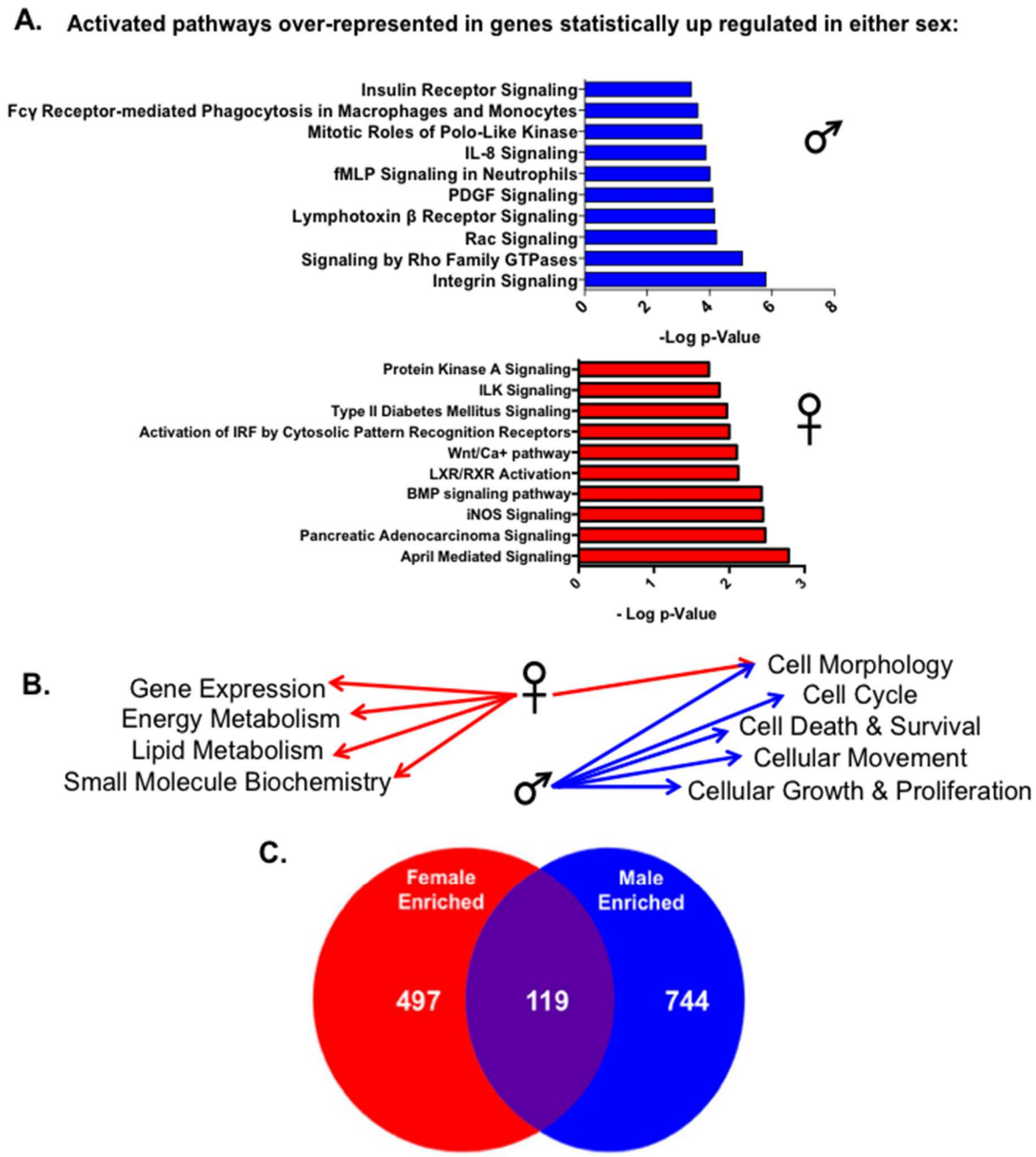

Figure 3.6: Specific pathways and functions are enriched in cardiac myocytes from either sex. IPA analysis of significantly expressed genes by at least 1.5 fold in either sex. **(A)** The top ten statistically significant canonical pathways predicted to be activated by IPA in genes unregulated in either male or female cardac myocytes. Pathways were deemed statistically significant by IPA if $p<0.05$ using the Fischer exact test. Activated pathways were indicated by positive z-scores calculated by IPA; for pathways that contained the same genes, the pathway with the lower p-value was listed. **(B)** The top five statistically significant (lower end of p-value overlap at least 0.05) molecular and cellular functions enriched in genes found to be upregulated in either male or female myocytes by IPA. **(C)** The number of statistically significant

($p<0.05$) upstream regulators enriched in up-regulated genes from either sex as measured by IPA analysis.

For example, the activation of the signaling proteins mTOR, Akt and p53 were higher in the male ARVMs (Figure 3.7). Activation of these proteins is associated with regulating cell growth, proliferation and division, which I observed to be enriched in the genes more highly expressed in the male ARVMs (Figure 3.6). However, when the activation of mTOR and Akt were analyzed by western blot to verify the array findings, the results of the westerns were not statistically different (data not shown).

To investigate the potential role estrogen may be playing in the differences I observed, I analyzed the genes that were statistically differentially expressed in one sex relative to the other by at least 1.5 fold for the enrichment of an estrogen response element (ERE) within 10kb of the start site (Figure 3.8). I observed only 30 genes that contained an ERE and were differentially expressed. However, when I performed hypergeometric probability analysis on this data, it appears that finding an enrichment of these 30 genes within the total 611 genes that were differentially expressed is statistically significant as the probability of drawing 30 or more successes from a population of 611 is 0.02 (Figure 3.8). Additionally, the majority of the genes shared between the two categories are more highly expressed in the female myocytes relative to the males.

3.3.4 Protein kinase A activity exhibits sex-specific profiles

Because PKA signaling is an important mediator in cardiac physiology (Parks & Howlett, 2013) and our IPA analysis indicated this pathway was activated in female myocytes (Figure 3.6A), we measured PKA activity in male and female cells. We observed that female cardiac myocytes displayed increased PKA activity compared to their male counterparts, consistent with our IPA analysis (Figure 3.6A). We next sought to perturb the PKA pathway and perform contractility assays in ARVMs from both sexes to determine the functional relevance of the

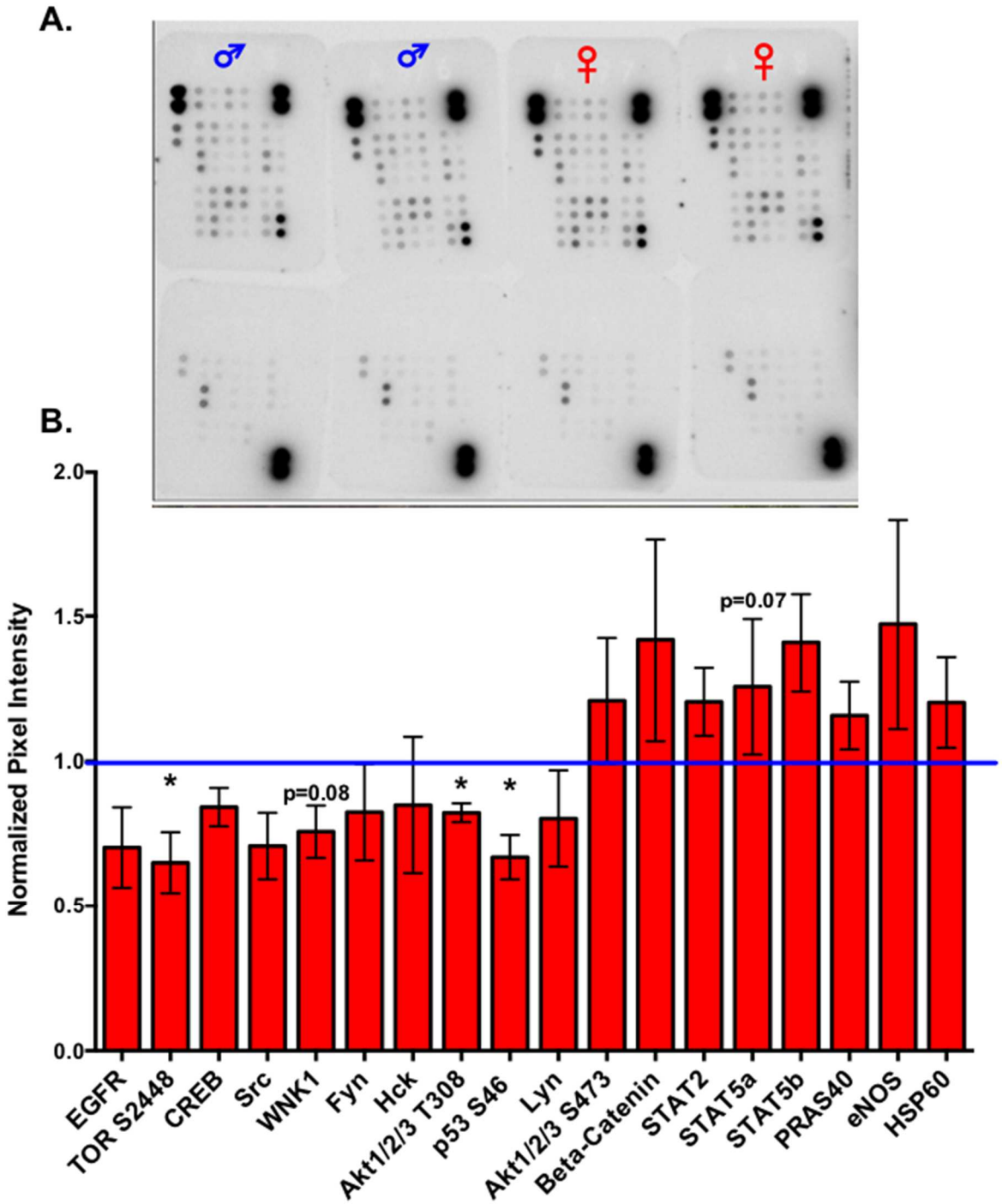

Figure 3.7 Sex differences in signaling pathway activation. (A) Representative antibody arrays analyzing the activation state of signaling molecules in male (left) and female (right) ARVM lysates. **(B)** Activation status of signaling molecules in female ARVMs that were at least 15% different compared to the males. Average pixel intensity for a given protein was normalized to the male samples (blue line). * $p<0.05$ by student's t-test; n= 4 arrays per sex with myocyte lysates from 2 animals pooled per array; error bars: ± SEM.

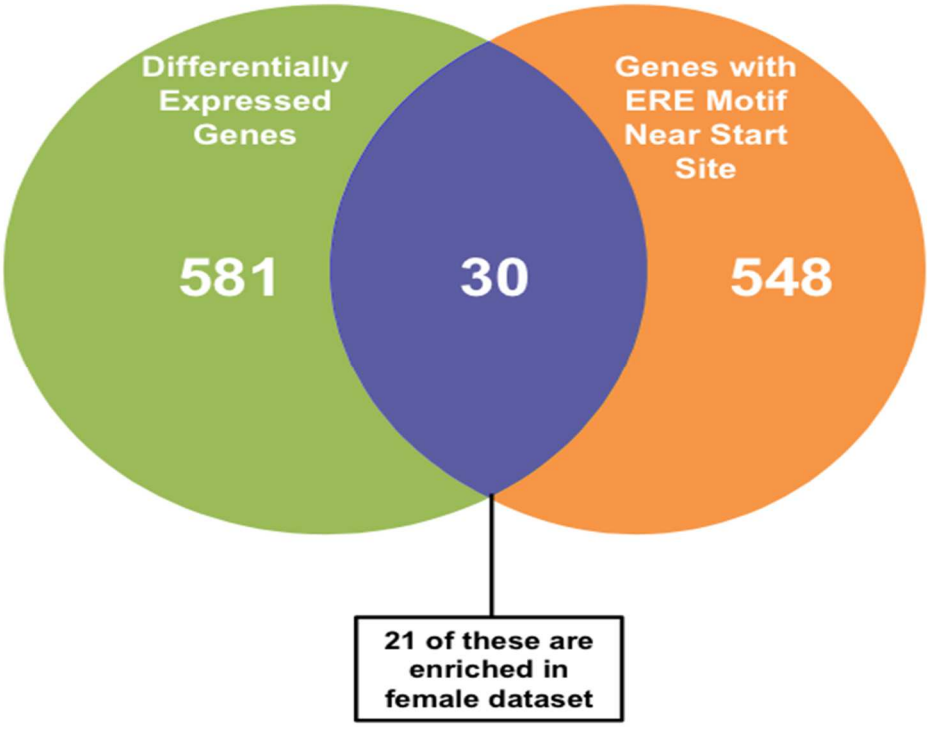

Figure 3.8: Sexually dimorphic cardiac myocyte genes contain EREs. Enrichment analysis of EREs within 10kb of start sites of genes that were significantly differentially expressed between male and female myocytes performed with genome-wide position weight matrix (PWM) scanner. Probability of discovering these 30 genes within the list of differentially expressed genes = 0.02 by hypergeometric probability analysis.

increased PKA activity we observed in the female cells. To perform this experiment we treated male and female ARVMs with the cyclic adenosine monophosphate (cAMP) mimic, Bucladesine, for 30 minutes to investigate how activating the PKA pathway in cells of both sexes affects contractile function. Similar to what we observe in non-treated cells (Figure 3.2B), the female DMSO treated cells took longer to reach peak shortening as well as to fully relax relative to their male counterparts (Figure 3.9B). However, the time it took the male and female bucladesine treated myocytes to reach peak shortening and relaxation was not statistically different from each other (Figure 3.9B). This suggests that activating the PKA pathway in both sexes is somehow mitigating the functional differences observed in the DMSO control cells. Because troponin I is a target of PKA, we assessed its phosphorylation status. Interestingly,

male ARVMs displayed a slight increase in p-troponin I in response to bucladesine treatment, but p-troponin I levels actually decreased after treatment in the female cells (Figure 3.9C).

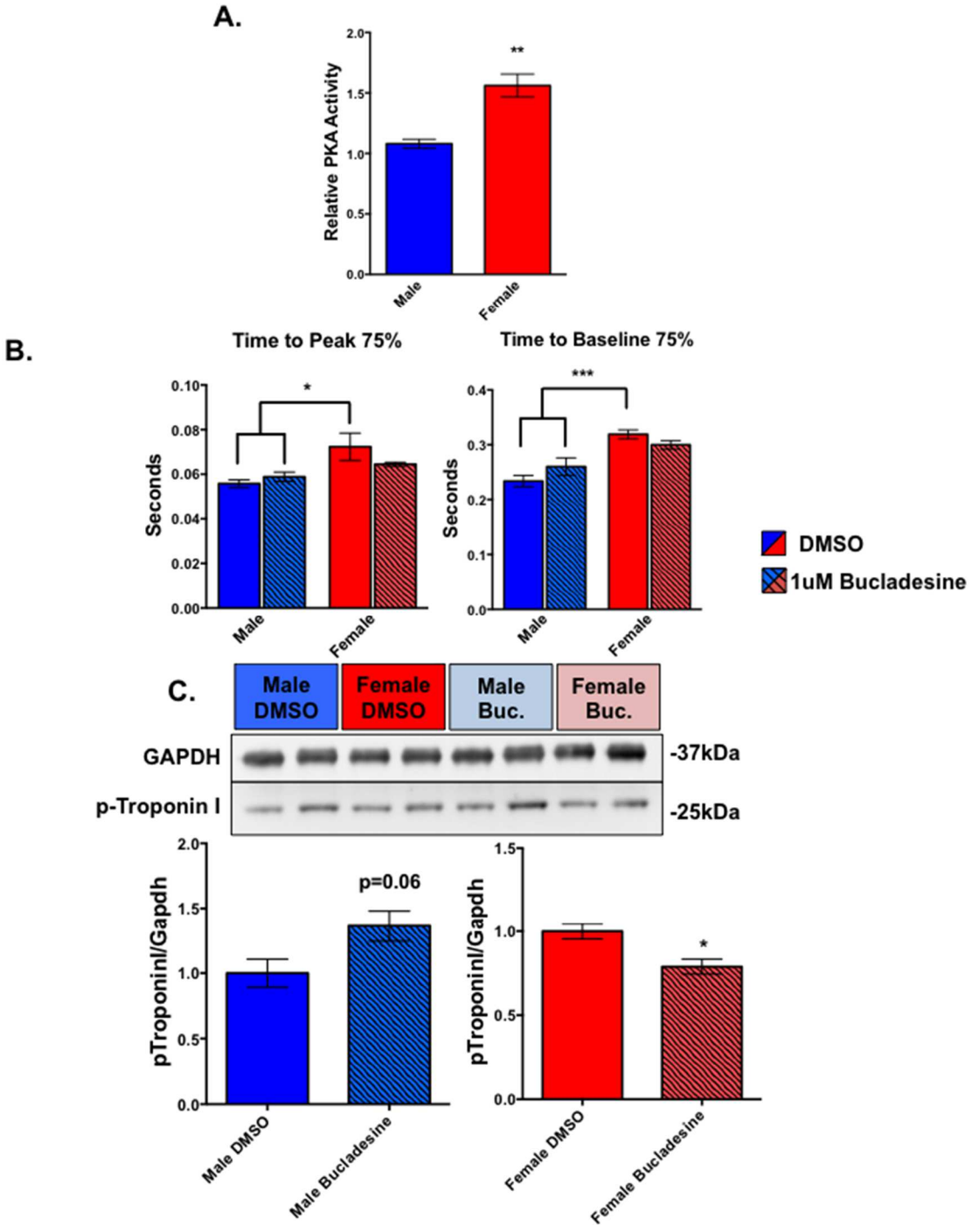

Figure 3.9: PKA activity is sexually dimorphic in cardiac myocytes. (A) Levels of PKA activity in male and female cardiac myocytes as measured by PKA activity assay. **p<0.01 female relative to male; n=4 animals of each sex. All data reported as mean ± SEM. **(B)** Contractile function of electrically paced ventricular myocytes treated with bucladesine or DMSO

for 30 minutes from rats of both sex. *p<0.05 relative to female DMSO; n= at least 19 cells per group pooled from 4 animals of each sex. **(C)** Quantification and representative immunoblot of p-Troponin I levels present in male and female ARVMs treated with bucladesine for 30 minutes.

3.4 Discussion

3.4.1 Baseline cardiac function is sexually dimorphic at multiple tissue levels

While there have been multiple reports analyzing the functional differences between male and female cardiac myocytes at baseline, to our knowledge, this is the first report to demonstrate that functional sex differences exist from the level of the whole heart to the myofibril. Sex differences in whole heart function have been debated within the literature. However, in our study we consistently observed female rats to have better function as indicated by higher fractional shortening compared to the males, which has been reported before in humans, mice and rats (Haines, Harvey, & Leinwand, 2012; Litwin et al., 1999; Prabhavathi et al., 2014). Our data also demonstrate this functional difference is apparent at the level of the cardiac myocyte with female cells displaying greater percent shortening but taking longer to contract and relax. While other studies have also observed that female myocytes reach peak shortening and relaxation more slowly that male cells, previous reports have commonly observed male myocytes to exhibit greater contractile function, which contrasts with our findings (Curl, Wendt, & Kotsanas, 2001). However, a variety of differences in procedures during the contractility studies, such as temperature or pacing frequency, (Reviewed in(Parks & Howlett, 2013)) could account for these differences and it is promising that our *in vivo* echocardiographic data support the functional differences we observed in the isolated myocytes. This is also the first report comparing isolated myofibrillar function between sexes, further validating that the duration of the relaxation phase is consistently longer in females which is most likely due to differences in the myofibril proteins themselves since we observed this in both isolated cells and myofibrils. These results are particularly interesting considering that women are more likely to develop HFpEF, which is characterized by diastolic left ventricular dysfunction, stiffness as well

as reduced ventricular relaxation (den Ruijter et al., 2015). The prolonged relaxation times we observed in female cardiac myocytes and myofibrils at baseline, in combination with aging, may provide the underlying mechanism that predisposes women to developing HFpEF.

3.4.2 Sexually dimorphic gene expression mediates the functional differences observed at baseline

Many past studies have focused on how estrogen signaling mediates the sexual dimorphisms in cardiac disease development and while we acknowledge the importance of estrogen in the heart, we also sought to understand what other mechanisms could be involved. Additionally, we have previously described that ER transcript expression is quite low, restricted to ERα and not sexually dimorphic in cardiac myocytes (Pugach et al., 2016), prompting our interest in understanding what other pathways are involved in mediating the functional sex differences we observed at baseline. By exploring broad gene expression differences between sexes in myocytes from healthy animals, we aimed to gain further insight into how biological sex influences cardiac function and eventually disease development within the cardiac myocyte.

Sexually dimorphic gene expression differences have been previously reported in multiple somatic tissues including, liver, adipose, brain and muscle (X. Yang et al., 2006; Yu et al., 2014). Similar to what we observed in the isolated cardiac myocytes, there are many genes that are differentially expressed between the sexes with modest fold-changes, however, the genes changes are highly tissue specific and are enriched for distinct signaling pathways (X. Yang et al., 2006). While not many exist, there are several previous reports have that sought to describe sex differences in cardiac gene expression. A study analyzing healthy human as well as mouse hearts reported only a modest number of genes (~30-125) that were expressed in a sexually dimorphic manner (Isensee et al., 2008). However, a previous microarray study in our lab analyzing mouse left ventricles reported sex-specific expression of ~2000 genes with most of the genes being enriched in the male samples (Haines, Harvey, et al., 2012b). While we

detected around 600 genes that were differentially expressed in cardiac myocytes from either sex, we did not observe a difference in the overall number of genes that were more highly expressed in one sex relative to the other (Figure 2B). These previous studies analyzed whole heart and ventricle samples, which due to the many different cardiac cell types could account for the contrast between our findings. Additionally, the previous studies utilized microarray methods to detect differential expression, which would have missed genes not present on the array, whereas our RNA-sequencing data provides an unbiased and large-scale approach to detect differences. Interestingly, a large number of genes (~1800) were differentially expressed in left ventricle samples from male and female patients with dilated cardiomyopathy (Fermin et al., 2008). Similar to our findings, the majority of the fold changes in gene expression reported in the study were modest (~1.5-2.0), suggesting that biological sex does not mediate large individual changes, but perhaps the enriched pathways are the most important for mediating functional differences.

Irrespective of tissue type, all studies reporting sex specific differences in gene expression also observed enrichment for distinct pathways. Sexually dimorphic enrichment of pathways such as the immune response and lipid metabolism appear to be strongly conserved among a variety of tissues such as liver, adipose, heart as well as in our cardiac myocyte samples (Figure 3.6) (Isensee et al., 2008; X. Yang et al., 2006; Yu et al., 2014). Previous reports in the heart have observed GeneOntology categories such as metabolism, signaling transduction, regulation of cell growth, size and cell death to be enriched in a sex-specific manner (Haines, Harvey, et al., 2012b; Isensee et al., 2008). Our results agree with these reports as Rho and Rac signaling and genes involved in regulating cell growth and death were enriched in male cardiac myocytes, whereas female myocytes were enriched for processes such as energy metabolism and gene expression (Figure 3.6). Our dataset allows a more focused view of which pathways are sex-specific within the cardiac myocytes themselves. For example, I observed enrichment of the integrin signaling pathway and cell cycle functions in the

genes up-regulated in male cardiac myocytes, but these were not consistently seen between the previous whole heart studies. While it may seem surprising that genes involved in regulating cell cycle functions were enriched in adult cardiac myocytes, reports have reviewed the idea that a variety of cell cycle genes, such as cyclin G1 and c-myc, are actually involved in regulating the cardiac response to hypertrophic stimuli (Ahuja, Sdek, & MacLellan, 2007). I observed the PKA and inducible nitric oxide synthase (iNOS) pathways to be enriched in genes that were more highly expressed in female cardiac myocytes, which also appear to be myocyte specific, however a more thorough gene expression analysis in the whole heart would need to be performed to definitively understand this observation. I also observed sex specific differences at the protein level in my phospho-kinase analysis of ARVM lysates with proteins involved in cell growth, proliferation and cell division being more highly activated in the males relative to the female cells (Figure 3.7) (Manning & Cantley, 2007). While these differences were not confirmed with western blot, this could be due to variations in the protein epitopes of the antibodies used in each of the two methods.

Many of the pathways and processes we observed to be sex-specific are extremely important in maintaining cardiac function. Integrin signaling, which we observed to be enriched in male cardiac myocytes relative to the females, is an integral pathway within the cardiac myocyte as it is involved in maintaining adhesions with the extracellular matrix, but also in mechanotransduction and responding to hypertrophic stimuli (Israeli-Rosenberg, Manso, Okada, & Ross, 2014). Additionally, estrogen supplementation of cardiac fibroblasts attenuated the angiotensin-II increases in β1-integrin expression (Stewart, Cashatt, Borck, Brown, & Carver, 2006), suggesting a potential mechanism by which integrin signaling is lower in female cardiac myocytes. Of the genes that were differentially expressed between male and female cardiac myocytes, I only observed 30 that contained an ERE, but this enrichment appears to be statistically significant, further implicating an influence of estrogen on mediating this differential expression (Figure 3.8). However, this data must be considered carefully, since estrogen

signaling is extremely complex and just because a gene contains an ERE does not mean that it is regulated by estrogen, especially in cardiac cells (Heldring et al., 2007; Knowlton & Lee, 2012).

PKA signaling is extremely important in maintaining proper cardiac function as well as in responding to increases in metabolic demands that was enriched in a sexually dimorphic manner in cardiac myocytes. We also observed the female cardiac myocytes exhibit higher PKA activity at baseline relative to their male counterparts, further validating our RNA-sequencing results (Figure 3.9A). Additionally, treating ARVMs with the cAMP mimic bucladesine abrogated the sex specific difference in the time it took the cells to reach peak shortening or relax (Figure 3.9B). This suggests altering PKA signaling is somehow affecting the cells from either sex differently since the males experienced a slight, but not statistically significant, increase in the time it took them to reach peak shortening and baseline, but the opposite was observed in the female cells. Because PKA signaling generally results in decreased calcium sensitivity in addition to increased relaxation rates, the increased PKA activity in the female cells was surprising. However, there are conflicting reports regarding the effect PKA activation has on myofibril relaxation rates, and it appears, based on our data, that sex mediates differences in this pathway (Rao et al., 2014; Walker, Walker, Margulies, Buttrick, & de Tombe, 2011).

Because tropoinin I is a common target phosphorylation target of PKA at Ser23/24, we analyzed p-troponin I levels in response to bucladesine in order to measure the effectiveness of the treatment. While we observed an increase in p-troponin I levels in the male cells, p-troponin I actually decreased in the female cells (Figure 3.9C). This was particularly surprising because even though phosphorylation of troponin I reduces the sensitivity of the myofilament to calcium, it has also been reported to accelerate relaxation, but this is not what we observed (Layland, Solaro, & Shah, 2005). However, our results could be due to a variety of different factors such as the bucladesine treatment protocol. A common dose of bucladesine or its equivalent Dibutyryl cAMP in the literature is 1mmol/liter (Somekawa et al., 2005), which is much higher

than the dose we used for our experiments. However, when we initially performed our contractility experiments with the 1mmol/liter dose, the cells could not maintain proper contraction upon electrical pacing (Figure 3.10A). This prompted us to perform a dose response study, which led to both an increase in p-troponin I levels as well as consistent, reliable contractions in male ARVMs (Figure 3.10A,B). A more likely explanation of our results is most likely a difference in the expression or phosphorylation of other proteins such as phospholamban or myosin binding protein-C, which are also know to be phosphorylated in response to PKA activation and should be investigated in the future.

To our knowledge, this study is the first to observe sex differences a multiple levels of the cardiac structure in a single model as well as report sexually dimorphic gene expression within cardiac myocytes. Additionally, our RNA-sequencing analysis was able to identify an important cardiac signaling pathway, the PKA pathway, which appears to be differentially regulated between the sexes. While understanding the influence biological sex exerts on the cardiovascular system is complex, more studies, particularly during healthy baseline conditions, are needed. By obtaining a more thorough picture of how the cardiovascular system differs between men and women, we will be better prepared to effectively treat all CVD patients.

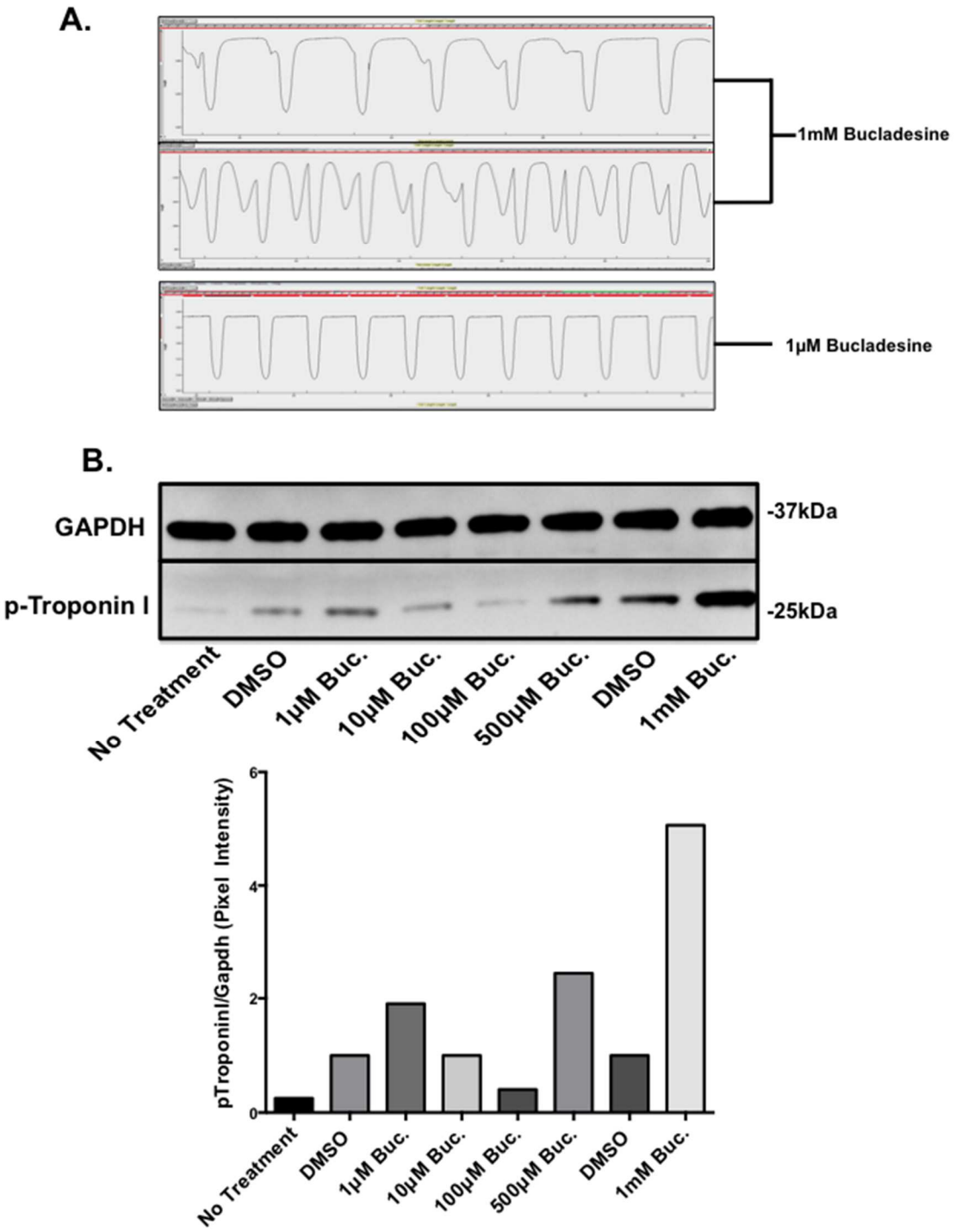

Figure 3.10: Determining appropriate bucladesine dose treatment in ARVMs. (A) Representative myocyte contractility traces obtained with IonOptix software of ARVMs treated with either 1mM bucladesine (top) or 1µM bucladesine for 30 minutes prior to contractility experiment. **(B)** Analysis of PKA pathway activation in ARVMs in response to varying doses of bucladesine (Buc.) treatment for 30 minutes by measuring p-troponin I levels relative to GAPDH by western blot (top), quantification of western blot (bottom).

Chapter 4 Conclusions and Future Directions

In this thesis I present work that helps elucidate the complex nature of ERα signaling within neonatal and adult cardiac myocytes. Through these experiments I unexpectedly discovered that ERα expression and localization both in the presence or absence of physiological levels of estrogen, is not different between male and female myocytes. Because sex differences in cardiovascular function and disease development have been well documented, I sought to further understand how biological sex could be influencing cardiac myocyte function since estrogen signaling between the sexes was not different. I revealed that cardiac functional differences are present in the rat model at the level of the whole heart, isolated cardiac myocytes and myofibrils, further warranting more information about the importance of biological sex in the heart. I discovered that cardiac gene myocyte expression is sexually dimorphic with around 600 genes being differentially expressed between the sexes. Furthermore, this sex-specific gene expression appears to be functionally relevant as distinct signaling pathways, such as the integrin and PKA pathways, were enriched in a sexually dimorphic manner. I also provided evidence that the PKA pathway plays an important role in mediating the functional differences observed in cardiac myocytes from either sex. While these studies have provided valuable information about the baseline sex differences and the role of ERα within cardiac myocytes, there are still some remaining questions.

4.1 ERα isoform signaling in adult cardiac myocytes

In chapter 2, in collaboration with Dr. Emily Pugach, ERα signaling was extensively characterized in neonatal (NRVMs) and adult cardiac myocytes (Pugach et al., 2016). However, there are some unique findings in the adult cardiac myocytes experiments that warrant further investigation. For example, while all three EGFP-tagged ERα variants primarily displayed nuclear localization, independent of estrogen treatment in the NRVMs, we consistently observed that the *ERα36-EGFP* construct also localized to the cytoplasm and intercalated disks within

transfected ARVMs (Figure 4.1). This non-nuclear localization was observed in both the male and female ARVMs, independent of estrogen treatment. However, while we observed that full-length ERα is the functionally relevant isoform for cardiac myocytes and its principal

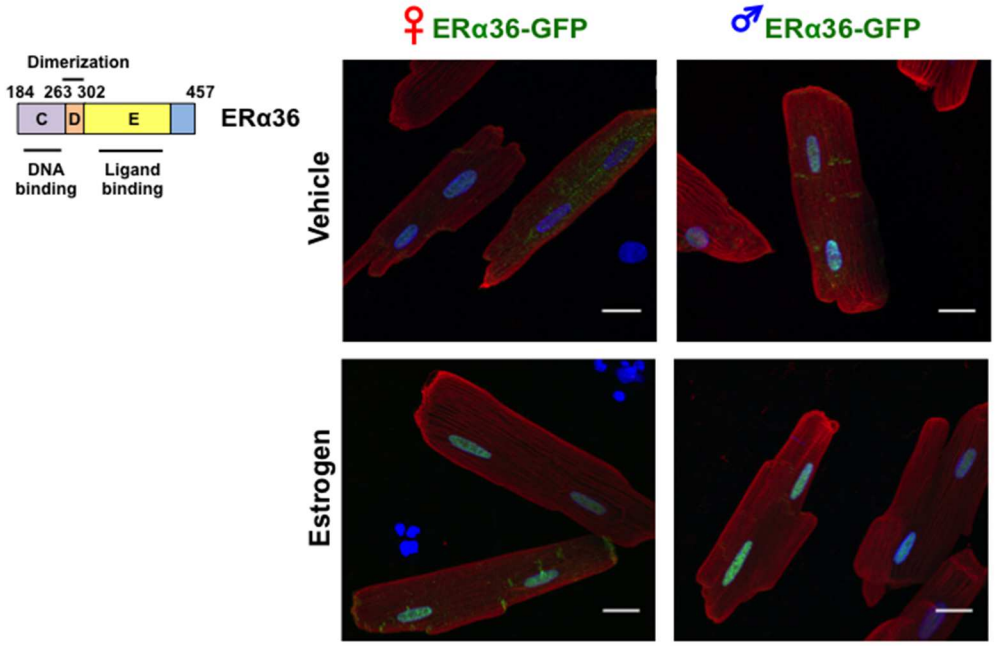

Figure 4.1: *ERα36-EGFP* localization is cytoplasmic and nuclear in ARVMs. Fluorescence based subcellular localization of each GFP-tagged ERα36 variant relative to DNA (DAPI) or myosin (F59) following treatment with either vehicle or 100 pM 17β-estradiol using confocal microscopy. 100X magnification; scale bar: 15μm.

mechanism of signaling is through transcriptional activation, we only performed the transcriptional activity and rapid signaling assays in the neonatal cardiac myocytes, not in the adult cells (Figure 2.10A). Therefore, the unique localization of ERα36 in the ARVMs could potentially be indicative of a specialized rapid-signaling role of ERα36 in the adult cells, but further experimentation is required to elucidate the role of ERα36 outside of the nucleus. Additionally, the intercalated disk localization suggests ERα36 could also be interacting with gap junction proteins, such as connexin-43. Previous reports have implicated that estrogen signaling affects the phosphorylation of connexin-43 in cardiac myocytes potentially through membrane initiated signaling pathways (T. H. Chung, Wang, & Wu, 2004). Future experiments, such as

analyzing co-localization of both connexin-43 and ERα36, in *ERα36-EGFP* infected ARVMs from both sexes, could shed light on this question.

4.2 Sex differences in cardiac myocyte function and gene expression

Data presented in chapter 3 revealed that gene expression and enriched signaling pathways are sexually dimorphic in cardiac myocytes during baseline conditions. Specifically, the PKA pathway appears to be an important mediator of the functional contractility and gene expression differences observed between male and female cardiac myocytes. However, as mentioned in chapter 3, the functional response of both the male and female myocytes to the cAMP mimic bucladesine, was unexpected and brought up some future experimental questions. For example, after bucladesine treatment, I observed an increase in p-troponin I levels in the male cells, p-troponin I actually decreased in the female cells (Figure 3.9C). This decreased p-troponin I in the female myocytes was observed in conjunction with these cells taking less time to relax, which is generally the opposite of what is described in the literature. However, because contractility is highly dependent on calcium handling within the cardiac myocytes, and calcium is tightly controlled within the cells, there are many calcium-handling proteins that are also regulated by PKA signaling that could be involved in this unexpected result.

PKA mediated phosphorylation of the L-type calcium channel leads to an increase size of the calcium current causing enhanced contractions (Reviewed in(Parks & Howlett, 2013)). Phosphorylation of phospholamban by PKA relieves phospholamban's inhibition on the activity of the sarcoendoplasmic reticulum calcium ATPase (SERCA) allowing for a more rapid decay of the calcium transient. Additionally, the calcium-calmodulin kinase II (CamKII) pathway can also regulate the activity of these proteins, altering contractile function. All of this taken together suggests that the expression and phosphorylation status of the L-type calcium channel and phospholamban as well as CamKII activity should be analyzed in cardiac myocytes from both sexes to better understand the functional sexual dimorphisms that exist at baseline.

Furthermore, because PKA itself is activated by stimulation of the β- adrenergic pathway, analyzing the expression and activity of the different components of this signaling pathway such as adenylyl-cyclase, guanine nucleotide binding proteins (G-proteins) and the adrenergic receptors themselves, would also help elucidate the complicated signaling differences that exist in cardiac myocytes from either sex.

As previously mentioned, calcium handling is a critical mediator of cardiac function primarily through regulating the cardiac action potential. There have been many previous studies that have analyzed sex differences in calcium levels as well as action potential waveforms between male and female cardiac myocytes. While differences in calcium levels as well as action potential duration have been observed in a variety of studies, the results are not consistent between reports. This could be due to a variety of reasons such as differences in animal models and experimental conditions, but it makes drawing conclusions challenging (Reviewed in:(Parks & Howlett, 2013)). One of the most common methods used to measure calcium levels and action potentials rely on the use of calcium or voltage-sensitive dyes, however there are drawbacks to these methods that may be contributing to the variations in results between studies. For example, depending on which calcium indicator that is used, the dye can be sequestered to other parts of the cell such as the sarcoplasmic reticulum or the nucleus, which can make quantifying the signal difficult (Hagen, Boyman, Kao, & Lederer, 2012). Another draw back of using dyes, especially voltage-sensitive dyes for measuring action potentials, is phototoxicity that can occur during while recording data (Hou, Kralj, Douglass, Engert, & Cohen, 2014).

To overcome these obstacles, using genetically encoded calcium or voltage indicators is generally the preferred method. To this end, I sought to develop a reliable tool in the lab to effectively analyze calcium and voltage differences in adult cardiac myocytes from either sex to further understand the functional and signaling differences I had been observing. Recently Dr. Joel Kralj and his colleagues developed a lentiviral dual calcium-voltage reporter (CaViar) that

allows for the measurement of calcium and voltage transients simultaneously within cells and even whole hearts (Hou et al., 2014). Dr. Kralj graciously allowed me to use his construct to develop an adenovirus capable of expressing the CaViar reporter since adult cardiac myocytes are notoriously difficult to infect with lentivirus (Kaestner et al., 2014). Adenovirus production was performed using the AdEasy-1 kit (Qbiogene) as described in chapter 2 and pictured in Figure 4.2. I have been able to infect adult cardiac myocytes with this adenovirus and effectively quantify the rate of calcium transients within the cells upon electrically pacing at a frequency of 1Hz (Figure 4.3). However, I have only been able to detect and quantify changes in the voltage reporter in the neonatal cells, but have been unsuccessful in the adult cardiac myocytes (data not shown). This could be due to a variety of factors, but it is most likely due to differences in the required concentration of retinol that the cells must be treated with prior to the experiment in order to activate the voltage-reporter. Further experimentation is needed to optimize these experiments, but once completed, this could be an incredibly valuable tool for the lab.

4.3 Sexual dimorphisms in the cardiac myocyte during pathological hypertropy

All of the data presented and discussed so far have been investigating the sex differences within cardiac myocytes during baseline, non-pathological conditions. However, as discussed in chapter 1, there are many sex-specific differences in the development and presentation of a variety of cardiovascular diseases, both in humans as well as in animal models. This leads to investigating if the sex differences in function, gene expression and signaling pathways in cardiac myocytes detected at baseline play a role in mediating the differences that exist in response to pathologic conditions. In collaboration with a post-doctoral fellow in our lab, Dr. Angela Peter, we have started to investigate this question by analyzing cardiac myocytes that have been isolated from rats of both sexes that were treated with

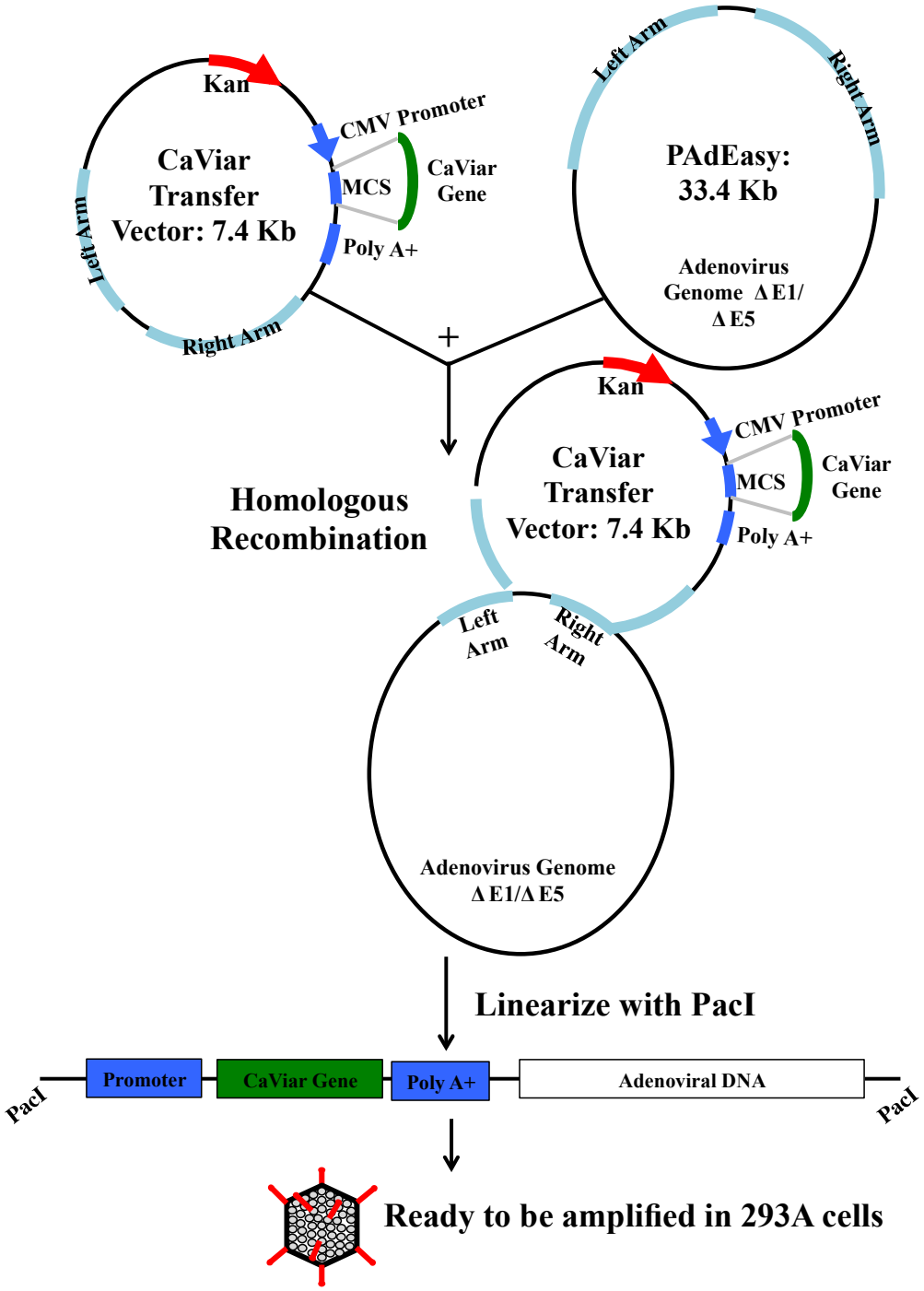

Figure 4.2: Generation of CaViar adenovirus using the AdEasy system.

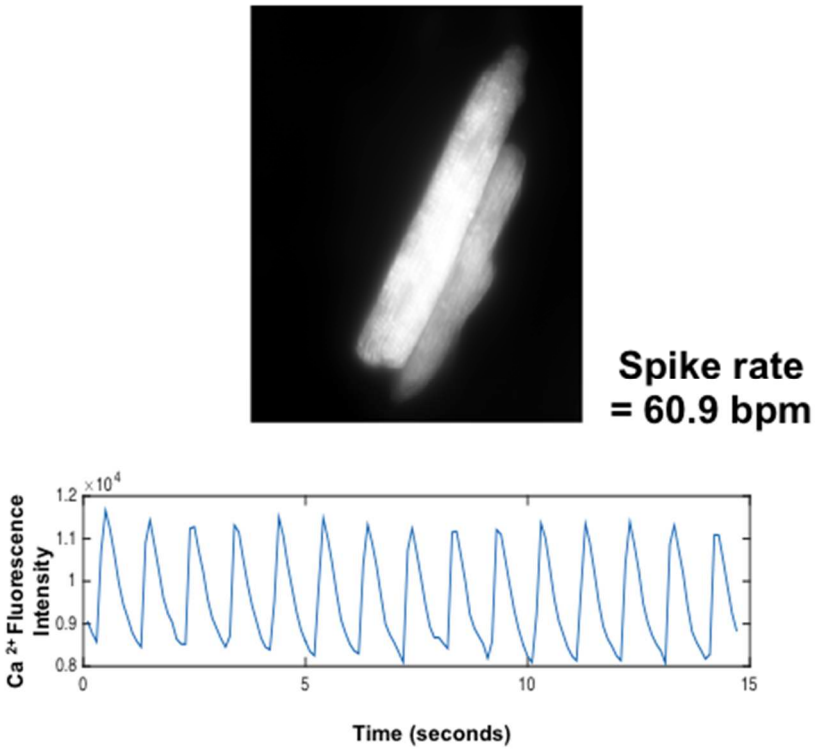

Figure 4.3: Quantification of calcium transients in CaViar infected ARVMs. Representative analysis of calcium transients in CaViar infected ARVMs analyzed with MatLab.

with either vehicle (1μM ascorbic acid in saline) or the β-adrenergic agonist, isoproterenol (ISO) for 7 days via osmotic minipump. This study is particularly interesting because while previous investigators have analyzed sex differences in response to ISO treatment, these studies only analyzed the effect of a short, acute treatment, whereas we are interested in what happens in the myocyte after a chronic disease state is induced (J. Chen et al., 2003; Curl et al., 2000; Vizgirda et al., 2002). Echocardiography and cardiac myocyte contractility analysis were performed in the same manner as described in chapter 3 to investigate if sex differences exist in the whole heart and cardiac myocytes in response to drug treatment.

First, we needed to establish an effective ISO concentration in the rat model. In a pilot experiment testing three different doses of ISO in male rats, we found that a dose of 4mg/kg/day of ISO was the most effective dose at inducing significant cardiac hypertrophy (Figure 4.4). ISO treated male and female rats both showed a significant increase in heart and left ventricle

weight (Figure 4.5). However, we only observed an increase in right ventricle weight in the ISO treated male samples (Figure 4.5). Isolated cardiac myocytes used for the contractility assay were shorter in the females relative to the males, irrespective of ISO treatment (Figure 4.6A), which is likely indicative of the smaller baseline heart weight of the females (Figure 4.5A). Similar to the echocardiography data in Figure 4.4B, we did not observe a statistical increase in peak shortening in response to ISO treatment in cells of either sex (Figure 4.6A). In both sexes, myocytes isolated from ISO treated animals took less time to reach peak shortening as well as displayed an increased departure velocity (Figure 4.6B,C). However, only myocytes isolated from male ISO treated animals took less time to relax and exhibited an increased return velocity (Figure 4.6B,C). These differences in relaxation parameters are similar to what we observed at baseline conditions and could potentially be cardioprotective for the female animals as the male rats were much more likely to die in response to ISO treatment (data not shown). Further experiments analyzing gene expression and activated signaling pathways in the whole heart and myocyte samples from this study will hopefully provide more insight into the mechanisms responsible for the relaxation differences observed in the isolated myocytes.

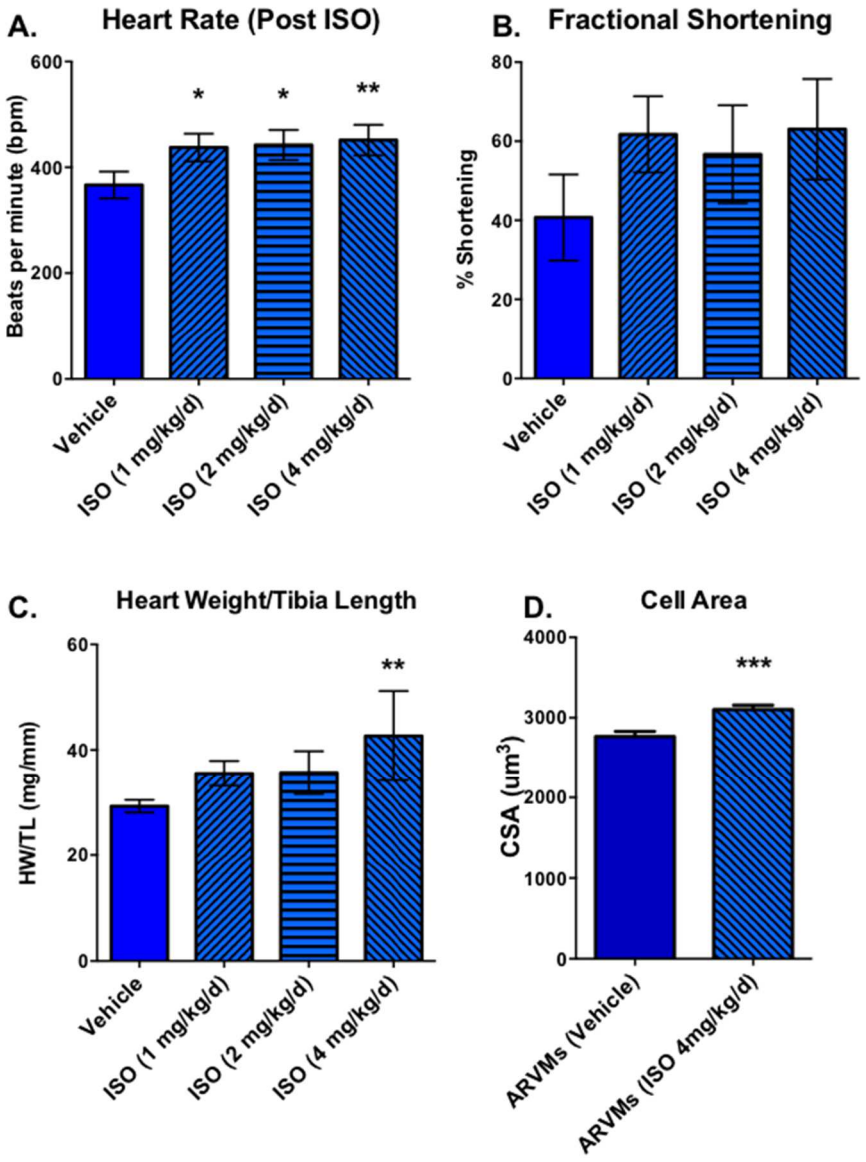

Figure 4.4: Determining appropriate isoproterenol (ISO) treatment in male rats. (A, B) *In vivo* echocardiograph data analyzing whole heart function. *p<0.05 vs. vehicle group with One-way ANOVA, Dunnett's *post hoc*; n= 2-4 animals per group. **(C)** Whole heart weight normalized to tibia length in vehicle or ISO treated animals. **p<0.01 vs. vehicle group with One-way ANOVA, Dunnett's *post hoc;* n=4-5 animals per group. **(D)** Cell area measurements performed with ImageJ software. ***p<0.001 vs. vehicle with student's t-test; n=at least 150 cells per group. All data reported as ± SEM.

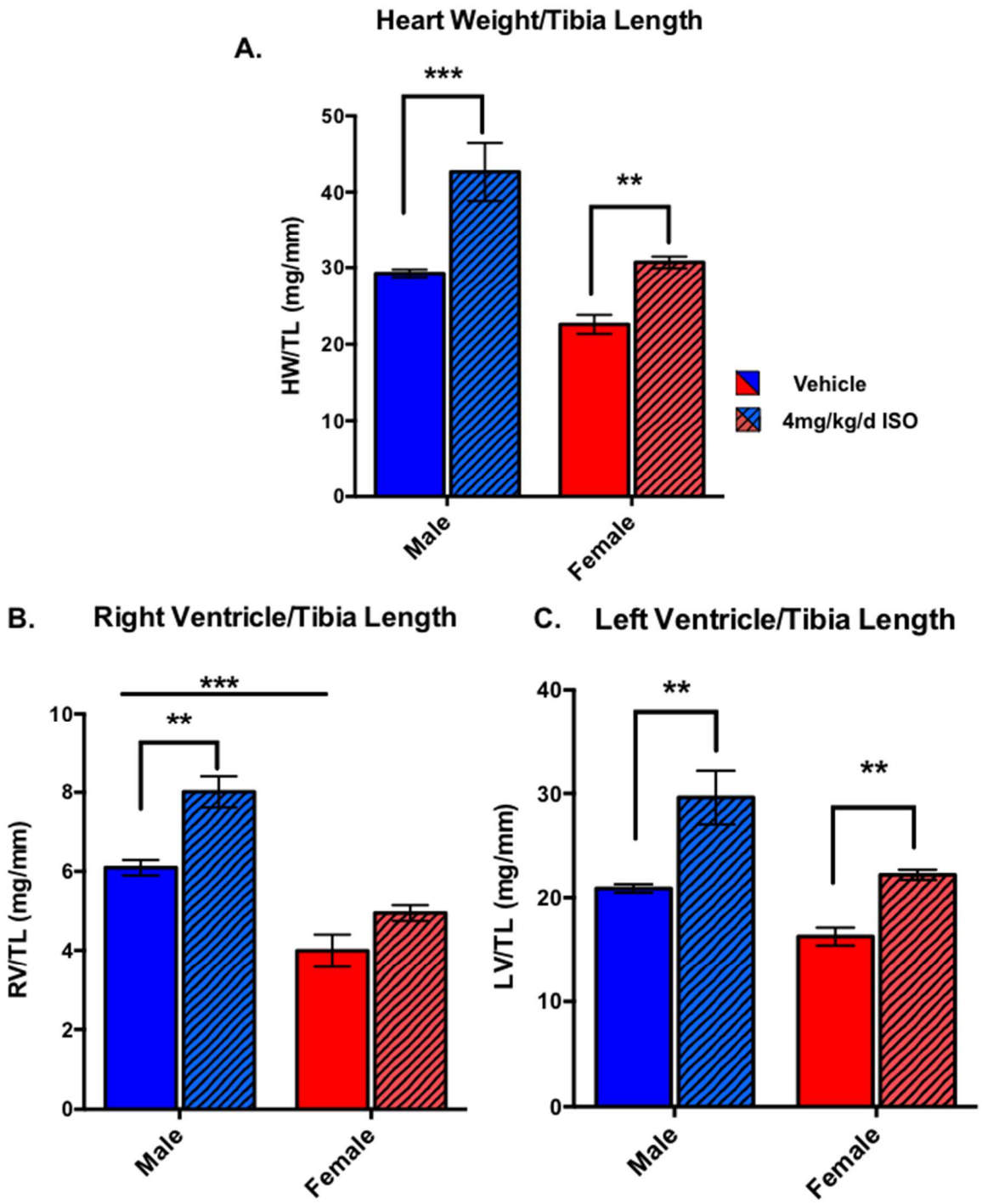

Figure 4.5: Heart and left ventricle weight increases in response to ISO treatment in both sexes. Whole heart **(A**) right ventricle, RV **(B)**, and left ventricle, LV **(C)** weight normalized to tibia length in vehicle or ISO treated animals of both sexes. *p<0.05 with Two-way ANOVA, Tukey's *post hoc;* n=4-9 animals per group. All data reported as ± SEM.

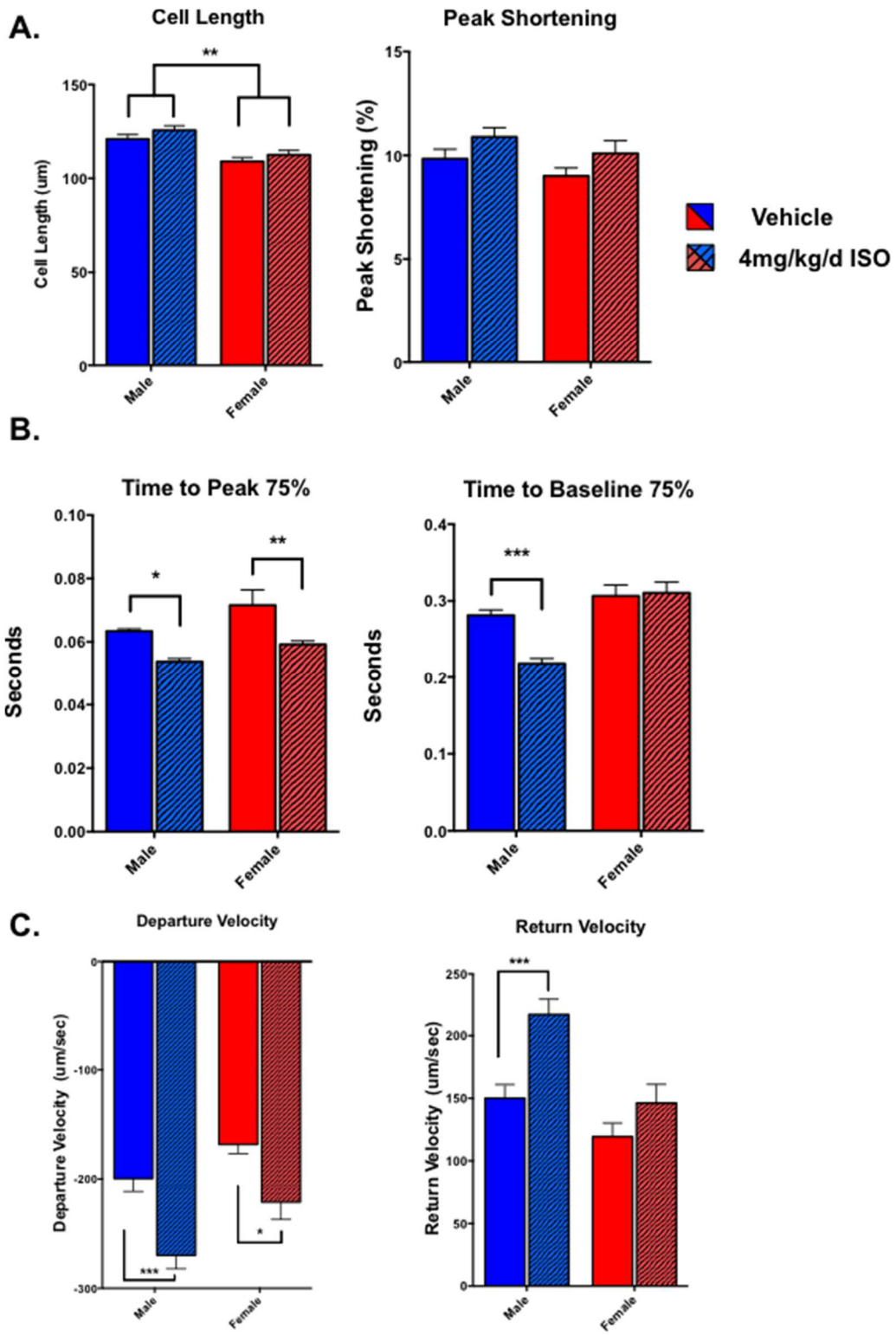

Figure 4.6: Sex differences in cardiac myocyte relaxation measures exist in response to chronic ISO treatment. (A-D) Contractility analysis performed with myocytes isolated from male or female rats treated with vehicle or ISO for 7 days. *p<0.05 with Two-way ANOVA using Tukey's *post hoc*; n= at least 40 cells pooled from at least 5 animals per group. All data reported as ± SEM.

References

Ahuja, P., Sdek, P., & MacLellan, W. R. (2007). Cardiac myocyte cell cycle control in development, disease, and regeneration. *Physiol Rev, 87*(2), 521-544. doi:10.1152/physrev.00032.2006

Arad, M., Seidman, J. G., & Seidman, C. E. (2002). Phenotypic diversity in hypertrophic cardiomyopathy. *Hum Mol Genet, 11*(20), 2499-2506.

Babiker, F. A., Lips, D., Meyer, R., Delvaux, E., Zandberg, P., Janssen, B., . . . Doevendans, P. A. (2006). Estrogen receptor beta protects the murine heart against left ventricular hypertrophy. *Arterioscler Thromb Vasc Biol, 26*(7), 1524-1530. doi:10.1161/01.ATV.0000223344.11128.23

Babiker, F. A., Lips, D. J., Delvaux, E., Zandberg, P., Janssen, B. J., Prinzen, F., . . . Doevendans, P. A. (2007). Oestrogen modulates cardiac ischaemic remodelling through oestrogen receptor-specific mechanisms. *Acta Physiol (Oxf), 189*(1), 23-31. doi:10.1111/j.1748-1716.2006.01633.x

Bai, C. X., Kurokawa, J., Tamagawa, M., Nakaya, H., & Furukawa, T. (2005). Nontranscriptional regulation of cardiac repolarization currents by testosterone. *Circulation, 112*(12), 1701-1710. doi:10.1161/CIRCULATIONAHA.104.523217

Banerjee, I., Fuseler, J. W., Price, R. L., Borg, T. K., & Baudino, T. A. (2007). Determination of cell types and numbers during cardiac development in the neonatal and adult rat and mouse. *Am J Physiol Heart Circ Physiol, 293*(3), H1883-1891. doi:10.1152/ajpheart.00514.2007

Batistuzzo de Medeiros, S. R., Krey, G., Hihi, A. K., & Wahli, W. (1997). Functional interactions between the estrogen receptor and the transcription activator Sp1 regulate the estrogen-dependent transcriptional activity of the vitellogenin A1 io promoter. *J Biol Chem, 272*(29), 18250-18260.

Bayorh, M. A., Bayorh, M. A., Socci, R. R., Eatman, D., Wang, M., & Thierry-Palmer, M. (2001). The Role of Gender in Salt-Induced Hypertension. *Clinical and Experimental Hypertension, 23*(3), 241-255. doi:10.1081/ceh-100102663

Berg, J. M. (1989). DNA binding specificity of steroid receptors. *Cell, 57*(7), 1065-1068.

Berger, F., Borchard, U., Hafner, D., Putz, I., & Weis, T. M. (1997). Effects of 17beta-estradiol on action potentials and ionic currents in male rat ventricular myocytes. *Naunyn Schmiedebergs Arch Pharmacol, 356*(6), 788-796.

Bergmann, O., Bhardwaj, R. D., Bernard, S., Zdunek, S., Barnabe-Heider, F., Walsh, S., . . . Frisen, J. (2009). Evidence for cardiomyocyte renewal in humans. *Science, 324*(5923), 98-102. doi:10.1126/science.1164680

Bernardo, B. C., Weeks, K. L., Pretorius, L., & McMullen, J. R. (2010). Molecular distinction between physiological and pathological cardiac hypertrophy: experimental findings and therapeutic strategies. *Pharmacol Ther, 128*(1), 191-227. doi:10.1016/j.pharmthera.2010.04.005

Bernelot Moens, S. J., Schnitzler, G. R., Nickerson, M., Guo, H., Ueda, K., Lu, Q., . . . Karas, R. H. (2012). Rapid estrogen receptor signaling is essential for the protective effects of estrogen

against vascular injury. *Circulation, 126*(16), 1993-2004. doi:10.1161/CIRCULATIONAHA.112.124529

Bers, D. M. (1991). Control of cardiac contraction by SR-Ca release and sarcolemmal-Ca fluxes. In D. M. Bers (Ed.), *Excitation-contraction coupling and cardiac contractile force. Developments in cardiovascular medicine* (Vol. 122, pp. 149-170). Dordrecht, Boston, London: Kluver Academic Publishers.

Bers, D. M. (2002). Cardiac excitation-contraction coupling. *Nature, 415*(6868), 198-205. doi:10.1038/415198a

Bhupathy, P., Haines, C. D., & Leinwand, L. A. (2010). Influence of sex hormones and phytoestrogens on heart disease in men and women. *Womens Health (Lond Engl), 6*(1), 77-95. doi:10.2217/whe.09.80

Bjornstrom, L., & Sjoberg, M. (2005). Mechanisms of estrogen receptor signaling: convergence of genomic and nongenomic actions on target genes. *Mol Endocrinol, 19*(4), 833-842. doi:10.1210/me.2004-0486

Blenck, C. L., Harvey, P. A., Reckelhoff, J. F., & Leinwand, L. A. (2016). The Importance of Biological Sex and Estrogen in Rodent Models of Cardiovascular Health and Disease. *Circ Res, 118*(8), 1294-1312. doi:10.1161/CIRCRESAHA.116.307509

Bodi, I., Mikala, G., Koch, S. E., Akhter, S. A., & Schwartz, A. (2005). The L-type calcium channel in the heart: the beat goes on. *J Clin Invest, 115*(12), 3306-3317. doi:10.1172/JCI27167

Bogatyryov, Y., Tomanek, R. J., & Dedkov, E. I. (2013). Structural composition of myocardial infarction scar in middle-aged male and female rats: does sex matter? *J Histochem Cytochem, 61*(11), 833-848. doi:10.1369/0022155413499794

Boynton, R. E., & Todd, R. L. (1947). Blood pressure readings of 75,258 university students. *Arch Intern Med (Chic), 80*(4), 454-462.

Brinson, K. N., Elmarakby, A. A., Tipton, A. J., Crislip, G. R., Yamamoto, T., Baban, B., & Sullivan, J. C. (2013). Female SHR have greater blood pressure sensitivity and renal T cell infiltration following chronic NOS inhibition than males. *Am J Physiol Regul Integr Comp Physiol, 305*(7), R701-710. doi:10.1152/ajpregu.00226.2013

Brinson, K. N., Rafikova, O., & Sullivan, J. C. (2014). Female sex hormones protect against salt-sensitive hypertension but not essential hypertension. *Am J Physiol Regul Integr Comp Physiol, 307*(2), R149-157. doi:10.1152/ajpregu.00061.2014

Brown, D. A., Lynch, J. M., Armstrong, C. J., Caruso, N. M., Ehlers, L. B., Johnson, M. S., & Moore, R. L. (2005). Susceptibility of the heart to ischaemia-reperfusion injury and exercise-induced cardioprotection are sex-dependent in the rat. *J Physiol, 564*(Pt 2), 619-630. doi:10.1113/jphysiol.2004.081323

Bryzgalova, G., Gao, H., Ahren, B., Zierath, J. R., Galuska, D., Steiler, T. L., . . . Khan, A. (2006). Evidence that oestrogen receptor-alpha plays an important role in the regulation of glucose homeostasis in mice: insulin sensitivity in the liver. *Diabetologia, 49*(3), 588-597. doi:10.1007/s00125-005-0105-3

Bueno, O. F., De Windt, L. J., Tymitz, K. M., Witt, S. A., Kimball, T. R., Klevitsky, R., . . . Molkentin, J. D. (2000). The MEK1-ERK1/2 signaling pathway promotes compensated cardiac hypertrophy in transgenic mice. *EMBO J, 19*(23), 6341-6350. doi:10.1093/emboj/19.23.6341

Bursztyn, M., & Ben-Dov, I. Z. (2013). Sex differences in salt-sensitivity risk approximated from ambulatory blood pressure monitoring and mortality. *J Hypertens, 31*(5), 900-905. doi:10.1097/HJH.0b013e32835f29f4

Cain, P. A., Ahl, R., Hedstrom, E., Ugander, M., Allansdotter-Johnsson, A., Friberg, P., & Arheden, H. (2009). Age and gender specific normal values of left ventricular mass, volume and function for gradient echo magnetic resonance imaging: a cross sectional study. *BMC Med Imaging, 9*, 2. doi:10.1186/1471-2342-9-2

Calovini, T., Haase, H., & Morano, I. (1995). Steroid-hormone regulation of myosin subunit expression in smooth and cardiac muscle. *J Cell Biochem, 59*(1), 69-78. doi:10.1002/jcb.240590109

Carretero, O. A., & Oparil, S. (2000). Essential hypertension. Part I: definition and etiology. *Circulation, 101*(3), 329-335.

Carroll, J. D., Carroll, E. P., Feldman, T., Ward, D. M., Lang, R. M., McGaughey, D., & Karp, R. B. (1992). Sex-associated differences in left ventricular function in aortic stenosis of the elderly. *Circulation, 86*(4), 1099-1107.

Cavasin, M. A., Sankey, S. S., Yu, A. L., Menon, S., & Yang, X. P. (2003). Estrogen and testosterone have opposing effects on chronic cardiac remodeling and function in mice with myocardial infarction. *Am J Physiol Heart Circ Physiol, 284*(5), H1560-1569. doi:10.1152/ajpheart.01087.2002

Cavasin, M. A., Tao, Z., Menon, S., & Yang, X. P. (2004). Gender differences in cardiac function during early remodeling after acute myocardial infarction in mice. *Life Sci, 75*(18), 2181-2192. doi:10.1016/j.lfs.2004.04.024

Cavasin, M. A., Yang, X. P., Liu, Y. H., Mehta, D., Karumanchi, R., Bulagannawar, M., & Carretero, O. A. (2000). Effects of ACE inhibitor, AT1 antagonist, and combined treatment in mice with heart failure. *J Cardiovasc Pharmacol, 36*(4), 472-480.

Chan, V., Fenning, A., Levick, S., Loch, D., Chunduri, P., Iyer, A., Teo, Y.L., Hoey, A., Wilson, K., Burstow, D., Brown, L. (2011). Cardiovascular Changes During Maturation and Ageing in Male anf Female Spontaneously Hypertensive Rats. *Journal of Cardiovascular Pharmacology, 57*, 469-478.

Chen, C., Hu, L. X., Dong, T., Wang, G. Q., Wang, L. H., Zhou, X. P., . . . Zhang, G. X. (2013). Apoptosis and autophagy contribute to gender difference in cardiac ischemia-reperfusion induced injury in rats. *Life Sci, 93*(7), 265-270. doi:10.1016/j.lfs.2013.06.019

Chen, C. C., Lin, C. C., & Lee, T. M. (2010). 17beta-Estradiol decreases vulnerability to ventricular arrhythmias by preserving connexin43 protein in infarcted rats. *Eur J Pharmacol, 629*(1-3), 73-81. doi:10.1016/j.ejphar.2009.11.050

Chen, J., Petranka, J., Yamamura, K., London, R. E., Steenbergen, C., & Murphy, E. (2003). Gender differences in sarcoplasmic reticulum calcium loading after isoproterenol. *Am J Physiol Heart Circ Physiol, 285*(6), H2657-2662. doi:10.1152/ajpheart.00557.2003

Chen, Q., Williams, R., Healy, C. L., Wright, C. D., Wu, S. C., & O'Connell, T. D. (2010). An association between gene expression and better survival in female mice following myocardial infarction. *J Mol Cell Cardiol, 49*(5), 801-811. doi:10.1016/j.yjmcc.2010.08.002

Chen, Y., Zhang, Z., Hu, F., Yang, W., Yuan, J., Cui, J., . . . Qiao, S. (2015). 17beta-estradiol prevents cardiac diastolic dysfunction by stimulating mitochondrial function: a preclinical study in a mouse model of a human hypertrophic cardiomyopathy mutation. *J Steroid Biochem Mol Biol, 147*, 92-102. doi:10.1016/j.jsbmb.2014.12.011

Chen, Y. F., Redetzke, R. A., Sivertson, R. M., Coburn, T. S., Cypher, L. R., & Gerdes, A. M. (2011). Post-myocardial infarction left ventricular myocyte remodeling: are there gender differences in rats? *Cardiovasc Pathol, 20*(5), e189-195. doi:10.1016/j.carpath.2010.09.007

Chu, S. H., Goldspink, P., Kowalski, J., Beck, J., & Schwertz, D. W. (2006). Effect of estrogen on calcium-handling proteins, beta-adrenergic receptors, and function in rat heart. *Life Sci, 79*(13), 1257-1267. doi:10.1016/j.lfs.2006.03.037

Chung, A. K., Das, S. R., Leonard, D., Peshock, R. M., Kazi, F., Abdullah, S. M., . . . Drazner, M. H. (2006). Women have higher left ventricular ejection fractions than men independent of differences in left ventricular volume: the Dallas Heart Study. *Circulation, 113*(12), 1597-1604. doi:10.1161/CIRCULATIONAHA.105.574400

Chung, T. H., Wang, S. M., & Wu, J. C. (2004). 17beta-estradiol reduces the effect of metabolic inhibition on gap junction intercellular communication in rat cardiomyocytes via the estrogen receptor. *J Mol Cell Cardiol, 37*(5), 1013-1022. doi:10.1016/j.yjmcc.2004.08.003

Clayton, J. A., & Collins, F. S. (2014). Policy: NIH to balance sex in cell and animal studies. *Nature, 509*(7500), 282-283.

Colom, B., Oliver, J., Roca, P., & Garcia-Palmer, F. J. (2007). Caloric restriction and gender modulate cardiac muscle mitochondrial H2O2 production and oxidative damage. *Cardiovasc Res, 74*(3), 456-465. doi:10.1016/j.cardiores.2007.02.001

Colomo, F., Nencini, S., Piroddi, N., Poggesi, C., & Tesi, C. (1998). Calcium dependence of the apparent rate of force generation in single striated muscle myofibrils activated by rapid solution changes. *Adv Exp Med Biol, 453*, 373-381; discussion 381-372.

Consideration of Sex as a Biological Variable in NIH-funded Research. (2015). Retrieved from Bethesda, MD: https://grants.nih.gov/grants/guide/notice-files/NOT-OD-15-102.html

Cowley, A. W., Jr. (2006). The genetic dissection of essential hypertension. *Nat Rev Genet, 7*(11), 829-840. doi:10.1038/nrg1967

Cross, H. R., Lu, L., Steenbergen, C., Philipson, K. D., & Murphy, E. (1998). Overexpression of the cardiac Na+/Ca2+ exchanger increases susceptibility to ischemia/reperfusion injury in male, but not female, transgenic mice. *Circ Res, 83*(12), 1215-1223.

Cross, H. R., Murphy, E., & Steenbergen, C. (2002). Ca(2+) loading and adrenergic stimulation reveal male/female differences in susceptibility to ischemia-reperfusion injury. *Am J Physiol Heart Circ Physiol, 283*(2), H481-489. doi:10.1152/ajpheart.00790.2001

Curl, C. L., Wendt, I. R., & Kotsanas, G. (2000). Effects of gender on intracellular [Ca2+] in rat cardiac myocytes. *Pflügers Archiv, 441*(5), 709-716. doi:10.1007/s004240000473

Curl, C. L., Wendt, I. R., & Kotsanas, G. (2001). Effects of gender on intracellular. *Pflugers Arch, 441*(5), 709-716.

Czubryt, M. P., Espira, L., Lamoureux, L., & Abrenica, B. (2006). The role of sex in cardiac function and disease. *Can J Physiol Pharmacol, 84*(1), 93-109. doi:10.1139/y05-151

deAlmeida, A. C., van Oort, R. J., & Wehrens, X. H. (2010). Transverse aortic constriction in mice. *J Vis Exp*(38). doi:10.3791/1729

Dedkov, E. I., Oak, K., Christensen, L. P., & Tomanek, R. J. (2014). Coronary vessels and cardiac myocytes of middle-aged rats demonstrate regional sex-specific adaptation in response to postmyocardial infarction remodeling. *Biol Sex Differ, 5*(1), 1. doi:10.1186/2042-6410-5-1

Demos-Davies, K. M., Ferguson, B. S., Cavasin, M. A., Mahaffey, J. H., Williams, S. M., Spiltoir, J. I., . . . McKinsey, T. A. (2014). HDAC6 contributes to pathological responses of heart and skeletal muscle to chronic angiotensin-II signaling. *Am J Physiol Heart Circ Physiol, 307*(2), H252-258. doi:10.1152/ajpheart.00149.2014

den Ruijter, H., Pasterkamp, G., Rutten, F. H., Lam, C. S., Chi, C., Tan, K. H., . . . de Kleijn, D. P. (2015). Heart failure with preserved ejection fraction in women: the Dutch Queen of Hearts program. *Neth Heart J, 23*(2), 89-93. doi:10.1007/s12471-014-0613-1

Dent, M. R., Tappia, P. S., & Dhalla, N. S. (2010a). Gender differences in apoptotic signaling in heart failure due to volume overload. *Apoptosis, 15*(4), 499-510. doi:10.1007/s10495-009-0441-8

Dent, M. R., Tappia, P. S., & Dhalla, N. S. (2010b). Gender differences in cardiac dysfunction and remodeling due to volume overload. *J Card Fail, 16*(5), 439-449. doi:10.1016/j.cardfail.2009.12.017

Dent, M. R., Tappia, P. S., & Dhalla, N. S. (2011). Gender differences in beta-adrenoceptor system in cardiac hypertrophy due to arteriovenous fistula. *J Cell Physiol, 226*(1), 181-186. doi:10.1002/jcp.22321

Doggrell, S., Brown, L. (1998). Rat models of hypertension, cardiac hypertrophy and failure. *Cardiovasc Res, 39*, 89-105.

Douglas, P. S., Katz, S. E., Weinberg, E. O., Chen, M. H., Bishop, S. P., & Lorell, B. H. (1998). Hypertrophic remodeling: gender differences in the early response to left ventricular pressure overload. *J Am Coll Cardiol, 32*(4), 1118-1125.

Dubal, D. B., Kashon, M. L., Pettigrew, L. C., Ren, J. M., Finklestein, S. P., Rau, S. W., & Wise, P. M. (1998). Estradiol protects against ischemic injury. *J Cereb Blood Flow Metab, 18*(11), 1253-1258. doi:10.1097/00004647-199811000-00012

Eisner, D. A., & Sipido, K. R. (2004). Sodium calcium exchange in the heart: necessity or luxury? *Circ Res, 95*(6), 549-551. doi:10.1161/01.RES.0000143419.87518.9e

Escande, A., Pillon, A., Servant, N., Cravedi, J. P., Larrea, F., Muhn, P., . . . Balaguer, P. (2006). Evaluation of ligand selectivity using reporter cell lines stably expressing estrogen receptor alpha or beta. *Biochem Pharmacol, 71*(10), 1459-1469. doi:10.1016/j.bcp.2006.02.002

Fang, L., Gao, X. M., Moore, X. L., Kiriazis, H., Su, Y., Ming, Z., . . . Du, X. J. (2007). Differences in inflammation, MMP activation and collagen damage account for gender difference in murine cardiac rupture following myocardial infarction. *J Mol Cell Cardiol, 43*(5), 535-544. doi:10.1016/j.yjmcc.2007.06.011

Farach-Carson, M. C., & Davis, P. J. (2003). Steroid hormone interactions with target cells: cross talk between membrane and nuclear pathways. *J Pharmacol Exp Ther, 307*(3), 839-845. doi:10.1124/jpet.103.055038

Farrell, S. R., Ross, J. L., & Howlett, S. E. (2010). Sex differences in mechanisms of cardiac excitation-contraction coupling in rat ventricular myocytes. *Am J Physiol Heart Circ Physiol, 299*(1), H36-45. doi:10.1152/ajpheart.00299.2010

Fermin, D. R., Barac, A., Lee, S., Polster, S. P., Hannenhalli, S., Bergemann, T. L., . . . Hall, J. L. (2008). Sex and age dimorphism of myocardial gene expression in nonischemic human heart failure. *Circ Cardiovasc Genet, 1*(2), 117-125. doi:10.1161/CIRCGENETICS.108.802652

Figtree, G. A., McDonald, D., Watkins, H., & Channon, K. M. (2003). Truncated estrogen receptor alpha 46-kDa isoform in human endothelial cells: relationship to acute activation of nitric oxide synthase. *Circulation, 107*(1), 120-126.

Fliegner, D., Schubert, C., Penkalla, A., Witt, H., Kararigas, G., Dworatzek, E., . . . Regitz-Zagrosek, V. (2010). Female sex and estrogen receptor-beta attenuate cardiac remodeling and apoptosis in pressure overload. *Am J Physiol Regul Integr Comp Physiol, 298*(6), R1597-1606. doi:10.1152/ajpregu.00825.2009

Flouriot, G., Brand, H., Denger, S., Metivier, R., Kos, M., Reid, G., . . . Gannon, F. (2000). Identification of a new isoform of the human estrogen receptor-alpha (hER-alpha) that is encoded by distinct transcripts and that is able to repress hER-alpha activation function 1. *EMBO J, 19*(17), 4688-4700. doi:10.1093/emboj/19.17.4688

Flouriot, G., Griffin, C., Kenealy, M., Sonntag-Buck, V., & Gannon, F. (1998). Differentially expressed messenger RNA isoforms of the human estrogen receptor-alpha gene are generated by alternative splicing and promoter usage. *Mol Endocrinol, 12*(12), 1939-1954. doi:10.1210/mend.12.12.0209

Fujimoto, N., Jinno, N., & Kitamura, S. (2004). Activation of estrogen response element dependent transcription by thyroid hormone with increase in estrogen receptor levels in a rat pituitary cell line, GH3. *J Endocrinol, 181*(1), 77-83.

Gabel, S. A., Walker, V. R., London, R. E., Steenbergen, C., Korach, K. S., & Murphy, E. (2005). Estrogen receptor beta mediates gender differences in ischemia/reperfusion injury. *J Mol Cell Cardiol, 38*(2), 289-297. doi:10.1016/j.yjmcc.2004.11.013

Gaborit, N., Varro, A., Le Bouter, S., Szuts, V., Escande, D., Nattel, S., & Demolombe, S. (2010). Gender-related differences in ion-channel and transporter subunit expression in non-diseased human hearts. *J Mol Cell Cardiol, 49*(4), 639-646. doi:10.1016/j.yjmcc.2010.06.005

Galien, R., & Garcia, T. (1997). Estrogen receptor impairs interleukin-6 expression by preventing protein binding on the NF-kappaB site. *Nucleic Acids Res, 25*(12), 2424-2429.

Gardner, J. D., Brower, G. L., & Janicki, J. S. (2002). Gender differences in cardiac remodeling secondary to chronic volume overload. *Journal of Cardiac Failure, 8*(2), 101-107. doi:10.1054/jcaf.2002.32195

Gender Mainstreaming in the 6th Framework Programme – Reference Guide for Scientific Officers/Project Officers. (2003). Retrieved from ftp://ftp.cordis.europa.eu/pub/science-society/docs/gendervademecum.pdf

Glushkovskaya-Semyachkina, O. V., Anishchenko, T. G., Sindyakova, T. A., Leksina, O. V., & Berdnikova, V. A. (2006). Sex-related differences in nitric oxide content in healthy and hypertensive rats at rest and under stress conditions. *Bull Exp Biol Med, 142*(1), 9-11.

Gorski, J., & Hansen, J. C. (1987). The "one and only" step model of estrogen action. *Steroids, 49*(6), 461-475.

Grandy, S. A., & Howlett, S. E. (2006). Cardiac excitation-contraction coupling is altered in myocytes from aged male mice but not in cells from aged female mice. *Am J Physiol Heart Circ Physiol, 291*(5), H2362-2370. doi:10.1152/ajpheart.00070.2006

Grohe, C., Kahlert, S., Lobbert, K., & Vetter, H. (1998). Expression of oestrogen receptor alpha and beta in rat heart: role of local oestrogen synthesis. *J Endocrinol, 156*(2), R1-7.

Guerra, S., Leri, A., Wang, X., Finato, N., Di Loreto, C., Beltrami, C. A., . . . Anversa, P. (1999). Myocyte death in the failing human heart is gender dependent. *Circ Res, 85*(9), 856-866.

Hagen, B. M., Boyman, L., Kao, J. P., & Lederer, W. J. (2012). A comparative assessment of fluo Ca2+ indicators in rat ventricular myocytes. *Cell Calcium, 52*(2), 170-181. doi:10.1016/j.ceca.2012.05.010

Haines, C. D., Harvey, P. A., & Leinwand, L. A. (2012). Estrogens mediate cardiac hypertrophy in a stimulus-dependent manner. *Endocrinology, 153*(9), 4480-4490. doi:10.1210/en.2012-1353

Haines, C. D., Harvey, P. A., Luczak, E. D., Barthel, K. K., Konhilas, J. P., Watson, P. A., . . . Leinwand, L. A. (2012a). Estrogenic compounds are not always cardioprotective and can be lethal in males with genetic heart disease. *Endocrinology, 153*(9), 4470-4479. doi:10.1210/en.2012-1391

Haines, C. D., Harvey, P. A., Luczak, E. D., Barthel, K. K., Konhilas, J. P., Watson, P. A., . . . Leinwand, L. A. (2012b). Estrogenic Compounds Are Not Always Cardioprotective and Can Be Lethal in Males with Genetic Heart Disease. *Endocrinology*. doi:10.1210/en.2012-1391

Hall, J. E., Guyton, A. C., & Brands, M. J. (1995). *Hypertension, Pathophysiology, Diagnosis, and Management.* (J. H. Laragh & B. M. Brenner Eds. 2 ed.): Raven Press.

Hall, J. E., Guyton, A. C., & Brands, M. W. (1996). Pressure-volume regulation in hypertension. *Kidney Int Suppl, 55*, S35-41.

Han, G., Li, F., Yu, X., & White, R. E. (2013). GPER: a novel target for non-genomic estrogen action in the cardiovascular system. *Pharmacol Res, 71*, 53-60. doi:10.1016/j.phrs.2013.02.008

Harman, S. M., Black, D. M., Naftolin, F., Brinton, E. A., Budoff, M. J., Cedars, M. I., . . . Hodis, H. N. (2014). Arterial imaging outcomes and cardiovascular risk factors in recently menopausal women: a randomized trial. *Ann Intern Med, 161*(4), 249-260. doi:10.7326/M14-0353

Harvey, P. A., & Leinwand, L. A. (2011). The cell biology of disease: cellular mechanisms of cardiomyopathy. *J Cell Biol, 194*(3), 355-365. doi:10.1083/jcb.201101100

Heldring, N., Pike, A., Andersson, S., Matthews, J., Cheng, G., Hartman, J., . . . Gustafsson, J. A. (2007). Estrogen receptors: how do they signal and what are their targets. *Physiol Rev, 87*(3), 905-931. doi:10.1152/physrev.00026.2006

Himmelmann, A. (1999). Hypertension: an important precursor of heart failure. *Blood Press, 8*(5-6), 253-260.

Hou, J. H., Kralj, J. M., Douglass, A. D., Engert, F., & Cohen, A. E. (2014). Simultaneous mapping of membrane voltage and calcium in zebrafish heart in vivo reveals chamber-specific developmental transitions in ionic currents. *Front Physiol, 5*, 344. doi:10.3389/fphys.2014.00344

Hove-Madsen, L., & Bers, D. M. (1993). Sarcoplasmic reticulum Ca2+ uptake and thapsigargin sensitivity in permeabilized rabbit and rat ventricular myocytes. *Circ Res, 73*(5), 820-828.

Howlett, S. E. (2010). Age-associated changes in excitation-contraction coupling are more prominent in ventricular myocytes from male rats than in myocytes from female rats. *Am J Physiol Heart Circ Physiol, 298*(2), H659-670. doi:10.1152/ajpheart.00214.2009

Htun, H., Holth, L. T., Walker, D., Davie, J. R., & Hager, G. L. (1999). Direct visualization of the human estrogen receptor alpha reveals a role for ligand in the nuclear distribution of the receptor. *Mol Biol Cell, 10*(2), 471-486.

Hubner, N., Wallace, C. A., Zimdahl, H., Petretto, E., Schulz, H., Maciver, F., . . . Aitman, T. J. (2005). Integrated transcriptional profiling and linkage analysis for identification of genes underlying disease. *Nat Genet, 37*(3), 243-253. doi:10.1038/ng1522

Hulley, S., Grady, D., Bush, T., Furberg, C., Herrington, D., Riggs, B., & Vittinghoff, E. (1998). Randomized trial of estrogen plus progestin for secondary prevention of coronary heart disease in postmenopausal women. Heart and Estrogen/progestin Replacement Study (HERS) Research Group. *JAMA, 280*(7), 605-613.

Huxley, V. H. (2007). Sex and the cardiovascular system: the intriguing tale of how women and men regulate cardiovascular function differently. *Adv Physiol Educ, 31*(1), 17-22. doi:10.1152/advan.00099.2006

Imahashi, K., London, R. E., Steenbergen, C., & Murphy, E. (2004). Male/female differences in intracellular Na+ regulation during ischemia/reperfusion in mouse heart. *J Mol Cell Cardiol, 37*(3), 747-753. doi:10.1016/j.yjmcc.2004.06.010

Irsik, D. L., Carmines, P. K., & Lane, P. H. (2013). Classical estrogen receptors and ERalpha splice variants in the mouse. *PLoS One, 8*(8), e70926. doi:10.1371/journal.pone.0070926

Isensee, J., Witt, H., Pregla, R., Hetzer, R., Regitz-Zagrosek, V., & Noppinger, P. R. (2008). Sexually dimorphic gene expression in the heart of mice and men. *J Mol Med (Berl), 86*(1), 61-74. doi:10.1007/s00109-007-0240-z

Israeli-Rosenberg, S., Manso, A. M., Okada, H., & Ross, R. S. (2014). Integrins and integrin-associated proteins in the cardiac myocyte. *Circ Res, 114*(3), 572-586. doi:10.1161/CIRCRESAHA.114.301275

Jayachandran, M., Preston, C. C., Hunter, L. W., Jahangir, A., Owen, W. G., Korach, K. S., & Miller, V. M. (2010). Loss of estrogen receptor beta decreases mitochondrial energetic potential and increases thrombogenicity of platelets in aged female mice. *Age (Dordr), 32*(1), 109-121. doi:10.1007/s11357-009-9119-y

Jazbutyte, V., Hu, K., Kruchten, P., Bey, E., Maier, S. K., Fritzemeier, K. H., . . . Pelzer, T. (2006). Aging reduces the efficacy of estrogen substitution to attenuate cardiac hypertrophy in female spontaneously hypertensive rats. *Hypertension, 48*(4), 579-586. doi:10.1161/01.HYP.0000240053.48517.c7

Jhund, P. S., & McMurray, J. J. (2008). Heart failure after acute myocardial infarction: a lost battle in the war on heart failure? *Circulation, 118*(20), 2019-2021. doi:10.1161/CIRCULATIONAHA.108.813493

Johnson, B. D., Zheng, W., Korach, K. S., Scheuer, T., Catterall, W. A., & Rubanyi, G. M. (1997). Increased expression of the cardiac L-type calcium channel in estrogen receptor-deficient mice. *J Gen Physiol, 110*(2), 135-140.

Johnson, M. S., Moore, R. L., & Brown, D. A. (2006). Sex differences in myocardial infarct size are abolished by sarcolemmal KATP channel blockade in rat. *Am J Physiol Heart Circ Physiol, 290*(6), H2644-2647. doi:10.1152/ajpheart.01291.2005

Jones, D. W., & Hall, J. E. (2004). Seventh report of the Joint National Committee on Prevention, Detection, Evaluation, and Treatment of High Blood Pressure and evidence from new hypertension trials. *Hypertension, 43*(1), 1-3. doi:10.1161/01.HYP.0000110061.06674.ca

Jugdutt, B. I. (2003). Ventricular remodeling after infarction and the extracellular collagen matrix: when is enough enough? *Circulation, 108*(11), 1395-1403. doi:10.1161/01.CIR.0000085658.98621.49

Kaestner, L., Scholz, A., Tian, Q., Ruppenthal, S., Tabellion, W., Wiesen, K., . . . Lipp, P. (2014). Genetically encoded Ca2+ indicators in cardiac myocytes. *Circ Res, 114*(10), 1623-1639. doi:10.1161/CIRCRESAHA.114.303475

Kahr, P. C., Piccini, I., Fabritz, L., Greber, B., Scholer, H., Scheld, H. H., . . . Kirchhof, P. (2011). Systematic analysis of gene expression differences between left and right atria in different mouse strains and in human atrial tissue. *PLoS One, 6*(10), e26389. doi:10.1371/journal.pone.0026389

Kalogeris, T., Baines, C. P., Krenz, M., & Korthuis, R. J. (2012). Cell biology of ischemia/reperfusion injury. *Int Rev Cell Mol Biol, 298*, 229-317. doi:10.1016/B978-0-12-394309-5.00006-7

Kam, K. W., Kravtsov, G. M., Liu, J., & Wong, T. M. (2005). Increased PKA activity and its influence on isoprenaline-stimulated L-type Ca2+ channels in the heart from ovariectomized rats. *Br J Pharmacol, 144*(7), 972-981. doi:10.1038/sj.bjp.0706123

Kang, L., Zhang, X., Xie, Y., Tu, Y., Wang, D., Liu, Z., & Wang, Z. Y. (2010). Involvement of estrogen receptor variant ER-alpha36, not GPR30, in nongenomic estrogen signaling. *Mol Endocrinol, 24*(4), 709-721. doi:10.1210/me.2009-0317

Kararigas, G., Fliegner, D., Forler, S., Klein, O., Schubert, C., Gustafsson, J. A., . . . Regitz-Zagrosek, V. (2014). Comparative proteomic analysis reveals sex and estrogen receptor beta effects in the pressure overloaded heart. *J Proteome Res, 13*(12), 5829-5836. doi:10.1021/pr500749j

Kararigas, G., Nguyen, B. T., & Jarry, H. (2014). Estrogen modulates cardiac growth through an estrogen receptor alpha-dependent mechanism in healthy ovariectomized mice. *Mol Cell Endocrinol, 382*(2), 909-914. doi:10.1016/j.mce.2013.11.011

Karlson, B. W., Herlitz, J., & Hartford, M. (1994). Prognosis in myocardial infarction in relation to gender. *Am Heart J, 128*(3), 477-483.

Kastner, P., Krust, A., Mendelsohn, C., Garnier, J. M., Zelent, A., Leroy, P., . . . Chambon, P. (1990). Murine isoforms of retinoic acid receptor gamma with specific patterns of expression. *Proc Natl Acad Sci U S A, 87*(7), 2700-2704.

Kelsey, S. F., James, M., Holubkov, A. L., Holubkov, R., Cowley, M. J., & Detre, K. M. (1993). Results of percutaneous transluminal coronary angioplasty in women. 1985-1986 National Heart, Lung, and Blood Institute's Coronary Angioplasty Registry. *Circulation, 87*(3), 720-727.

Kim, K. H., Toomre, D., & Bender, J. R. (2011). Splice isoform estrogen receptors as integral transmembrane proteins. *Mol Biol Cell, 22*(22), 4415-4423. doi:10.1091/mbc.E11-05-0416

Knowlton, A. A., & Korzick, D. H. (2014). Estrogen and the female heart. *Mol Cell Endocrinol, 389*(1-2), 31-39. doi:10.1016/j.mce.2014.01.002

Knowlton, A. A., & Lee, A. R. (2012). Estrogen and the cardiovascular system. *Pharmacol Ther, 135*(1), 54-70. doi:10.1016/j.pharmthera.2012.03.007

Komajda, M., & Lam, C. S. (2014). Heart failure with preserved ejection fraction: a clinical dilemma. *Eur Heart J, 35*(16), 1022-1032. doi:10.1093/eurheartj/ehu067

Konhilas, J. P., Maass, A. H., Luckey, S. W., Stauffer, B. L., Olson, E. N., & Leinwand, L. A. (2004). Sex modifies exercise and cardiac adaptation in mice. *Am J Physiol Heart Circ Physiol, 287*(6), H2768-2776. doi:10.1152/ajpheart.00292.2004

Korte, T., Fuchs, M., Arkudas, A., Geertz, S., Meyer, R., Gardiwal, A., . . . Grohe, C. (2005). Female mice lacking estrogen receptor beta display prolonged ventricular repolarization and

reduced ventricular automaticity after myocardial infarction. *Circulation, 111*(18), 2282-2290. doi:10.1161/01.CIR.0000164262.08004.BB

Krishnan, A., Samtani, R., Dhanantwari, P., Lee, E., Yamada, S., Shiota, K., . . . Lo, C. W. (2014). A detailed comparison of mouse and human cardiac development. *Pediatr Res, 76*(6), 500-507. doi:10.1038/pr.2014.128

Kubo, T., Kitaoka, H., Okawa, M., Hirota, T., Hayato, K., Yamasaki, N., . . . Doi, Y. L. (2010). Gender-specific differences in the clinical features of hypertrophic cardiomyopathy in a community-based Japanese population: results from Kochi RYOMA study. *J Cardiol, 56*(3), 314-319. doi:10.1016/j.jjcc.2010.07.004

Kuiper, G. G., Carlsson, B., Grandien, K., Enmark, E., Haggblad, J., Nilsson, S., & Gustafsson, J. A. (1997). Comparison of the ligand binding specificity and transcript tissue distribution of estrogen receptors alpha and beta. *Endocrinology, 138*(3), 863-870. doi:10.1210/endo.138.3.4979

Laborde, C. H., Lange, D., & Haywood, J. R. (2000). Role of Female Sex Hormones in Development and Reversal of Dahl Hypertension. *Hypertension, 35*, 484-489.

Lagranha, C. J., Deschamps, A., Aponte, A., Steenbergen, C., & Murphy, E. (2010). Sex differences in the phosphorylation of mitochondrial proteins result in reduced production of reactive oxygen species and cardioprotection in females. *Circ Res, 106*(11), 1681-1691. doi:10.1161/CIRCRESAHA.109.213645

Layland, J., Solaro, R. J., & Shah, A. M. (2005). Regulation of cardiac contractile function by troponin I phosphorylation. *Cardiovasc Res, 66*(1), 12-21. doi:10.1016/j.cardiores.2004.12.022

Le, T. Y., Ashton, A. W., Mardini, M., Stanton, P. G., Funder, J. W., Handelsman, D. J., & Mihailidou, A. S. (2014). Role of androgens in sex differences in cardiac damage during myocardial infarction. *Endocrinology, 155*(2), 568-575. doi:10.1210/en.2013-1755

Lee, L. M., Cao, J., Deng, H., Chen, P., Gatalica, Z., & Wang, Z. Y. (2008). ER-alpha36, a novel variant of ER-alpha, is expressed in ER-positive and -negative human breast carcinomas. *Anticancer Res, 28*(1B), 479-483.

Lehmann, M. H., Timothy, K. W., Frankovich, D., Fromm, B. S., Keating, M., Locati, E. H., . . . Vincent, G. M. (1997). Age-gender influence on the rate-corrected QT interval and the QT-heart rate relation in families with genotypically characterized long QT syndrome. *J Am Coll Cardiol, 29*(1), 93-99.

Leinwand, L. A. (2003). Sex is a potent modifier of the cardiovascular system. *Journal of Clinical Investigation, 112*(3), 302-307. doi:10.1172/jci200319429

Lenzen, M. J., Rosengren, A., Scholte op Reimer, W. J., Follath, F., Boersma, E., Simoons, M. L., . . . Komajda, M. (2008). Management of patients with heart failure in clinical practice: differences between men and women. *Heart, 94*(3), e10. doi:10.1136/hrt.2006.099523

Li, F., Wang, X., Capasso, J. M., & Gerdes, A. M. (1996). Rapid transition of cardiac myocytes from hyperplasia to hypertrophy during postnatal development. *J Mol Cell Cardiol, 28*(8), 1737-1746. doi:10.1006/jmcc.1996.0163

Li, H. J., Wang, L. Y., Qu, H. N., Yu, L. H., Burnstock, G., Ni, X., . . . Ma, B. (2011). P2Y2 receptor-mediated modulation of estrogen-induced proliferation of breast cancer cells. *Mol Cell Endocrinol, 338*(1-2), 28-37. doi:10.1016/j.mce.2011.02.014

Li, H. Y., Bian, J. S., Kwan, Y. W., & Wong, T. M. (2000). Enhanced responses to 17beta-estradiol in rat hearts treated with isoproterenol: involvement of a cyclic AMP-dependent pathway. *J Pharmacol Exp Ther, 293*(2), 592-598.

Li, L., Haynes, M. P., & Bender, J. R. (2003). Plasma membrane localization and function of the estrogen receptor alpha variant (ER46) in human endothelial cells. *Proc Natl Acad Sci U S A, 100*(8), 4807-4812. doi:10.1073/pnas.0831079100

Liew, R., Williams, J. K., Collins, P., & MacLeod, K. T. (2003). Soy-derived isoflavones exert opposing actions on Guinea pig ventricular myocytes. *J Pharmacol Exp Ther, 304*(3), 985-993. doi:10.1124/jpet.102.042986

Litwin, S. E., Katz, S. E., Litwin, C. M., Morgan, J. P., & Douglas, P. S. (1999). Gender differences in postinfarction left ventricular remodeling. *Cardiology, 91*(3), 173-183. doi:6906

Liu, J., Sadoshima, J., Zhai, P., Hong, C., Yang, G., Chen, W., . . . Vatner, D. E. (2006). Pressure overload induces greater hypertrophy and mortality in female mice with p38alpha MAPK inhibition. *J Mol Cell Cardiol, 41*(4), 680-688. doi:10.1016/j.yjmcc.2006.07.007

Liu, X. K., Katchman, A., Drici, M. D., Ebert, S. N., Ducic, I., Morad, M., & Woosley, R. L. (1998). Gender difference in the cycle length-dependent QT and potassium currents in rabbits. *J Pharmacol Exp Ther, 285*(2), 672-679.

Liu, Y., Ding, J., Bush, T. L., Longenecker, J. C., Nieto, F. J., Golden, S. H., & Szklo, M. (2001). Relative androgen excess and increased cardiovascular risk after menopause: a hypothesized relation. *Am J Epidemiol, 154*(6), 489-494.

Lizotte, E., Grandy, S. A., Tremblay, A., Allen, B. G., & Fiset, C. (2009). Expression, distribution and regulation of sex steroid hormone receptors in mouse heart. *Cell Physiol Biochem, 23*(1-3), 75-86. doi:10.1159/000204096

Lompre, A. M., Mercadier, J. J., Wisnewsky, C., Bouveret, P., Pantaloni, C., D'Albis, A., & Schwartz, K. (1981). Species- and age-dependent changes in the relative amounts of cardiac myosin isoenzymes in mammals. *Dev Biol, 84*(2), 286-290.

Lorell, B. H., & Carabello, B. A. (2000). Left ventricular hypertrophy: pathogenesis, detection, and prognosis. *Circulation, 102*(4), 470-479.

Loyer, X., Oliviero, P., Damy, T., Robidel, E., Marotte, F., Heymes, C., & Samuel, J. L. (2007). Effects of sex differences on constitutive nitric oxide synthase expression and activity in response to pressure overload in rats. *Am J Physiol Heart Circ Physiol, 293*(5), H2650-2658. doi:10.1152/ajpheart.00883.2007

Lu, Q., Pallas, D. C., Surks, H. K., Baur, W. E., Mendelsohn, M. E., & Karas, R. H. (2004). Striatin assembles a membrane signaling complex necessary for rapid, nongenomic activation of endothelial NO synthase by estrogen receptor alpha. *Proc Natl Acad Sci U S A, 101*(49), 17126-17131. doi:10.1073/pnas.0407492101

Luckey, S. W., Mansoori, J., Fair, K., Antos, C. L., Olson, E. N., & Leinwand, L. A. (2007). Blocking cardiac growth in hypertrophic cardiomyopathy induces cardiac dysfunction and decreased survival only in males. *Am J Physiol Heart Circ Physiol, 292*(2), H838-845. doi:10.1152/ajpheart.00615.2006

Luczak, E. D., & Leinwand, L. A. (2009). Sex-based cardiac physiology. *Annu Rev Physiol, 71*, 1-18. doi:10.1146/annurev.physiol.010908.163156

Maass, A., & Leinwand, L. A. (2000). Animal models of hypertrophic cardiomyopathy. *Curr Opin Cardiol, 15*(3), 189-196.

Maass, A. H., & Buvoli, M. (2007). Cardiomyocyte preparation, culture, and gene transfer. *Methods Mol Biol, 366*, 321-330. doi:10.1007/978-1-59745-030-0_18

Maass, A. H., Ikeda, K., Oberdorf-Maass, S., Maier, S. K., & Leinwand, L. A. (2004). Hypertrophy, fibrosis, and sudden cardiac death in response to pathological stimuli in mice with mutations in cardiac troponin T. *Circulation, 110*(15), 2102-2109. doi:10.1161/01.CIR.0000144460.84795.E3

Mahmoodzadeh, S., Eder, S., Nordmeyer, J., Ehler, E., Huber, O., Martus, P., . . . Regitz-Zagrosek, V. (2006). Estrogen receptor alpha up-regulation and redistribution in human heart failure. *FASEB J, 20*(7), 926-934. doi:10.1096/fj.05-5148com

Mahmoodzadeh, S., Fliegner, D., & Dworatzek, E. (2012). Sex differences in animal models for cardiovascular diseases and the role of estrogen. *Handb Exp Pharmacol*(214), 23-48. doi:10.1007/978-3-642-30726-3_2

Mair, K. M., Johansen, A. K., Wright, A. F., Wallace, E., & MacLean, M. R. (2014). Pulmonary arterial hypertension: basis of sex differences in incidence and treatment response. *Br J Pharmacol, 171*(3), 567-579. doi:10.1111/bph.12281

Manning, B. D., & Cantley, L. C. (2007). AKT/PKB signaling: navigating downstream. *Cell, 129*(7), 1261-1274. doi:10.1016/j.cell.2007.06.009

Marcus, J. T., DeWaal, L. K., Gotte, M. J., van der Geest, R. J., Heethaar, R. M., & Van Rossum, A. C. (1999). MRI-derived left ventricular function parameters and mass in healthy young adults: relation with gender and body size. *Int J Card Imaging, 15*(5), 411-419.

Marquez, D. C., & Pietras, R. J. (2001). Membrane-associated binding sites for estrogen contribute to growth regulation of human breast cancer cells. *Oncogene, 20*(39), 5420-5430. doi:10.1038/sj.onc.1204729

Maruvada, P., Baumann, C. T., Hager, G. L., & Yen, P. M. (2003). Dynamic shuttling and intranuclear mobility of nuclear hormone receptors. *J Biol Chem, 278*(14), 12425-12432. doi:10.1074/jbc.M202752200

Matkovich, S. J., Edwards, J. R., Grossenheider, T. C., de Guzman Strong, C., & Dorn, G. W., 2nd. (2014). Epigenetic coordination of embryonic heart transcription by dynamically regulated long noncoding RNAs. *Proc Natl Acad Sci U S A, 111*(33), 12264-12269. doi:10.1073/pnas.1410622111

Mayer, L. P., Dyer, C. A., Eastgard, R. L., Hoyer, P. B., & Banka, C. L. (2005). Atherosclerotic lesion development in a novel ovary-intact mouse model of perimenopause. *Arterioscler Thromb Vasc Biol, 25*(9), 1910-1916. doi:10.1161/01.ATV.0000175767.46520.6a

McKee, L. A., Chen, H., Regan, J. A., Behunin, S. M., Walker, J. W., Walker, J. S., & Konhilas, J. P. (2013). Sexually dimorphic myofilament function and cardiac troponin I phosphospecies distribution in hypertrophic cardiomyopathy mice. *Arch Biochem Biophys, 535*(1), 39-48. doi:10.1016/j.abb.2012.12.023

McKee, P. A., Castelli, W. P., McNamara, P. M., & Kannel, W. B. (1971). The natural history of congestive heart failure: the Framingham study. *N Engl J Med, 285*(26), 1441-1446. doi:10.1056/NEJM197112232852601

McNamara, K. M., Harwood, D. T., Simanainen, U., Walters, K. A., Jimenez, M., & Handelsman, D. J. (2010). Measurement of sex steroids in murine blood and reproductive tissues by liquid chromatography-tandem mass spectrometry. *J Steroid Biochem Mol Biol, 121*(3-5), 611-618. doi:10.1016/j.jsbmb.2010.02.001

Mellor, K. M., Curl, C. L., Chandramouli, C., Pedrazzini, T., Wendt, I. R., & Delbridge, L. M. (2014). Ageing-related cardiomyocyte functional decline is sex and angiotensin II dependent. *Age (Dordr), 36*(3), 9630. doi:10.1007/s11357-014-9630-7

Mendelsohn, M. E., & Karas, R. H. (2005). Molecular and cellular basis of cardiovascular gender differences. *Science, 308*(5728), 1583-1587. doi:10.1126/science.1112062

Miller, V. M., & Best, P. J. (2011). Implications for reproductive medicine: Sex differences in cardiovascular disease. *Sex Reprod Menopause, 9*(3), 21-28.

Miyata, S., Minobe, W., Bristow, M. R., & Leinwand, L. A. (2000). Myosin heavy chain isoform expression in the failing and nonfailing human heart. *Circ Res, 86*(4), 386-390.

Morani, A., Barros, R. P., Imamov, O., Hultenby, K., Arner, A., Warner, M., & Gustafsson, J. A. (2006). Lung dysfunction causes systemic hypoxia in estrogen receptor beta knockout (ERbeta-/-) mice. *Proc Natl Acad Sci U S A, 103*(18), 7165-7169. doi:10.1073/pnas.0602194103

Mosca, L., Benjamin, E. J., Berra, K., Bezanson, J. L., Dolor, R. J., Lloyd-Jones, D. M., . . . American Heart, A. (2011). Effectiveness-based guidelines for the prevention of cardiovascular disease in women--2011 update: a guideline from the American Heart Association. *J Am Coll Cardiol, 57*(12), 1404-1423. doi:10.1016/j.jacc.2011.02.005

Motulsky, H. J., & Brown, R. E. (2006). Detecting outliers when fitting data with nonlinear regression - a new method based on robust nonlinear regression and the false discovery rate. *BMC Bioinformatics, 7*, 123. doi:10.1186/1471-2105-7-123

Mozaffarian, D., Benjamin, E. J., Go, A. S., Arnett, D. K., Blaha, M. J., Cushman, M., . . . Stroke Statistics, S. (2015). Heart disease and stroke statistics--2015 update: a report from the American Heart Association. *Circulation, 131*(4), e29-322. doi:10.1161/CIR.0000000000000152

Murphy, E. (2011). Estrogen signaling and cardiovascular disease. *Circ Res, 109*(6), 687-696. doi:10.1161/CIRCRESAHA.110.236687

Murphy, E., & Steenbergen, C. (2007). Cardioprotection in females: a role for nitric oxide and altered gene expression. *Heart Fail Rev, 12*(3-4), 293-300. doi:10.1007/s10741-007-9035-0

Najafi, A., Schlossarek, S., van Deel, E. D., van den Heuvel, N., Guclu, A., Goebel, M., . . . van der Velden, J. (2015). Sexual dimorphic response to exercise in hypertrophic cardiomyopathy-associated MYBPC3-targeted knock-in mice. *Pflugers Arch, 467*(6), 1303-1317. doi:10.1007/s00424-014-1570-7

Nakajima, T., Iwasawa, K., Oonuma, H., Morita, T., Goto, A., Wang, Y., & Hazama, H. (1999). Antiarrhythmic effect and its underlying ionic mechanism of 17beta-estradiol in cardiac myocytes. *Br J Pharmacol, 127*(2), 429-440. doi:10.1038/sj.bjp.0702576

Nattel, S. (2008). Delayed-rectifier potassium currents and the control of cardiac repolarization: Noble and Tsien 40 years after. *J Physiol, 586*(Pt 24), 5849-5852. doi:10.1113/jphysiol.2008.163089

Nelson, J. F., Felicio, L. S., Osterburg, H. H., & Finch, C. E. (1981). Altered profiles of estradiol and progesterone associated with prolonged estrous cycles and persistent vaginal cornification in aging C57BL/6J mice. *Biol Reprod, 24*(4), 784-794.

Nelson, J. F., Felicio, L. S., Randall, P. K., Sims, C., & Finch, C. E. (1982). A longitudinal study of estrous cyclicity in aging C57BL/6J mice: I. Cycle frequency, length and vaginal cytology. *Biol Reprod, 27*(2), 327-339.

Nerbonne, J. M. (2004). Studying cardiac arrhythmias in the mouse--a reasonable model for probing mechanisms? *Trends Cardiovasc Med, 14*(3), 83-93. doi:10.1016/j.tcm.2003.12.006

Nuedling, S., Kahlert, S., Loebbert, K., Doevendans, P. A., Meyer, R., Vetter, H., & Grohe, C. (1999). 17 Beta-estradiol stimulates expression of endothelial and inducible NO synthase in rat myocardium in-vitro and in-vivo. *Cardiovasc Res, 43*(3), 666-674.

Nuedling, S., Kahlert, S., Loebbert, K., Meyer, R., Vetter, H., & Grohe, C. (1999). Differential effects of 17beta-estradiol on mitogen-activated protein kinase pathways in rat cardiomyocytes. *FEBS Lett, 454*(3), 271-276.

O'Meara, C. C., Wamstad, J. A., Gladstone, R. A., Fomovsky, G. M., Butty, V. L., Shrikumar, A., . . . Lee, R. T. (2015). Transcriptional reversion of cardiac myocyte fate during mammalian cardiac regeneration. *Circ Res, 116*(5), 804-815. doi:10.1161/CIRCRESAHA.116.304269

Ohshiro, K., Schwartz, A. M., Levine, P. H., & Kumar, R. (2012). Alternate estrogen receptors promote invasion of inflammatory breast cancer cells via non-genomic signaling. *PLoS One, 7*(1), e30725. doi:10.1371/journal.pone.0030725

Okamoto, K., & Aoki, K. (1963). Development of a strain of spontaneously hypertensive rats. *Jpn Circ J, 27*, 282-293.

Olsson, M. C., Palmer, B. M., Leinwand, L. A., & Moore, R. L. (2001). Gender and aging in a transgenic mouse model of hypertrophic cardiomyopathy. *Am J Physiol Heart Circ Physiol, 280*(3), H1136-1144.

Palmer, B. M., Chen, Z., Lachapelle, R. R., Hendley, E. D., & LeWinter, M. M. (2006). Cardiomyocyte function associated with hyperactivity and/or hypertension in genetic models of LV hypertrophy. *Am J Physiol Heart Circ Physiol, 290*(1), H463-473. doi:10.1152/ajpheart.00310.2005

Palmer, B. M., Wang, Y., Teekakirikul, P., Hinson, J. T., Fatkin, D., Strouse, S., . . . Maughan, D. W. (2008). Myofilament mechanical performance is enhanced by R403Q myosin in mouse myocardium independent of sex. *Am J Physiol Heart Circ Physiol, 294*(4), H1939-1947. doi:10.1152/ajpheart.00644.2007

Pare, G., Krust, A., Karas, R. H., Dupont, S., Aronovitz, M., Chambon, P., & Mendelsohn, M. E. (2002). Estrogen receptor-alpha mediates the protective effects of estrogen against vascular injury. *Circ Res, 90*(10), 1087-1092.

Parks, R. J., & Howlett, S. E. (2013). Sex differences in mechanisms of cardiac excitation-contraction coupling. *Pflugers Arch, 465*(5), 747-763. doi:10.1007/s00424-013-1233-0

Patrizio, M., Musumeci, M., Piccone, A., Raggi, C., Mattei, E., & Marano, G. (2013). Hormonal regulation of beta-myosin heavy chain expression in the mouse left ventricle. *J Endocrinol, 216*(3), 287-296. doi:10.1530/JOE-12-0201

Patten, R. D., & Hall-Porter, M. R. (2009). Small animal models of heart failure: development of novel therapies, past and present. *Circ Heart Fail, 2*(2), 138-144. doi:10.1161/CIRCHEARTFAILURE.108.839761

Patten, R. D., Pourati, I., Aronovitz, M. J., Alsheikh-Ali, A., Eder, S., Force, T., . . . Karas, R. H. (2008). 17 Beta-estradiol differentially affects left ventricular and cardiomyocyte hypertrophy following myocardial infarction and pressure overload. *J Card Fail, 14*(3), 245-253. doi:10.1016/j.cardfail.2007.10.024

Pechere-Bertschi, A., & Burnier, M. (2004). Female sex hormones, salt, and blood pressure regulation. *Am J Hypertens, 17*(10), 994-1001. doi:10.1016/j.amjhyper.2004.08.009

Pedram, A., Razandi, M., Lubahn, D., Liu, J., Vannan, M., & Levin, E. R. (2008). Estrogen inhibits cardiac hypertrophy: role of estrogen receptor-beta to inhibit calcineurin. *Endocrinology, 149*(7), 3361-3369. doi:10.1210/en.2008-0133

Pedram, A., Razandi, M., O'Mahony, F., Lubahn, D., & Levin, E. R. (2010). Estrogen receptor-beta prevents cardiac fibrosis. *Mol Endocrinol, 24*(11), 2152-2165. doi:10.1210/me.2010-0154

Pelzer, T., Loza, P. A., Hu, K., Bayer, B., Dienesch, C., Calvillo, L., . . . Ertl, G. (2005). Increased mortality and aggravation of heart failure in estrogen receptor-beta knockout mice after myocardial infarction. *Circulation, 111*(12), 1492-1498. doi:10.1161/01.CIR.0000159262.18512.46

Peterson, L. R., Soto, P. F., Herrero, P., Schechtman, K. B., Dence, C., & Gropler, R. J. (2007). Sex differences in myocardial oxygen and glucose metabolism. *J Nucl Cardiol, 14*(4), 573-581. doi:10.1016/j.nuclcard.2007.03.001

Petrov, G., Regitz-Zagrosek, V., Lehmkuhl, E., Krabatsch, T., Dunkel, A., Dandel, M., . . . Hetzer, R. (2010). Regression of myocardial hypertrophy after aortic valve replacement: faster in women? *Circulation, 122*(11 Suppl), S23-28. doi:10.1161/CIRCULATIONAHA.109.927764

Pierce, K. L., Tohgo, A., Ahn, S., Field, M. E., Luttrell, L. M., & Lefkowitz, R. J. (2001). Epidermal growth factor (EGF) receptor-dependent ERK activation by G protein-coupled receptors: a co-culture system for identifying intermediates upstream and downstream of heparin-binding EGF shedding. *J Biol Chem, 276*(25), 23155-23160. doi:10.1074/jbc.M101303200

Pinto, Y. M., Paul, M., & Ganten, D. (1998). Lessons from rat models of hypertension: from Goldblatt to genetic engineering. *Cardiovasc Res, 39*(1), 77-88.

Prabhavathi, K., Selvi, K. T., Poornima, K. N., & Sarvanan, A. (2014). Role of biological sex in normal cardiac function and in its disease outcome - a review. *J Clin Diagn Res, 8*(8), BE01-04. doi:10.7860/JCDR/2014/9635.4771

Praktiknjo, S. D., Llamas, B., Scott-Boyer, M. P., Picard, S., Robert, F., Langlais, D., . . . Deschepper, C. F. (2013). Novel effects of chromosome Y on cardiac regulation, chromatin remodeling, and neonatal programming in male mice. *Endocrinology, 154*(12), 4746-4756. doi:10.1210/en.2013-1699

Previlon, M., Pezet, M., Vinet, L., Mercadier, J. J., & Rouet-Benzineb, P. (2014). Gender-specific potential inhibitory role of Ca2+/calmodulin dependent protein kinase phosphatase (CaMKP) in pressure-overloaded mouse heart. *PLoS One, 9*(6), e90822. doi:10.1371/journal.pone.0090822

Pugach, E. K., Blenck, C. L., Dragavon, J. M., Langer, S. J., & Leinwand, L. A. (2016). Estrogen receptor profiling and activity in cardiac myocytes. *Mol Cell Endocrinol, 431*, 62-70. doi:10.1016/j.mce.2016.05.004

Qin, D., Zhang, Z. H., Caref, E. B., Boutjdir, M., Jain, P., & el-Sherif, N. (1996). Cellular and ionic basis of arrhythmias in postinfarction remodeled ventricular myocardium. *Circ Res, 79*(3), 461-473.

Queiros, A. M., Eschen, C., Fliegner, D., Kararigas, G., Dworatzek, E., Westphal, C., . . . Regitz-Zagrosek, V. (2013). Sex- and estrogen-dependent regulation of a miRNA network in the healthy and hypertrophied heart. *Int J Cardiol, 169*(5), 331-338. doi:10.1016/j.ijcard.2013.09.002

Rao, V., Cheng, Y., Lindert, S., Wang, D., Oxenford, L., McCulloch, A. D., . . . Regnier, M. (2014). PKA phosphorylation of cardiac troponin I modulates activation and relaxation kinetics of ventricular myofibrils. *Biophys J, 107*(5), 1196-1204. doi:10.1016/j.bpj.2014.07.027

Rapp, J. P., & Dene, H. (1985). Development and Characteristics of Inbred Strains of Dahl Salt-Sensitive and Salt-Resistant Rats. *Hypertension, 7*, 340-349.

Reckelhoff, J. F., Zhang, H., Granger, J. (1998). Testosterone Exacerbates Hypertension and Reduces Pressure-Natriuresis in Male Spontaneously Hypertensive Rats. *Hypertension, 31*(2), 435-439.

Reckelhoff, J. F. Z., H., Srivastava, K. (2000). Gender Differences in Development of Hypertenion in Spontaneously Hypertensive Rats: Role of the Renin-Angiotensin System. *Hypertension, 35*(2), 480-483.

Regitz-Zagrosek, V. (2006). Therapeutic implications of the gender-specific aspects of cardiovascular disease. *Nat Rev Drug Discov, 5*(5), 425-438. doi:10.1038/nrd2032

Reiser, P. J., & Moravec, C. S. (2014). Sex differences in myosin heavy chain isoforms of human failing and nonfailing atria. *Am J Physiol Heart Circ Physiol, 307*(3), H265-272. doi:10.1152/ajpheart.00810.2013

Report on Governmental Health Research Policies - Promoting Gender or Sex Differences Sensitivity (2003). Retrieved from http://dsp-psd.pwgsc.gc.ca/collection_2008/cihr-irsc/MR21-103-2003E.pdf

Resnicow, D. I., Deacon, J. C., Warrick, H. M., Spudich, J. A., & Leinwand, L. A. (2010). Functional diversity among a family of human skeletal muscle myosin motors. *Proc Natl Acad Sci U S A, 107*(3), 1053-1058. doi:10.1073/pnas.0913527107

Rice, R., Guinto, P., Dowell-Martino, C., He, H., Hoyer, K., Krenz, M., . . . Tardiff, J. C. (2010). Cardiac myosin heavy chain isoform exchange alters the phenotype of cTnT-related cardiomyopathies in mouse hearts. *J Mol Cell Cardiol, 48*(5), 979-988. doi:10.1016/j.yjmcc.2009.11.018

Rissman, E. F., Wersinger, S. R., Taylor, J. A., & Lubahn, D. B. (1997). Estrogen receptor function as revealed by knockout studies: neuroendocrine and behavioral aspects. *Horm Behav, 31*(3), 232-243. doi:10.1006/hbeh.1997.1390

Roberts, J., & Maurer, K. (1977). Blood pressure levels of persons 6-74 years. United States, 1971-1974. *Vital Health Stat 11*(203), i-v, 1-103.

Rohini, A., Agrawal, N., Koyani, C. N., & Singh, R. (2010). Molecular targets and regulators of cardiac hypertrophy. *Pharmacol Res, 61*(4), 269-280. doi:10.1016/j.phrs.2009.11.012

Ropero, A. B., Eghbali, M., Minosyan, T. Y., Tang, G., Toro, L., & Stefani, E. (2006). Heart estrogen receptor alpha: distinct membrane and nuclear distribution patterns and regulation by estrogen. *J Mol Cell Cardiol, 41*(3), 496-510. doi:10.1016/j.yjmcc.2006.05.022

Rosenkranz-Weiss, P., Tomek, R. J., Mathew, J., & Eghbali, M. (1994). Gender-specific differences in expression of mRNAs for functional and structural proteins in rat ventricular myocardium. *J Mol Cell Cardiol, 26*(2), 261-270.

Sacks, F. M., Lichtenstein, A., Van Horn, L., Harris, W., Kris-Etherton, P., & Winston, M. (2006). Soy protein, isoflavones, and cardiovascular health: a summary of a statement for professionals from the american heart association nutrition committee. *Arterioscler Thromb Vasc Biol, 26*(8), 1689-1692. doi:10.1161/01.ATV.0000227471.00284.ef

Sainz, J., Osuna, A., Wangensteen, R., de Dios Luna, J., Rodriguez-Gomez, I., Duarte, J., . . . Vargas, F. (2004). Role of sex, gonadectomy and sex hormones in the development of nitric oxide inhibition-induced hypertension. *Exp Physiol, 89*(2), 155-162. doi:10.1113/expphysiol.2003.002652

Salton, C. J., Chuang, M. L., O'Donnell, C. J., Kupka, M. J., Larson, M. G., Kissinger, K. V., . . . Manning, W. J. (2002). Gender differences and normal left ventricular anatomy in an adult population free of hypertension. A cardiovascular magnetic resonance study of the Framingham Heart Study Offspring cohort. *J Am Coll Cardiol, 39*(6), 1055-1060.

Sandstede, J., Lipke, C., Beer, M., Hofmann, S., Pabst, T., Kenn, W., . . . Hahn, D. (2000). Age- and gender-specific differences in left and right ventricular cardiac function and mass determined by cine magnetic resonance imaging. *Eur Radiol, 10*(3), 438-442. doi:10.1007/s003300050072

Schaible, T. F., Malhotra, A., Ciambrone, G., & Scheuer, J. (1984). The effects of gonadectomy on left ventricular function and cardiac contractile proteins in male and female rats. *Circ Res, 54*(1), 38-49.

Scheuer, J., Malhotra, A., Schaible, T. F., & Capasso, J. (1987). Effects of gonadectomy and hormonal replacement on rat hearts. *Circ Res, 61*(1), 12-19.

Schmidt, O., Pfanner, N., & Meisinger, C. (2010). Mitochondrial protein import: from proteomics to functional mechanisms. *Nat Rev Mol Cell Biol, 11*(9), 655-667. doi:10.1038/nrm2959

Schmitt, N., Grunnet, M., & Olesen, S. P. (2014). Cardiac potassium channel subtypes: new roles in repolarization and arrhythmia. *Physiol Rev, 94*(2), 609-653. doi:10.1152/physrev.00022.2013

Schonbrunn, A. (2014). Editorial: Antibody can get it right: confronting problems of antibody specificity and irreproducibility. *Mol Endocrinol, 28*(9), 1403-1407. doi:10.1210/me.2014-1230

Severs, N. J., Bruce, A. F., Dupont, E., & Rothery, S. (2008). Remodelling of gap junctions and connexin expression in diseased myocardium. *Cardiovasc Res, 80*(1), 9-19. doi:10.1093/cvr/cvn133

Shaw, L. J., Bairey Merz, C. N., Pepine, C. J., Reis, S. E., Bittner, V., Kelsey, S. F., . . . Investigators, W. (2006). Insights from the NHLBI-Sponsored Women's Ischemia Syndrome Evaluation (WISE) Study: Part I: gender differences in traditional and novel risk factors, symptom evaluation, and gender-optimized diagnostic strategies. *J Am Coll Cardiol, 47*(3 Suppl), S4-S20. doi:10.1016/j.jacc.2005.01.072

Shioura, K. M., Geenen, D. L., & Goldspink, P. H. (2008). Sex-related changes in cardiac function following myocardial infarction in mice. *Am J Physiol Regul Integr Comp Physiol, 295*(2), R528-534. doi:10.1152/ajpregu.90342.2008

Simoncini, T., Hafezi-Moghadam, A., Brazil, D. P., Ley, K., Chin, W. W., & Liao, J. K. (2000). Interaction of oestrogen receptor with the regulatory subunit of phosphatidylinositol-3-OH kinase. *Nature, 407*(6803), 538-541. doi:10.1038/35035131

Skavdahl, M., Steenbergen, C., Clark, J., Myers, P., Demianenko, T., Mao, L., . . . Murphy, E. (2005). Estrogen receptor-beta mediates male-female differences in the development of pressure overload hypertrophy. *Am J Physiol Heart Circ Physiol, 288*(2), H469-476. doi:10.1152/ajpheart.00723.2004

Somekawa, S., Fukuhara, S., Nakaoka, Y., Fujita, H., Saito, Y., & Mochizuki, N. (2005). Enhanced functional gap junction neoformation by protein kinase A-dependent and Epac-dependent signals downstream of cAMP in cardiac myocytes. *Circ Res, 97*(7), 655-662. doi:10.1161/01.RES.0000183880.49270.f9

Stauffer, B. L., Konhilas, J. P., Luczak, E. D., & Leinwand, L. A. (2006). Soy diet worsens heart disease in mice. *J Clin Invest, 116*(1), 209-216. doi:10.1172/JCI24676

Stenoien, D. L., Mancini, M. G., Patel, K., Allegretto, E. A., Smith, C. L., & Mancini, M. A. (2000). Subnuclear trafficking of estrogen receptor-alpha and steroid receptor coactivator-1. *Mol Endocrinol, 14*(4), 518-534. doi:10.1210/mend.14.4.0436

Stewart, J. A., Jr., Cashatt, D. O., Borck, A. C., Brown, J. E., & Carver, W. E. (2006). 17beta-estradiol modulation of angiotensin II-stimulated response in cardiac fibroblasts. *J Mol Cell Cardiol, 41*(1), 97-107. doi:10.1016/j.yjmcc.2006.04.019

Stumpf, W. E. (1990). Steroid hormones and the cardiovascular system: direct actions of estradiol, progesterone, testosterone, gluco- and mineralcorticoids, and soltriol [vitamin D] on central nervous regulatory and peripheral tissues. *Experientia, 46*(1), 13-25.

Sugishita, K., Su, Z., Li, F., Philipson, K. D., & Barry, W. H. (2001). Gender influences [Ca(2+)](i) during metabolic inhibition in myocytes overexpressing the Na(+)-Ca(2+) exchanger. *Circulation, 104*(17), 2101-2106.

Sun, J., Picht, E., Ginsburg, K. S., Bers, D. M., Steenbergen, C., & Murphy, E. (2006). Hypercontractile female hearts exhibit increased S-nitrosylation of the L-type Ca2+ channel alpha1 subunit and reduced ischemia/reperfusion injury. *Circ Res, 98*(3), 403-411. doi:10.1161/01.RES.0000202707.79018.0a

Tesi, C., Colomo, F., Nencini, S., Piroddi, N., & Poggesi, C. (1999). Modulation by substrate concentration of maximal shortening velocity and isometric force in single myofibrils from frog and rabbit fast skeletal muscle. *J Physiol, 516 (Pt 3)*, 847-853.

Tesi, C., Colomo, F., Nencini, S., Piroddi, N., & Poggesi, C. (2000). The effect of inorganic phosphate on force generation in single myofibrils from rabbit skeletal muscle. *Biophys J, 78*(6), 3081-3092. doi:10.1016/S0006-3495(00)76845-7

Thigpen, J. E., Setchell, K. D., Ahlmark, K. B., Locklear, J., Spahr, T., Caviness, G. F., . . . Forsythe, D. B. (1999). Phytoestrogen content of purified, open- and closed-formula laboratory animal diets. *Lab Anim Sci, 49*(5), 530-536.

Tomaselli, G. F., & Marban, E. (1999). Electrophysiological remodeling in hypertrophy and heart failure. *Cardiovasc Res, 42*(2), 270-283.

Ueyama, T., Kawashima, S., Sakoda, T., Rikitake, Y., Ishida, T., Kawai, M., . . . Yokoyama, M. (2000). Requirement of activation of the extracellular signal-regulated kinase cascade in myocardial cell hypertrophy. *J Mol Cell Cardiol, 32*(6), 947-960. doi:10.1006/jmcc.2000.1135

Ushio-Fukai, M., Zafari, A. M., Fukui, T., Ishizaka, N., & Griendling, K. K. (1996). p22phox is a critical component of the superoxide-generating NADH/NADPH oxidase system and regulates

angiotensin II-induced hypertrophy in vascular smooth muscle cells. *J Biol Chem, 271*(38), 23317-23321.

van Rooij, E., Fielitz, J., Sutherland, L. B., Thijssen, V. L., Crijns, H. J., Dimaio, M. J., . . . Olson, E. N. (2010). Myocyte enhancer factor 2 and class II histone deacetylases control a gender-specific pathway of cardioprotection mediated by the estrogen receptor. *Circ Res, 106*(1), 155-165. doi:10.1161/CIRCRESAHA.109.207084

Vijay, V., Han, T., Moland, C. L., Kwekel, J. C., Fuscoe, J. C., & Desai, V. G. (2015). Sexual dimorphism in the expression of mitochondria-related genes in rat heart at different ages. *PLoS One, 10*(1), e0117047. doi:10.1371/journal.pone.0117047

Villareal, R. P., Woodruff, A. L., & Massumi, A. (2001). Gender and cardiac arrhythmias. *Tex Heart Inst J, 28*(4), 265-275.

Vizgirda, V. M., Wahler, G. M., Sondgeroth, K. L., Ziolo, M. T., & Schwertz, D. W. (2002). Mechanisms of sex differences in rat cardiac myocyte response to beta-adrenergic stimulation. *Am J Physiol Heart Circ Physiol, 282*(1), H256-263.

Walker, J. S., Walker, L. A., Margulies, K., Buttrick, P., & de Tombe, P. (2011). Protein kinase A changes calcium sensitivity but not crossbridge kinetics in human cardiac myofibrils. *Am J Physiol Heart Circ Physiol, 301*(1), H138-146. doi:10.1152/ajpheart.00838.2010

Wang, F., He, Q., Sun, Y., Dai, X., & Yang, X. P. (2010). Female adult mouse cardiomyocytes are protected against oxidative stress. *Hypertension, 55*(5), 1172-1178. doi:10.1161/HYPERTENSIONAHA.110.150839

Wang, H., Jessup, J. A., Zhao, Z., Da Silva, J., Lin, M., MacNamara, L. M., . . . Groban, L. (2013). Characterization of the cardiac renin angiotensin system in oophorectomized and estrogen-replete mRen2.Lewis rats. *PLoS One, 8*(10), e76992. doi:10.1371/journal.pone.0076992

Wang, M., Baker, L., Tsai, B. M., Meldrum, K. K., & Meldrum, D. R. (2005). Sex differences in the myocardial inflammatory response to ischemia-reperfusion injury. *Am J Physiol Endocrinol Metab, 288*(2), E321-326. doi:10.1152/ajpendo.00278.2004

Wang, Y. R., Yen, C. H., Sun, Y. F., & Laun, Y. T. (2003). Gender-dependent response in blood pressure changes following the inhibition of nitric oxide synthase. *Chin J Physiol, 46*(2), 91-94.

Wang, Z., Zhang, X., Shen, P., Loggie, B. W., Chang, Y., & Deuel, T. F. (2005). Identification, cloning, and expression of human estrogen receptor-alpha36, a novel variant of human estrogen receptor-alpha66. *Biochem Biophys Res Commun, 336*(4), 1023-1027. doi:10.1016/j.bbrc.2005.08.226

Wang, Z., Zhang, X., Shen, P., Loggie, B. W., Chang, Y., & Deuel, T. F. (2006). A variant of estrogen receptor-{alpha}, hER-{alpha}36: transduction of estrogen- and antiestrogen-dependent membrane-initiated mitogenic signaling. *Proc Natl Acad Sci U S A, 103*(24), 9063-9068. doi:10.1073/pnas.0603339103

Weigel, N. L., & Zhang, Y. (1998). Ligand-independent activation of steroid hormone receptors. *J Mol Med (Berl), 76*(7), 469-479.

Weinberg, E. O., Thienelt, C. D., Katz, S. E., Bartunek, J., Tajima, M., Rohrbach, S., . . . Lorell, B. H. (1999). Gender differences in molecular remodeling in pressure overload hypertrophy. *J Am Coll Cardiol, 34*(1), 264-273.

Weinberger, M. H., Miller, J. Z., Luft, F. C., Grim, C. E., & Fineberg, N. S. (1986). Definitions and characteristics of sodium sensitivity and blood pressure resistance. *Hypertension, 8*(6 Pt 2), II127-134.

Weiner, C. P., Lizasoain, I., Baylis, S. A., Knowles, R. G., Charles, I. G., & Moncada, S. (1994). Induction of calcium-dependent nitric oxide synthases by sex hormones. *Proc Natl Acad Sci U S A, 91*(11), 5212-5216.

Writing Group, M., Lloyd-Jones, D., Adams, R. J., Brown, T. M., Carnethon, M., Dai, S., . . . Stroke Statistics, S. (2010). Heart disease and stroke statistics--2010 update: a report from the American Heart Association. *Circulation, 121*(7), e46-e215. doi:10.1161/CIRCULATIONAHA.109.192667

Wu, Q., Zhao, Z., Sun, H., Hao, Y. L., Yan, C. D., & Gu, S. L. (2008). Oestrogen changed cardiomyocyte contraction and beta-adrenoceptor expression in rat hearts subjected to ischaemia-reperfusion. *Exp Physiol, 93*(9), 1034-1043. doi:10.1113/expphysiol.2007.041939

Wu, Y., Huang, A., Sun, D., Falck, J. R., Koller, A., & Kaley, G. (2001). Gender-specific compensation for the lack of NO in the mediation of flow-induced arteriolar dilation. *Am J Physiol Heart Circ Physiol, 280*(6), H2456-2461.

Xiao, L., Zhang, L., Han, W., Wang, Z., & Nattel, S. (2006). Sex-based transmural differences in cardiac repolarization and ionic-current properties in canine left ventricles. *Am J Physiol Heart Circ Physiol, 291*(2), H570-580. doi:10.1152/ajpheart.01288.2005

Xie, M., Burchfield, J. S., & Hill, J. A. (2013). Pathological ventricular remodeling: therapies: part 2 of 2. *Circulation, 128*(9), 1021-1030. doi:10.1161/CIRCULATIONAHA.113.001879

Xin, M., Olson, E. N., & Bassel-Duby, R. (2013). Mending broken hearts: cardiac development as a basis for adult heart regeneration and repair. *Nat Rev Mol Cell Biol, 14*(8), 529-541. doi:10.1038/nrm3619

Yamamoto, K. R. (1985). Steroid receptor regulated transcription of specific genes and gene networks. *Annu Rev Genet, 19*, 209-252. doi:10.1146/annurev.ge.19.120185.001233

Yan, L., Ge, H., Li, H., Lieber, S. C., Natividad, F., Resuello, R. R., . . . Vatner, D. E. (2004). Gender-specific proteomic alterations in glycolytic and mitochondrial pathways in aging monkey hearts. *J Mol Cell Cardiol, 37*(5), 921-929. doi:10.1016/j.yjmcc.2004.06.012

Yanes, L. L., Romero, D. G., Iles, J. W., Iliescu, R., Gomez-Sanchez, C., & Reckelhoff, J. F. (2006). Sexual dimorphism in the renin-angiotensin system in aging spontaneously hypertensive rats. *Am J Physiol Regul Integr Comp Physiol, 291*(2), R383-390. doi:10.1152/ajpregu.00510.2005

Yanes, L. L., Sartori-Valinotti, J. C., Iliescu, R., Romero, D. G., Racusen, L. C., Zhang, H., & Reckelhoff, J. F. (2009). Testosterone-dependent hypertension and upregulation of intrarenal

angiotensinogen in Dahl salt-sensitive rats. *Am J Physiol Renal Physiol, 296*(4), F771-779. doi:10.1152/ajprenal.90389.2008

Yang, X., Schadt, E. E., Wang, S., Wang, H., Arnold, A. P., Ingram-Drake, L., . . . Lusis, A. J. (2006). Tissue-specific expression and regulation of sexually dimorphic genes in mice. *Genome Res, 16*(8), 995-1004. doi:10.1101/gr.5217506

Yang, X. P., & Reckelhoff, J. F. (2011). Estrogen, hormonal replacement therapy and cardiovascular disease. *Curr Opin Nephrol Hypertens, 20*(2), 133-138. doi:10.1097/MNH.0b013e3283431921

Yu, Y., Fuscoe, J. C., Zhao, C., Guo, C., Jia, M., Qing, T., . . . Wang, C. (2014). A rat RNA-Seq transcriptomic BodyMap across 11 organs and 4 developmental stages. *Nat Commun, 5*, 3230. doi:10.1038/ncomms4230

Zhang, Z., Fang, J., Gillespie, C., Wang, G., Hong, Y., & Yoon, P. W. (2012). Age-specific gender differences in in-hospital mortality by type of acute myocardial infarction. *Am J Cardiol, 109*(8), 1097-1103. doi:10.1016/j.amjcard.2011.12.001

Zheng, Y., Zhang, J., Xu, Z. Z., Sheng, J. M., Zhang, X. C., Wang, H. H., . . . Teng, L. S. (2010). Quantitative profiles of the mRNAs of ER-alpha and its novel variant ER-alpha36 in breast cancers and matched normal tissues. *J Zhejiang Univ Sci B, 11*(2), 144-150. doi:10.1631/jzus.B0900266

Zipes, D. P., & Jalife, J. *Cardiac electrophysiology : from cell to bedside* (Sixth edition. ed.).

Zou, Y., Ding, L., Coleman, M., & Wang, Z. (2009). Estrogen receptor-alpha (ER-alpha) suppresses expression of its variant ER-alpha 36. *FEBS Lett, 583*(8), 1368-1374. doi:10.1016/j.febslet.2009.03.047

Appendix I Primer sequences

Primer/Gene Name	Sequence
18S Forward	gccgctagaggtgaaattcttg
18S Reverse	ctttcgctctggtcgtctt
rodentER-alpha Forward	gggaagctcctgtttgctc
rodentER-alpha Reverse	agccagcaacatgtcaaaga
humanER-alpha Forward	ccactcctccacctttgac
humanER-alpha Reverse	accctgttgctgtagcca
Gapdh Forward	aggtcggtgtgaacggatttg
Gapdh Reverse	tgtagaccatgtagttgaggtca
ER-beta Forward	gctgggccaagaaaatcc
ER-beta Reverse	gctttctaagagccggacttg
Nr4a1 Forward	tgctctggtcctcatcactg
Nr4a1 Reverse	gacagctagcaatgcggttc
Tfrc Forward	cgttattaaaggctatgaggaacc
Tfrc Reverse	gttcccacactggacttcg
Col3a1 Forward	ggcacagcagtccaatgtag
Col3a1 Reverse	cccgagtcgcagacacata
Ccng1 Forward	actggacagattcttgtctaaaatga
Ccng1 Reverse	ggacgttcctttcctcttca
Ucp2 Forward	gttctacaccaagggctcaga
Ucp2 Reverse	gacctttaccacatctgtaggttg
Cox6c Forward	gcgtctgcgggttcatattg
Cox6c Reverse	tctgcataagccttctttcttg
Por Forward	gccgtctgaagagctacgag
Por Reverse	tggttcagcttccggttg

Appendix II DESeq results of female vs. male myocytes: All genes with padj ≤ 0.01.

Gene id	baseMean Male (A)	baseMean Female (B)	foldChange	padj
Ddx3	2340.91	0.21	8.79E-05	1.85E-118
Eif2s3y	2215.25	0.58	0.000261022	5.12E-111
Tfrc	8298.02	2812.58	0.338946319	9.94E-26
Sh3bgrl	874.21	408.17	0.466906921	7.25E-08
Synpo	1156.93	2270.39	1.962432628	1.54E-07
Rcn1	1503.97	747.02	0.49669818	2.70E-07
C4a	1417.16	3353.66	2.366464963	3.20E-07
Casc5	80.20	10.09	0.125782718	5.34E-07
Itga7	9047.05	16031.98	1.772067319	1.01E-06
Por	1853.27	3395.06	1.831930954	1.08E-06
Apoe	1206.37	2256.63	1.870599792	1.76E-06
Dstn	6144.46	3489.83	0.567964155	1.76E-06
Nr4a1	800.13	1721.16	2.151087556	1.76E-06
Irf6	165.13	52.34	0.316970359	3.09E-06
Adamtsl4	904.72	1707.91	1.88778041	7.20E-06
Col3a1	10722.45	3914.72	0.365095802	1.16E-05
Junb	9242.11	16086.99	1.740618961	1.64E-05
Mlf1	3361.26	1956.33	0.582021325	1.79E-05
Pcsk6	3782.43	6386.60	1.688491473	1.79E-05
Emp1	2089.38	820.66	0.39277514	2.40E-05
Loxl2	230.02	93.30	0.405623935	2.86E-05
Zfp423	557.32	1017.85	1.826329727	3.18E-05
Ahdc1	472.02	966.97	2.048605809	3.98E-05
Ech1	18612.98	30110.38	1.617708355	4.12E-05
Eif2ak2	1565.79	815.40	0.520761536	4.12E-05
Zfp142	552.73	1006.07	1.820161537	4.12E-05
Zfp36	14086.77	23759.40	1.686645753	4.12E-05
Acacb	9197.83	16175.91	1.758665988	4.87E-05
Pdxp	178.00	370.08	2.079048374	5.66E-05
Prpf8	4303.35	7068.39	1.642532259	5.66E-05
Mki67	408.55	102.83	0.251705157	6.02E-05
Usp19	2533.41	4493.32	1.773627435	6.02E-05
Klf2	135.43	306.46	2.262878338	6.63E-05
Corin	3351.73	5734.17	1.710810696	8.36E-05
Mef2d	1970.43	3260.16	1.654544089	8.36E-05
Sept2	6802.92	4181.20	0.614618949	8.36E-05
Gcn1l1	2746.57	4570.49	1.664072367	8.46E-05
Ncln	562.60	1005.23	1.786756153	8.46E-05
Tacc2	8533.74	14783.06	1.732308148	8.46E-05
Ier2	2327.61	4269.26	1.834187549	9.97E-05
Cog1	842.86	1453.32	1.724276343	0.000117378
Fitm2	7091.57	11484.28	1.619427093	0.000117378
Myh6	831770.67	1330868.07	1.600042075	0.000117378
Dnaja1	5213.11	3241.49	0.621795234	0.000120513

Rnf31	490.34	860.39	1.754699012	0.000120513
Urgcp	1434.81	2376.86	1.656573796	0.000126236
Zfp691	325.54	599.71	1.842194814	0.000127126
Hhatl	4363.99	7012.22	1.606836165	0.00013806
Pc	833.13	1424.05	1.709276862	0.00013806
Rela	1602.37	2636.76	1.645534737	0.00013806
Csdc2	509.81	1326.19	2.601356953	0.000138332
Gaa	3608.89	5878.14	1.628796563	0.000140139
Hspa12b	240.72	493.28	2.04914986	0.000150176
Casp3	199.76	83.51	0.418067821	0.000151871
Cad	265.68	530.48	1.996671735	0.000163727
Rbm14	271.75	513.94	1.891240276	0.000177129
Mypn	4795.22	7645.74	1.594450495	0.000177884
Trim11	314.26	630.51	2.006344397	0.000177884
Bcas3	709.06	1331.35	1.877617699	0.000180746
Tmem214	698.75	1189.13	1.701787801	0.000186194
Mest	118.84	41.11	0.345902745	0.000186813
Mgp	2739.15	4438.92	1.620549938	0.000197705
Sf3a1	1996.92	3234.51	1.619751767	0.000207251
Ptprs	1826.35	2981.25	1.632352562	0.000217965
Gtpbp1	1186.78	2728.14	2.298773157	0.000224587
Pvrl3	246.75	112.26	0.454962742	0.000232491
Ucp2	3335.78	6485.26	1.944149478	0.000238318
Abcc8	990.33	1643.69	1.659747316	0.00025857
Cbx7	202.26	389.68	1.9265807	0.000262129
Sgce	461.81	246.29	0.533315438	0.000262129
Foxj2	841.40	1397.50	1.660911707	0.000287306
Per1	865.59	1433.58	1.656194815	0.000287306
Ubr4	3063.10	4822.85	1.574497876	0.00030279
Ttll12	358.43	649.68	1.812575874	0.000304999
Akap17a	588.33	1011.95	1.720042332	0.000305393
Colq	401.26	694.62	1.731087737	0.000305393
Nes	891.42	518.84	0.582041882	0.000310142
Cst3	6931.00	10669.63	1.539408326	0.000326523
RGD1310507	530.87	882.04	1.661512904	0.000342741
Armcx3	4615.39	2867.91	0.621380453	0.000356436
Phldb1	4645.99	7223.57	1.55479673	0.000363393
Rbm42	357.00	682.72	1.912416317	0.000401948
Krt19	48.86	133.34	2.72884226	0.000435925
Mob1a	1554.86	946.81	0.608935369	0.000435925
Mfap1a	3094.25	1976.27	0.638690575	0.000437375
Pik3r3	605.77	347.78	0.574107163	0.000437375
Prcp	408.58	207.48	0.507821168	0.000437375
Pdcd4	599.19	338.38	0.564727365	0.000468561
Stard10	491.23	849.83	1.730010889	0.000481795
Xab2	421.42	727.79	1.726999834	0.000489295
Lrg1	70.42	188.29	2.673729302	0.000490561
Tmod3	1186.99	634.70	0.534714322	0.000490561
Dyrk1b	301.67	586.43	1.943948659	0.000496959

Scap	1240.39	1971.82	1.589679849	0.000497062
Aspa	38.19	5.01	0.131281738	0.000497168
Hspbp1	174.73	355.91	2.036895185	0.000497168
Irs3	15.55	65.42	4.205735544	0.000507709
Myh14	4653.57	7244.12	1.556680022	0.000509505
Vasn	242.65	451.33	1.859983577	0.000510923
Edc4	866.48	1470.10	1.696637845	0.00055366
Eif3f	2171.79	3852.94	1.774082147	0.000572897
Ankrd13c	698.66	404.63	0.579146744	0.00057942
Pelp1	427.89	757.07	1.769330219	0.000590685
Hdac5	2021.36	3140.80	1.553800419	0.000593213
Ptpla	1591.35	950.54	0.597315389	0.000593213
Tbc1d17	646.06	1072.85	1.660614228	0.000593213
Tlk1	226.88	104.40	0.460146353	0.000593213
Vps18	489.16	958.38	1.959236276	0.000593213
Rabac1	505.43	865.73	1.71287356	0.000636372
Slc35a3	250.31	120.39	0.48096013	0.000636372
Kif23	71.48	18.04	0.252408908	0.000683819
Repin1	121.77	255.20	2.09584721	0.00070889
Magi3	4515.77	2692.69	0.596285497	0.000711894
Hyou1	5597.38	8512.77	1.520849955	0.00074139
Lrrc4b	6709.49	10307.85	1.536308832	0.00074139
Trim37	292.79	149.76	0.511480757	0.00074139
Usp36	745.30	1223.95	1.642224361	0.00074139
Nampt	11669.60	6581.32	0.563971782	0.000746481
Pigy	2928.69	1729.17	0.590425568	0.000767795
Amotl2	3928.69	6013.42	1.530642541	0.000772681
Nin	478.69	249.55	0.521310182	0.000775285
Jak3	61.64	149.93	2.432162166	0.000786232
Mlycd	2038.03	3160.72	1.550867939	0.000792409
Slc3a2	2146.29	3308.43	1.541470396	0.000794037
Gstm2	5956.41	9712.32	1.630568074	0.000794417
Xbp1	2379.00	3904.14	1.641082539	0.000794417
Man2c1	912.68	1441.57	1.579502432	0.00080325
Akr7a2	967.79	1533.70	1.584742307	0.00080679
Hsf4	108.35	229.40	2.117225494	0.00080679
Plaa	3958.89	2584.80	0.652909739	0.00080679
Serp1	749.20	438.34	0.585072092	0.00080679
Tmtc4	602.99	327.21	0.542656785	0.00080679
Tns1	15689.84	23680.06	1.509260247	0.00080679
Vars	2555.07	4039.26	1.580879769	0.00080679
Atg9a	2281.22	3654.48	1.601983368	0.000825347
Acsf2	4494.29	6923.88	1.540595314	0.000828267
Rhbdf1	252.09	450.06	1.785338416	0.000828267
Tubb4b	11202.11	18294.94	1.633168795	0.000828267
Ubc	5844.12	8805.02	1.506646658	0.000828267
Cep290	353.34	133.17	0.376897971	0.000833214
Itgb1	10162.38	6750.59	0.664272104	0.000833214
Anxa10	611.22	356.70	0.583593353	0.000874379

Capza1	1269.87	794.78	0.625878971	0.000874379
Fam65a	873.35	1396.19	1.598668311	0.000874379
Slc4a3	5847.67	8835.01	1.510860336	0.000874379
Hmgn3	1215.36	698.72	0.574907799	0.000874869
Ap3s1	321.19	170.09	0.5295715	0.000885397
Rab8b	323.22	153.11	0.473708243	0.000885397
Slc27a1	1395.39	2291.05	1.641871942	0.000885397
Zdhhc21	281.91	135.92	0.482123487	0.000885397
Nfix	733.38	1164.92	1.588424036	0.000897513
Atg2a	713.06	1366.07	1.915792506	0.000925658
Herpud1	6645.71	10008.36	1.505989793	0.000925658
Cpsf1	640.04	1048.85	1.638721334	0.000925974
Mllt1	1257.08	1981.04	1.575906028	0.000935409
Tbx5	1706.38	2656.91	1.557044359	0.000939868
Zbtb45	177.49	332.89	1.875578337	0.000944402
Gga1	831.72	1328.01	1.596711189	0.000959387
Sec16a	1429.84	2214.52	1.548789669	0.000959387
Dnm1l	6703.82	4469.08	0.666646777	0.000962573
Top2a	181.68	44.99	0.247632036	0.000962573
Irf2bp1	205.73	443.70	2.156733328	0.00096707
Mroh1	1089.00	1731.19	1.589713859	0.000981133
Wbp2	423.19	720.02	1.701416868	0.000981133
Prrc2a	1694.21	3370.88	1.98964665	0.00098914
Nasp	867.87	533.47	0.614685712	0.001003049
Cand2	2397.18	4109.78	1.714427715	0.0010094
Calcrl	599.64	293.71	0.489813124	0.001009455
Entpd6	503.60	894.30	1.775800116	0.001018514
Leng8	292.76	511.12	1.745820674	0.001018514
Sec24c	1074.38	1691.90	1.574764465	0.001026323
Wnk2	1537.18	3034.45	1.974037943	0.001044489
Vcan	357.15	162.10	0.453874868	0.001051965
Pign	348.70	190.22	0.545513219	0.001094411
Slc9a8	483.16	797.66	1.650937806	0.001094411
Kras	284.47	128.52	0.451774097	0.001097881
Adar	1413.72	2167.49	1.53318394	0.001101556
Csgalnact1	112.86	44.32	0.392662922	0.001101556
Mfge8	3140.49	5084.65	1.619058948	0.001101556
Tapbp	391.11	707.64	1.809307999	0.001101556
Fam73b	1581.29	2413.90	1.526536886	0.001113704
Myo18a	2969.35	4825.88	1.625232655	0.001113704
Crk	3731.30	2438.04	0.653402833	0.001115028
Ccp110	135.61	54.95	0.405165193	0.001141143
Cep55	29.69	3.61	0.121569628	0.001141143
Pon2	586.67	346.90	0.591313177	0.001141143
Agpat1	558.56	894.39	1.601246102	0.001175769
Hcfc1	1837.76	2889.76	1.57244112	0.001175769
Map1s	139.59	376.95	2.700412477	0.001175769
Nckipsd	172.26	317.48	1.842983679	0.001186926
Cul9	343.47	587.90	1.711620196	0.001204309

Dnajc3	1911.60	1221.53	0.639008826	0.001204309
Syde1	584.53	938.19	1.60504635	0.001205057
Pdcd10	661.64	392.87	0.593788081	0.001206719
Lamb2	11227.77	16736.70	1.490651298	0.001214717
Fbxo31	1021.91	1695.29	1.658951788	0.001314443
Fmo1	585.30	1129.86	1.930380884	0.001331006
Lzts2	690.60	1071.43	1.551459661	0.001331006
Ppp2r3a	9505.41	6280.33	0.660710805	0.001331006
Tax1bp1	4530.68	3031.92	0.66919753	0.001331006
Dyrk3	272.48	514.97	1.88994546	0.001372218
Lrp5	3469.63	5185.64	1.494579562	0.001372218
Psme4	11693.63	7588.26	0.648922433	0.001372218
Rogdi	1028.52	1590.22	1.546133813	0.001372218
Trim54	9735.63	14302.29	1.469067435	0.001372218
Speg	5665.40	8460.28	1.493325213	0.001373469
Nrep	180.32	84.61	0.469253951	0.001388774
Abracl	182.45	84.57	0.463517388	0.001420554
Gpt	931.32	1459.99	1.567653359	0.001420554
Pacs1	387.07	645.69	1.668139502	0.001423725
Ptov1	995.68	1547.77	1.55447658	0.001433734
Rps14	1440.00	2155.02	1.496544802	0.001433734
Dock11	260.89	125.13	0.479630069	0.001436025
Jup	5115.99	8891.73	1.738025941	0.001436025
Minos1	7153.54	4663.34	0.651891611	0.001436025
Nfkb2	835.91	1398.80	1.673376201	0.001436025
Plbd2	496.25	829.36	1.671239144	0.001436025
Rala	927.62	535.80	0.577599864	0.001436025
Rnf2	1953.34	1196.82	0.612705345	0.001437018
Plekhm2	3901.98	5867.70	1.503775069	0.001453291
Nr1h2	1005.40	1541.63	1.533351299	0.001455898
Fmnl1	84.26	182.86	2.170187591	0.001477787
Pom121	123.37	244.91	1.985200884	0.001532567
Ass1	33.59	91.49	2.723575586	0.001553737
Gtf3c1	3197.75	4756.59	1.487477744	0.001553737
Hmgb2	605.84	346.87	0.572542999	0.001553737
Map4k4	3305.91	2197.15	0.664612505	0.001553737
Arpc2	6118.42	3863.17	0.631399847	0.001568424
Atg4al1	689.17	421.29	0.611297436	0.001568424
Gata5	1572.32	2402.72	1.528135285	0.001568424
LOC310926	1981.27	8549.81	4.315323845	0.001577701
Lipe	585.25	1020.10	1.743032217	0.001577701
Ppt2	889.52	1375.41	1.546251301	0.001584302
Alg2	317.25	537.75	1.695045222	0.001639566
Ccz1b	897.73	517.18	0.576095764	0.001663477
Alpl	836.89	1583.86	1.892543105	0.001694254
Gnai3	1538.77	713.29	0.463543203	0.001694254
Bcl9l	166.26	304.10	1.829093959	0.00170063
Hsp90aa1	720.31	2.12	0.002942903	0.00170063
March7	2943.89	1812.26	0.615602103	0.00170063

Sqstm1	7583.31	12105.24	1.596300624	0.00170063
Pds5a	1958.53	1145.51	0.584880428	0.001716559
Rab11b	1965.79	2955.32	1.503378389	0.001716559
LOC499602	1738.60	1142.12	0.656920304	0.001735969
Bckdha	4980.12	7504.61	1.506913989	0.00173782
Rrm2	74.94	16.60	0.221507516	0.00173782
Prrg1	225.79	113.41	0.502303318	0.001809172
Aarsd1	904.27	1485.84	1.643143403	0.001811732
Ap2a1	956.07	1472.88	1.540561629	0.001811732
Calu	21541.39	14823.18	0.68812551	0.001811732
Cyp2e1	344.76	929.51	2.696122954	0.001811732
H6pd	410.01	670.87	1.636198389	0.001811732
Msln	110.79	238.29	2.150818995	0.001811732
Plxnb2	1284.02	1984.85	1.54580474	0.001811732
Ptpn23	134.08	257.94	1.923748253	0.001811732
Sema3d	246.88	114.43	0.463520675	0.001811732
Slc25a34	783.01	1210.56	1.546034634	0.001811732
Timm44	4592.51	3102.30	0.675513098	0.001811732
Rnf123	1593.32	2659.50	1.669162233	0.001814677
Pygm	51691.68	75438.47	1.459392969	0.001843801
Zdhhc17	524.08	286.44	0.54656149	0.001884849
Nckap1	6077.74	4125.32	0.678759633	0.001887287
Klf6	6427.77	4050.57	0.630168323	0.001913275
Pbxip1	2414.35	3775.58	1.563804558	0.001926319
Rab1a	3615.37	2378.29	0.657828259	0.001926319
Ola1	2867.32	1927.80	0.672334159	0.001942735
Map1lc3a	8436.51	12270.33	1.454430911	0.001993514
Bag6	4349.72	6870.35	1.579492813	0.002004002
Flii	6082.87	9040.54	1.486231066	0.002004002
Sugp1	1274.11	1933.76	1.517733745	0.002004002
Fem1a	7058.29	10271.49	1.455238059	0.002015417
Itm2c	2867.36	4219.18	1.471449649	0.002015417
Klhl4	152.43	67.97	0.445910622	0.002015417
Trappc9	473.47	803.68	1.697428812	0.002015417
Arrdc3	1127.98	623.61	0.552859099	0.002068209
Dok7	208.17	370.22	1.778397205	0.002083643
Lrch4	135.36	269.17	1.988529805	0.002083643
Scaf1	323.27	555.09	1.717142597	0.0020843
Fmr1	572.46	216.28	0.377801147	0.002099636
Dusp1	5818.91	10371.90	1.782446082	0.002116553
Des	88155.95	138958.37	1.5762789	0.002147592
Tomm20	4271.34	2653.88	0.621323386	0.002176409
Nkx2-5	352.69	668.19	1.894568454	0.002199762
Hist1h1d	731.32	1477.78	2.020710415	0.00220507
Flad1	1653.50	2621.03	1.585139422	0.00220959
Dctn1	5282.37	7734.35	1.46418032	0.002237784
Tpra1	527.08	829.25	1.573308516	0.002237784
Tuba8	14240.84	20778.94	1.459109795	0.002237784
Vopp1	7898.15	5378.68	0.681005843	0.002237784

Aldoa	50502.46	84264.82	1.668528933	0.002247075
Mrpl32	1742.33	1148.46	0.659149661	0.002252473
Sympk	1012.46	1702.25	1.681302863	0.002252473
Gigyf1	527.66	834.36	1.581222732	0.00227031
Camta2	416.12	678.26	1.629946784	0.002298251
Lnpep	6940.35	4225.49	0.608830148	0.002298251
Gata4	1686.99	2506.91	1.486019994	0.002308912
Usp10	1457.05	2377.48	1.631713693	0.002308912
Csnk1a1	4546.34	3014.67	0.663098557	0.002318326
Ncl	6820.66	4590.36	0.673008335	0.002318326
Dld	16649.65	10667.79	0.640721535	0.002327102
Syap1	780.01	468.26	0.600324913	0.002350431
Phf10	929.87	581.40	0.625253864	0.002358494
Cav2	1086.76	503.78	0.46355636	0.002360931
Gtf2h1	987.22	634.97	0.643192032	0.002360931
Hopx	1862.78	992.11	0.532596095	0.002360931
Mn1	343.65	628.68	1.829436086	0.002513398
Stmn1	1512.82	999.73	0.660840196	0.002513398
Ralbp1	2054.65	1364.46	0.664084769	0.00251999
Slc35a4	729.54	1129.36	1.548043421	0.00251999
Usp46	950.23	579.53	0.609889782	0.00251999
Llgl2	233.99	420.06	1.795203478	0.002524584
Homer2	796.74	471.84	0.592214926	0.002536125
Hk1	4167.31	6387.33	1.532724664	0.002549141
Ccdc85a	909.14	581.54	0.639655386	0.002568344
Fbxo21	719.59	1107.23	1.538696854	0.002568344
Zer1	1282.79	1927.01	1.5022061	0.002568344
Fos	19955.14	29061.29	1.456330961	0.002613883
Mapk6	2279.03	1454.28	0.638112781	0.002613883
Rab30	343.85	197.38	0.574010569	0.002613883
Hspd1	14236.49	9944.36	0.698511852	0.002629852
Chchd10	26763.39	40081.48	1.497623584	0.002647165
Foxk1	65.89	146.86	2.228992193	0.002647165
Npr2	346.51	563.97	1.627563232	0.002647165
Tpt1	42770.09	26544.58	0.620634086	0.002656157
Yipf3	622.47	990.86	1.591813838	0.002656157
Dmtn	36.99	96.70	2.613945896	0.002660115
Kif11	77.11	14.88	0.192918996	0.002660115
Canx	17966.38	11627.93	0.647205158	0.002667124
Llph	591.59	331.78	0.560823185	0.002667279
Kpna5	439.93	255.93	0.581744769	0.002708816
Pank3	1092.49	586.44	0.536790317	0.002793466
Prkcsh	1818.75	2682.06	1.47467116	0.002793466
Rpa1	1448.85	2140.83	1.477606241	0.002793466
Tada3	1284.03	1898.16	1.478275416	0.002793466
Ttc39b	871.28	551.63	0.633132292	0.002793466
Lrp4	656.04	1031.89	1.572911034	0.00281026
Angel1	187.52	332.22	1.771673696	0.00284044
Cmpk1	1402.24	774.17	0.552095143	0.002869806

Prkx	344.36	198.28	0.575784663	0.002877368
Postn	107.76	43.84	0.406778791	0.00287907
Ptpn12	1558.27	1040.94	0.668008413	0.00287907
Tsc2	1610.58	2392.74	1.485637536	0.002890627
Phrf1	1153.29	1724.08	1.494930068	0.002895898
Tnrc18	385.21	629.66	1.634575636	0.002972846
Disp1	311.16	557.05	1.790228051	0.003003607
Aspm	75.96	24.00	0.315930088	0.003016769
Gbp2	862.16	464.19	0.538401728	0.003032824
Lims2	6887.32	11351.12	1.648118957	0.003036929
Ppard	882.10	1337.30	1.516045729	0.0030463
Apaf1	337.16	194.17	0.575895029	0.003105218
Naga	615.74	950.68	1.543966728	0.003105218
Akirin1	836.64	534.24	0.638555095	0.00312586
Dgkb	1249.09	508.67	0.407231365	0.00312586
Ptbp3	317.67	144.26	0.45411742	0.00312586
Ipo13	1578.81	2565.41	1.62489857	0.003138102
Nucb1	3316.72	5060.27	1.525683704	0.003141814
Cycs	60457.55	37963.96	0.627944091	0.003144964
Med25	438.65	715.78	1.631756399	0.003224247
Picalm	3689.40	2371.53	0.642796706	0.003230417
Tmem115	332.24	539.49	1.623791814	0.003230417
Them4	1140.45	743.02	0.651512373	0.003238311
Kcng2	1671.92	2553.49	1.52728347	0.00323978
Myo1e	482.22	753.04	1.561613358	0.003240142
Mapk12	347.93	558.02	1.603804079	0.003249199
Maged1	2371.91	3472.55	1.464031183	0.003278163
Top3b	568.83	901.61	1.585022571	0.003301364
Sucla2	20241.97	14268.06	0.704874981	0.003301806
Numa1	2126.29	3138.61	1.476093477	0.003302135
Prc1	150.74	23.78	0.157738546	0.003308361
Rbm7	823.41	527.45	0.640570039	0.003308361
Alg13	206.46	107.27	0.519579237	0.003309955
RGD1305110	903.84	424.08	0.469199161	0.003309955
Clk1	2234.42	1515.73	0.678357444	0.003314515
Gkap1	1193.72	784.52	0.657205456	0.003314515
Rap1b	459.25	268.97	0.585670653	0.003337542
Serbp1	9178.92	6174.21	0.672651106	0.003337542
Usp32	2227.33	1374.83	0.617254269	0.003354363
Ppat	3757.32	2380.04	0.633439509	0.003376242
Chmp3	4236.77	2719.08	0.641782676	0.003380465
Cops2	2816.77	1658.62	0.588837214	0.003393798
Srebf1	264.04	611.73	2.316838062	0.003435218
RGD1308706	1374.44	718.58	0.522820672	0.003462681
Scn5a	6662.42	9652.07	1.448733664	0.003462681
Tbc1d25	97.61	187.39	1.919836678	0.003462681
Ugp2	19651.49	12558.29	0.639050461	0.00347608
Bzw1	2312.74	1577.16	0.681942032	0.003495318
Nab1	1560.05	987.63	0.633074064	0.003495318

Plekhh3	496.42	808.35	1.628366927	0.003495318
Tuba4a	14126.18	20092.64	1.422368949	0.003495318
Il1b	92.86	36.71	0.395367048	0.003543523
Abcd1	781.36	1182.07	1.512841448	0.003597485
Cpsf3l	483.86	759.95	1.57060392	0.003597485
Tceal8	1942.44	1106.38	0.569584481	0.003597485
Zswim8	918.80	1552.89	1.690134258	0.003597485
Rhbdd2	383.47	614.84	1.603360375	0.003637946
Thop1	495.65	765.99	1.545446645	0.003637946
Hlx	108.72	245.36	2.256773051	0.003662514
Zfp148	1674.37	1114.70	0.665740737	0.003662514
Ctsd	8564.62	12261.74	1.431673734	0.003713702
Frg1	1342.52	877.34	0.653503144	0.003713702
Gorasp1	1052.34	1599.08	1.519548381	0.003713702
Ift172	892.21	1347.26	1.510023594	0.003713702
Slc12a2	880.03	567.69	0.645073934	0.003720195
Rras2	4985.78	3460.28	0.694030393	0.003805849
Ccnd2	10605.13	6174.91	0.582256551	0.0038522
Htr2a	41.70	9.49	0.227677145	0.0038522
Pde11a	41.14	9.51	0.231186605	0.0038522
Pla2g15	96.93	199.13	2.054351259	0.0038522
Scrib	998.98	1527.74	1.529305151	0.0038522
Sts	1344.76	2410.36	1.792415707	0.0038522
Abca2	789.75	1225.26	1.551442403	0.003929129
Arc	206.72	370.00	1.789864298	0.003929129
Eif4e3	1032.95	675.97	0.654410817	0.003929129
Metap2	4584.74	3021.53	0.659040709	0.003929129
Chrng	12.05	0.18	0.015024916	0.003963479
Pdzd2	937.06	1392.30	1.485815852	0.003975444
Rbbp8	209.74	110.54	0.527033201	0.004037711
Mcee	2108.10	1444.37	0.685150638	0.004046507
Creb3l2	671.64	1047.60	1.55976721	0.004075603
Mybbp1a	2151.63	3144.16	1.461295131	0.004158446
Tlk2	1572.65	1059.28	0.673562343	0.004158446
Tspan2	1062.69	434.40	0.408774012	0.004173853
Jtb	1057.80	699.58	0.661352736	0.004212276
Vps36	720.63	377.33	0.523613678	0.004215759
Afap1	379.37	610.52	1.609284858	0.004223317
Pik3c2a	1426.13	608.85	0.426922932	0.004248805
Cd83	195.31	91.63	0.469126739	0.00425168
Eef2	33262.29	46900.98	1.410034667	0.00425168
ENSRNOG00000030371	1405569.40	822079.91	0.584873228	0.004252223
Klhl21	1205.52	1790.51	1.48526269	0.004252223
Larp1b	6809.79	3741.35	0.549407469	0.004252223
Mospd2	233.36	125.91	0.539559443	0.004252223
Mrpl18	925.73	584.71	0.631614134	0.004252223
Nfic	297.33	477.12	1.604713986	0.004252223
Mib1	550.50	345.58	0.627750204	0.004271514
Asb2	16857.93	28315.89	1.679677428	0.004277551

Chst15	545.85	830.55	1.521585497	0.004297943
Eif2b2	438.73	689.76	1.572174317	0.004338617
Pros1	408.88	249.51	0.610218544	0.004338617
Crkl	512.16	792.55	1.547456032	0.00436349
Slc12a7	9913.41	14409.81	1.453567621	0.00436349
Syngr2	1642.72	2367.53	1.441228389	0.004364961
Mtx2	1058.42	672.47	0.635350788	0.004497656
Lrrc41	959.81	1434.30	1.494345752	0.00452106
Rab2a	4573.80	3177.56	0.694729147	0.004521932
Zfp444	246.06	409.01	1.662207734	0.004521932
Usmg5	38783.42	24586.04	0.633931875	0.004529262
Bub1	161.08	81.70	0.507179636	0.004626864
Smc2	400.52	204.40	0.510328327	0.004626864
Jak2	841.82	462.02	0.548829702	0.004636212
Sf1	768.39	1161.64	1.511775899	0.004636212
Lpar4	23.67	3.21	0.135659856	0.004642076
Plekhf1	662.75	1061.86	1.602190676	0.004645357
Gng12	334.60	200.04	0.597859337	0.004675517
Apool	2052.84	1248.04	0.607957196	0.004733124
Atg3	1404.01	915.54	0.652087791	0.00474457
Myef2	638.16	359.97	0.56407864	0.004750296
Ell	826.42	1232.54	1.491417192	0.004781444
Pdha1	52675.18	34588.08	0.656629414	0.004781444
Rasa1	2707.34	1455.99	0.537792748	0.004781444
Rtn4	8831.04	6211.67	0.703390719	0.004781444
Tcof1	663.19	997.60	1.504255115	0.004781444
Tarsl2	1593.32	1009.05	0.633301833	0.004839819
Btbd1	14714.61	9589.76	0.65171697	0.004877502
Eapp	763.33	470.42	0.616272711	0.004886246
Golim4	3144.36	2122.30	0.674956572	0.004886246
Tmem184b	860.40	1293.86	1.503779776	0.004886246
Tpk1	289.54	168.35	0.581423701	0.004886246
Cpt1b	21358.84	30165.66	1.41232709	0.004898566
Rbm38	3743.37	5370.30	1.434616064	0.004909136
Zfp367	306.40	158.11	0.5160185	0.004909136
Fbxw8	259.17	447.56	1.726910298	0.004910374
Vars2	853.25	1272.57	1.491447268	0.004910374
Cyp2j4	484.08	260.10	0.537314858	0.004951105
Ece1	1607.26	2344.69	1.458817903	0.004951105
Tfeb	553.82	886.05	1.599879549	0.004951105
Ccdc43	1440.74	946.18	0.65673545	0.004953141
Gabpa	1739.42	1015.53	0.583833526	0.00496217
Plekha1	1319.97	892.63	0.676249453	0.004980255
Tmtc3	1571.21	934.46	0.5947412	0.004980255
Apoo	1767.32	1202.19	0.680230952	0.00498711
Abhd12	1101.98	1605.11	1.456566477	0.00500556
Sec63	1467.42	997.21	0.67956233	0.00500556
Odc1	3417.06	2371.53	0.694025696	0.00500851
Pten	1978.58	1038.40	0.524818966	0.005010403

Arhgap11a	115.11	45.29	0.393451792	0.005038606
Bche	1194.23	792.57	0.663671104	0.005038606
Gstm1	1076.02	1691.15	1.571678556	0.005038606
Snx33	741.19	1121.62	1.513264746	0.005038606
Tgfbr1	793.43	485.59	0.612018235	0.005038606
Zmat2	1422.13	957.04	0.672960799	0.005038606
Cenpf	116.89	27.88	0.238535433	0.005049511
Neurl4	1172.85	1734.96	1.479276757	0.005087708
Casp8ap2	667.58	309.76	0.463999734	0.005145184
Decr1	10303.68	15007.50	1.456518694	0.005145184
Grina	2101.73	3293.93	1.567244574	0.005148223
Ptms	2591.82	3891.05	1.501282654	0.005154632
Gys1	10115.93	16069.75	1.588558766	0.0051567
Sgsm2	2471.77	3687.79	1.491965361	0.005158447
Ddx6	3192.75	2209.09	0.691910697	0.005236566
Srrm2	2856.11	4090.41	1.432161859	0.005236566
Synpo2	12956.32	18418.95	1.421618451	0.005236566
Akt1s1	1232.53	1785.41	1.448573225	0.005242049
Csrp2	200.65	74.74	0.372468635	0.005242049
Ctps1	3518.67	2334.18	0.663369152	0.005303734
MGC95208	705.42	450.62	0.638804811	0.005303734
Ppp1r14c	4651.09	2839.22	0.61044225	0.005303734
Baz2a	549.65	836.16	1.521269561	0.005303929
Hmgb1	3000.58	1932.28	0.643969377	0.005303929
Wdr26	4915.21	3238.62	0.65889638	0.005303929
Eif1a	1164.38	662.66	0.569105237	0.005331304
Cyb5r4	371.80	209.16	0.562561701	0.005356995
Emc10	984.78	1487.47	1.510454818	0.005356995
Pogz	674.72	1008.81	1.495149922	0.005356995
RGD1308147	871.91	571.03	0.654917088	0.005356995
Usp1	1151.40	694.00	0.602748562	0.005386445
Rmdn1	3557.56	2089.76	0.587413054	0.005437038
Ap3d1	3322.19	4895.74	1.473648525	0.005479579
Mum1l1	302.38	158.70	0.524831929	0.005499537
Bhlhb9	215.19	120.11	0.558181516	0.005511466
Memo1	1078.41	599.30	0.555724839	0.005511466
Sgol2	41.20	3.80	0.09231603	0.005511466
Rangap1	314.28	506.08	1.610268313	0.005525283
Rnf152	263.16	129.47	0.49199405	0.005525283
Sod2	10452.91	7290.86	0.697496268	0.005525283
Psap	16314.00	22951.69	1.406870807	0.005562885
Skiv2l	486.81	837.78	1.720967669	0.005562885
Abce1	3194.01	2241.75	0.701860073	0.005671099
Ccdc97	827.02	1250.82	1.512449997	0.005671099
Dbf4	30.76	5.39	0.175337914	0.005671099
Oplah	667.51	1071.75	1.605601808	0.005671099
Acap2	537.64	339.80	0.632022166	0.005743006
Ap5s1	67.08	138.50	2.064605253	0.005743006
Fmc1	739.82	1140.15	1.541113437	0.005743006

Ilvbl	427.04	655.56	1.53512703	0.005743006
Pafah1b2	2872.41	1955.54	0.680800938	0.005743006
Pcif1	352.33	553.61	1.571282071	0.005743006
Pwwp2b	395.47	640.12	1.618614336	0.005743006
Skp1	16829.41	11920.00	0.70828357	0.005750879
Chd1	1805.16	1153.56	0.639034612	0.005760076
Mrc1	194.33	85.92	0.442157597	0.005776331
Shroom3	2222.49	4349.03	1.956827823	0.00579856
Atf1	1851.64	1188.40	0.641811955	0.005854939
Ccnb2	67.81	21.56	0.317962639	0.005854939
Tmem109	2120.96	3210.89	1.513884898	0.005854939
Ier5l	80.04	236.98	2.96085283	0.005867627
Mtmr6	2558.16	1673.20	0.65406344	0.005868764
Sbf1	2050.41	2955.19	1.441267734	0.005868883
Htatsf1	1205.91	660.46	0.547682842	0.005869247
Pafah1b1	5832.23	3612.39	0.619384552	0.005921645
Clcn6	215.31	358.17	1.663464445	0.005984862
Efnb2	362.43	218.27	0.602238523	0.005984862
Mex3c	782.45	495.07	0.632708913	0.005984862
Sh3glb1	15266.00	9613.56	0.629737046	0.005984862
Slc9a1	146.17	255.43	1.747519541	0.005984862
Zfp710	613.02	928.31	1.514323447	0.005984862
Cast	3892.46	2592.50	0.666031028	0.005995766
Txn2	3347.65	4883.09	1.458660739	0.006021621
Tlr3	218.19	121.70	0.557755214	0.006052266
Adcy6	2890.12	4141.62	1.433029528	0.006096475
Cx3cl1	430.43	781.84	1.816411065	0.006149063
Mfn2	8587.21	12152.13	1.41514242	0.006149063
Ergic2	3190.28	1915.96	0.600560245	0.006202713
Ggct	403.06	247.66	0.614447798	0.006202713
Nr3c1	5595.33	3340.97	0.597101058	0.006202713
Pde4a	353.08	564.21	1.597979446	0.006202713
Fap	94.94	40.80	0.42975125	0.006223007
Pbld1	123.35	220.17	1.784928867	0.00622362
Kctd18	249.64	140.28	0.561925836	0.006225884
Cdc37l1	3665.85	2564.21	0.699484552	0.006237856
Ppm1a	3646.85	2432.59	0.667038548	0.006237856
Rsrc2	3718.56	2447.54	0.658193957	0.006237856
Tmed5	965.01	435.59	0.451383179	0.006237856
Ypel5	1365.27	936.96	0.686280875	0.006237856
Farsa	594.15	886.14	1.49143212	0.006247117
Jrk	136.33	244.48	1.793306492	0.006276659
Dynlt3	1736.74	914.93	0.526808647	0.0063312
ENSRNOG00000030700	1604051.86	1032735.60	0.643829307	0.006331333
Cnot3	241.36	392.93	1.627959509	0.006380209
Foxp3	111.17	202.58	1.822229963	0.006380209
Ighmbp2	505.15	761.32	1.507128439	0.006380209
Mapk8	1513.53	1033.68	0.68295537	0.006380209
Sema4b	311.58	499.26	1.6023801	0.006421637

Tubgcp6	457.15	686.48	1.501647351	0.006421637
Gbf1	2170.24	3166.73	1.45915643	0.006490991
Mrpl51	3258.39	2295.77	0.704571718	0.006531299
Mcts1	1080.54	720.26	0.666571486	0.006542747
Fxyd1	10212.02	14080.72	1.378837888	0.006560149
Cbx5	1546.87	1077.18	0.696362087	0.006581272
Ccng1	48379.01	24823.63	0.513107417	0.006581272
Exosc4	138.27	239.90	1.734973776	0.006581272
Ireb2	664.34	399.44	0.60124833	0.006581272
Ngrn	933.66	621.47	0.665620294	0.006581272
Dus3l	276.71	467.03	1.687820504	0.006606692
Kdm4b	1094.08	1596.27	1.459003902	0.006606692
Pycard	118.01	38.03	0.3223012	0.006606692
Supt5h	4490.04	6329.51	1.409677348	0.006606692
Zfyve1	384.02	593.40	1.545227306	0.006622453
Tceb1	1164.27	788.58	0.677320201	0.006624338
Slk	4746.47	2890.80	0.609041659	0.006628821
Acaa1a	293.33	473.85	1.615423988	0.006646152
Pop4	1217.74	830.88	0.682311036	0.006667374
Myo9a	2806.68	1625.13	0.579024727	0.00671498
Rfx1	83.31	160.69	1.928769378	0.006777268
Ndc80	27.59	4.62	0.167307393	0.006820607
Rmnd1	1531.69	1057.53	0.690432882	0.006820607
Pomgnt2	310.57	492.11	1.584554825	0.006834941
Rnd3	4275.62	2273.96	0.531843789	0.006834941
Smek1	1330.05	849.50	0.638701469	0.006834941
Phospho2	638.44	393.35	0.616102829	0.006873965
Sept7	10949.15	6839.92	0.624699038	0.006873965
Cfl2	8924.37	5707.11	0.639496419	0.006882403
Fgd1	571.81	894.07	1.563564143	0.006882403
Spag9	7147.67	4846.04	0.677988795	0.006889262
Abhd16a	1391.02	1983.67	1.426054911	0.006931307
Baz1a	503.73	293.83	0.583316758	0.006953276
Kctd9	418.74	262.33	0.62648734	0.006991842
Zfp777	607.10	907.24	1.49437758	0.006991842
Sec31a	1278.62	1971.15	1.541625892	0.007017384
Arl5b	541.79	248.82	0.459247819	0.007024791
Gpatch11	395.49	246.69	0.623750357	0.007024791
Vps4b	1491.97	907.37	0.608169548	0.007024791
Nr1d1	2192.37	3318.02	1.513439652	0.007036166
Sars2	680.86	1021.30	1.500016901	0.007042255
Tom1	3450.02	4845.83	1.404581633	0.007052795
Cggbp1	1484.34	883.84	0.595442984	0.007077847
Cdh23	329.25	512.09	1.555296213	0.00716871
Phactr3	54.19	16.03	0.295869491	0.00716871
Rab6a	2786.56	1679.30	0.602643618	0.00716871
Ap1s2	1381.46	816.43	0.590991487	0.007178776
Cox6c	60540.28	39579.16	0.653765836	0.007178776
Uba3	3665.73	2237.73	0.610444378	0.007178776

Fbxw5	2943.76	4147.77	1.409005336	0.007301141
Jade2	295.14	469.09	1.589381638	0.007307244
Birc2	1139.05	708.17	0.621716185	0.007309447
Bmi1	1447.51	830.86	0.573993774	0.007309447
Chm	1013.48	585.97	0.578178976	0.007309447
Cnksr1	212.66	395.02	1.857518317	0.007309447
Prss23	1029.81	694.30	0.674199415	0.007309447
Psmc6	5655.41	4039.66	0.714300013	0.007309447
Raver1	471.63	795.43	1.686564555	0.007309447
Scp2	5669.77	3987.98	0.703375546	0.007309447
Tmem126a	2849.59	1800.92	0.631995164	0.007309447
Cox6a2	62551.33	86126.49	1.376893089	0.007317458
Psma4	4916.08	3501.63	0.712280678	0.007326664
Snrpe	948.36	637.44	0.672144824	0.007337169
Tpcn1	936.20	1415.77	1.512258703	0.007386618
Evl	379.96	239.42	0.630124967	0.007388442
Strn3	6292.21	3788.89	0.602154946	0.00744073
Tjap1	182.87	311.08	1.701082501	0.007444343
Sptb	6965.27	9816.85	1.409400597	0.00761679
Col1a1	707.97	377.07	0.532605261	0.007623453
Arpc5l	1632.07	980.55	0.60079878	0.007645135
Kif5b	23556.34	12067.77	0.512294031	0.007645135
Pld3	170.06	291.03	1.71140226	0.007645135
Snap23	1237.87	807.01	0.651933349	0.007645135
Ranbp10	927.16	1349.74	1.455778864	0.007752674
Wdr24	531.21	795.35	1.497226393	0.007782518
March5	1112.77	723.95	0.650582909	0.007795343
Kcnh2	985.76	1467.08	1.488277091	0.007795425
Cyr61	7336.95	12746.93	1.73735926	0.007817107
Rb1cc1	2882.18	1622.49	0.562938856	0.007836352
Cdk14	2070.30	1368.90	0.661210445	0.00786694
Msantd3	529.51	336.83	0.636118499	0.00786694
S100a10	705.73	375.86	0.532587101	0.00786694
Capza2	4004.74	2557.15	0.638531072	0.00788093
Hibch	2217.73	1563.12	0.704826271	0.00788093
Atp6v1d	6709.80	4828.92	0.719681825	0.007907935
Mocs1	247.42	395.89	1.600103683	0.00793717
Mtf2	235.04	124.08	0.527919729	0.007949617
Apoa1bp	1226.22	1745.88	1.423791615	0.008075182
Col5a2	704.99	381.40	0.540996418	0.008114144
Bsg	25862.52	37646.39	1.455635073	0.008114347
Usp25	3512.91	2270.70	0.646387447	0.008128154
C1qtnf6	95.72	42.42	0.44315811	0.00812842
Rps6kb1	1755.00	942.21	0.536875425	0.00812842
Urb1	362.30	567.45	1.566269301	0.00812842
Gadd45a	4219.52	2457.09	0.582314688	0.008143971
Guf1	3328.03	2128.06	0.639434868	0.008149167
Manbal	643.89	947.69	1.471817137	0.008200339
Plcd3	405.99	635.75	1.565904878	0.008204049

Tln1	4873.86	7362.87	1.510686318	0.008320493
Aip	599.36	885.66	1.477664209	0.00844826
Fiz1	321.09	498.04	1.551078103	0.00844826
Gcat	180.18	300.68	1.66871066	0.00844826
Pitpnb	3365.86	2316.42	0.688210787	0.00844826
Plekha3	965.66	606.60	0.628171844	0.00844826
Sar1a	3493.30	2487.25	0.712004566	0.00844826
Tom1l2	2357.29	3303.96	1.401595702	0.00844826
Usp12	534.43	296.45	0.55470732	0.00844826
Clstn1	2047.83	2910.96	1.421485529	0.008459087
Fam185a	883.41	599.24	0.678325215	0.008459087
Lims1	3914.99	2568.71	0.656120913	0.008459087
Wdr81	126.14	225.41	1.786972579	0.008459087
Pex14	539.17	802.64	1.488655904	0.008717485
Fastkd2	1144.25	777.00	0.679051648	0.008726694
Pknox2	261.49	416.36	1.592259274	0.008730365
Cdv3	2721.01	1537.84	0.565172715	0.008818173
Ctdsp1	3912.00	5386.36	1.376882324	0.008826447
Emc2	3847.05	2197.98	0.571341085	0.008826447
Gnai1	149.13	77.06	0.516736362	0.008826447
Idi1	383.79	197.26	0.513991322	0.008826447
Phtf2	3325.60	2256.80	0.678613076	0.008826447
Rbm25	4013.87	2406.12	0.599450332	0.008826447
Caskin2	361.03	550.90	1.525925038	0.008876638
Nfatc1	147.50	251.06	1.702113154	0.00895383
Kpna4	2458.99	1665.54	0.677325443	0.0089863
Csnk1g3	1198.14	760.07	0.634374446	0.009002598
Mical1	299.86	482.25	1.608239926	0.009010888
Pbk	37.80	6.15	0.162810072	0.009010888
Slc29a1	908.18	1311.24	1.443818456	0.009010888
LOC367515	391.77	195.45	0.49890275	0.009048656
Irgq	440.71	706.53	1.603167309	0.009116758
Rps15	4477.18	6160.43	1.375961904	0.009116758
Tysnd1	145.08	272.89	1.880987186	0.009116758
Setd2	1956.74	1246.58	0.637068856	0.00913531
Cd302	151.95	77.95	0.512986296	0.009165102
Frem2	335.49	528.77	1.576129057	0.009165102
Slc35f5	3060.67	2187.02	0.714556209	0.009165102
Tle2	116.52	204.09	1.75155578	0.009165102
Xpr1	532.06	341.54	0.641920429	0.009184679
Acot9	2066.74	1451.42	0.70227199	0.009267961
Jun	10961.71	15352.38	1.400546891	0.009267961
Notch2	141.67	255.92	1.806524967	0.009267961
Zhx1	1153.55	626.99	0.543534466	0.009267961
Tdg	384.15	240.67	0.626497391	0.009290212
Lrrc8b	852.98	577.80	0.677396278	0.009309077
Tex264	1359.47	1919.84	1.412191672	0.009309077
Vwf	890.26	1415.96	1.590505658	0.009318517
Agpat3	4137.96	5762.15	1.392509153	0.009327764

Ddx46	4156.89	3003.79	0.722606195	0.009327764
Gimap4	870.93	600.73	0.689757598	0.009327764
Zfand6	1706.91	1184.37	0.693871092	0.009327764
Ncoa5	789.17	1141.87	1.446931936	0.009368272
Otud6b	2083.18	1267.65	0.608518501	0.009368272
Rfc1	1820.77	1205.07	0.661844466	0.009368272
Ythdf3	3916.45	2673.74	0.682694955	0.009368272
Atp1a2	14625.05	20165.15	1.378809097	0.009382994
Krit1	2388.21	1632.71	0.683655894	0.009392007
Reep3	281.10	167.51	0.595912533	0.009394172
Rimbp2	1026.56	1485.21	1.446774232	0.009436774
Gga3	275.71	426.92	1.548470676	0.00945236
Rab21	2059.16	1259.25	0.611537224	0.00945236
Tulp4	397.64	248.59	0.625169068	0.00945236
Azin1	4583.32	2680.92	0.58492975	0.009462854
Fbn1	575.50	341.87	0.594045332	0.009462854
Ogfrl1	619.78	386.38	0.623406014	0.009462854
Ripk2	954.90	640.13	0.6703602	0.009462854
Hist2h4	1341.05	3563.72	2.657420543	0.009555447
Rreb1	1409.65	2000.98	1.419487136	0.009557614
Bola1	290.22	455.47	1.569383935	0.009571651
Csde1	39635.10	21332.77	0.538229154	0.009571651
Nup210	157.83	270.52	1.714026118	0.009571651
Slc22a17	460.30	706.02	1.533813605	0.009571651
Atp6v1c1	1572.99	1100.12	0.69938244	0.009636261
Murc	7536.35	5483.59	0.727619557	0.009870002
Atp13a1	324.64	502.29	1.547229513	0.00995244
Inha	1894.50	3082.14	1.626883804	0.009968757
Mkks	1646.15	1139.09	0.691969201	0.009968757